Mathematical modeling of the ductile-brittle-transition and an application to ferritic steel

Von der Carl-Friedrich-Gauß-Fakultät
der Technischen Universität Carolo-Wilhelmina zu Braunschweig

zur Erlangung des Grades eines

Doktors der Naturwissenschaften (Dr. rer. nat.)

genehmigte

Dissertation

von Thomas Hennecke
geboren am 29.03.1978
in Stadtoldendorf

Eingereicht am: 29.10.2012

Disputation am: 13.03.2013

1. Referent: Prof. Dr. Thomas Sonar

2. Referent: PD Dr. Peter Hähner

(2013)

I am only in it for the mechanics.

(Frei nach The Mothers of Invention.)

Danksagung

Für einen Wissenschaftler sind gute Gründe schlechte Gründe, denn sie verstellen den Blick auf die Besseren. Für einen Politiker sind gute Gründe gute Gründe, aus dem gleichen Grund. Solche und ähnliche Dinge lernt man bei einem interessanten Arbeitgeber wie der Europäischen Kommission. Die wichtigsten Ideen dieser Arbeit entstanden während meiner Zeit in den Niederlanden am Institute for Energy des Joint Research Center eben dieser Kommission und die Zeit dort hat mich nicht unerheblich geprägt. Sehr viele Personen haben zum Gelingen dieser Arbeit beigetragen und ich kann hier nur die wichtigsten hervorheben.

Ich danke Privatdozent Dr. Peter Hähner am Institute for Energy, dem jetzigen Institute for Energy and Transport, herzlich für die Stellung des interessanten Themas und die Betreuung während der Arbeit. Mein Blick auf die Festkörpermechanik hat sich durch diese Arbeit grundlegend geändert. Ebenfalls danke ich herzlich Prof. Dr. Thomas Sonar, der sich an der TU Braunschweig als Mentor zur Verfügung gestellt hat und damit auch einem ungewöhnlichen Thema am Rande seines Hauptforschungsgebiets und der Grenze zwischen Mathematik und Physik eine Chance gegeben hat, genauso wie für die Zusammenarbeit während des Wintersemesters 2008/2009 und Sommersemesters 2009. Auch mit Prof. Dr. Andreas Meister an der Uni Kassel habe ich immer sehr gut kooperieren können, dafür danke ich ebenfalls herzlich.

Von den vielen Personen in den erwähnten Arbeitsgruppen, mit denen ich sehr viele positive Erfahrungen im menschlichen Umgang teile, möchte ich drei namentlich hervorheben: Felix Hagemann, mit dem ich mehrere Jahre das Büro und zeitweise auch die Wohnung teilte, für die vielen guten Diskussionen über Bruchmechanik und die Welt, die stete Hilfsbereitschaft bei den verschiedensten Dingen und die Freundschaft sowie Dr. Bettina Messerschmidt und Dr. Sigrun Ortleb für das Korrekturlesen.

Prof. Steve Roberts in Oxford danke ich für die finanzielle Unterstützung für einen Kurzaufenthalt in Oxford und ihm und seiner Arbeitsgruppe, insbesondere Ed Tarleton, für die umfangreiche Betreuung vor Ort.

Diese Arbeit wurde im Rahmen des Großprojekts PERFECT im sechsten Rahmenprogramm von EURATOM gefördert, dabei danke ich für die finanzielle Unterstützung sowie den Kooperationspartnern Bernard Marini und David Lidbury (†) und dem Koordinator Jean-Paul Massoud für das Interesse an meiner Arbeit und dem Fortgang der Entwicklung.

Meine Eltern und meine Familie haben mich in den vielen Jahren stets unterstützt, all dies wäre ohne sie so nicht denkbar gewesen. Dafür danke ich von ganzem Herzen.

Zusammenfassung

Diese Dissertation beschäftigt sich mit der mathematischen Modellierung des Spröd-duktil-Übergangs auf Basis der Versetzungsdynamik, wobei der Beschreibung qualitativer Eigenschaften des Übergangs und der Abhängigkeit der Bruchzähigkeit von der Temperatur bei ferritischen Stählen besondere Beachtung geschenkt wird.
Nach einer Einführung anhand historischer Zusammenhänge und der technischen Bedeutung sowie einer Beschreibung der zu erklärenden empirischen Tatsachen und versetzungstheoretischen Grundlagen werden dafür zwei Modelle auf Basis der elastischen Wechselwirkung von Rissen und Kerben mit Versetzungen eingeführt und eine Analogie zur Supraleitung diskutiert.
Mit dem auf der Spannungsintensität an einer Rissspitze basierenden ersten Modell erhält man neben einer Beschreibung der Temperaturabhängigkeit der Bruchzähigkeit auch ein explizites Kriterium für den Übergang. Die im Übergangsbereich auftretende Streuung der Messwerte wird erstmals aufgrund der intrinsischen Dynamik erklärt und somit auch für Reinstoffe wie Silizium verständlich; dabei kann auch erklärt werden, warum sie nur im Übergangsbereich besonders groß ist. Unter anderem wird auch das Auftreten von Spaltbruch bei gleichzeitigem erheblichen plastischen Fluss erklärt. Auch wegen des Bezugs auf die Rissspitze kann dieses Modell aber noch nicht auf Stähle angewendet werden.
Das zweite Modell verwendet einen Vergleich der Versetzungsgeschwindigkeit mit der Ausbreitungsgeschwindigkeit von Niveaus gleicher Spannung, um den Anstieg der Bruchzähigkeit mit der Temperatur zu beschreiben, wobei der Bruchvorgang nicht mehr an der Rissspitze einzusetzen braucht. Seine Anwendbarkeit auf eine große Klasse von Spannungsfeldern wird gezeigt und anschließend ein Beispiel explizit durchgerechnet. Mithilfe dieses Modells gelingt die Erklärung der starken Streuung im Übergangsbereich aufgrund von Schwankungen in der lokalen Bruchspannung und warum auch bei diesen Schwankungen die Streuung außerhalb des Übergangsbereichs viel geringer ist. Das Modell sagt eine Temperaturabhängigkeit der Rissinitierungsposition vorher. Lokale Plastizität, duktiles Risswachstum und Spaltbruch schließen sich nicht gegenseitig aus. Eine physikalische Rechtfertigung des Master-Curve-Ansatzes für die Temperaturabhängigkeit der Bruchzähigkeit unter Bestrahlung wird erstmals aufgrund der Versetzungsgeschwindigkeit direkt gegeben, wobei der Master-Curve-Ansatz nur dann näherungsweise korrekt ist, wenn die thermische Energie klein gegen die effektive Energiebarriere für Versetzungsbewegung und die Strahlenbelastung nicht zu groß ist. Es wird erklärt, warum Verschiebung der Übergangsregion zu höheren Temperaturen und der Anstieg der Fließspannung als Funktionen der Bestrahlung

miteinander korrelieren, obwohl sie das als Funktionen der Temperatur in erheblich geringerem Maße tun. Ein explizites Übergangskriterium, das unabhängig von der Probengeometrie ist, kann in diesem Zusammenhang nicht mehr angegeben werden. Dies erscheint aber nicht als Nachteil zum ersten Modell, sondern notwendige Konsequenz aus dem allgemeineren Ansatz. Es wird an verschiedenen Stellen deutlich, dass eine genaue Beschreibung des Übergangs explizite Berücksichtigung von duktilem Risswachstum und durch plastische Verformung ausgelöstem Spaltbruch erfordert.
Anstatt die Untersuchungen aufgrund der gegebenen Modelle zu vertiefen, wird im letzten Kapitel eine Analogie zwischen Festkörpermechanik und Supraleitung diskutiert, weil sie eine völlig neue Perspektive auf das Problem eröffnet. Der Festkörper wird dabei als Supraleiter für mechanische Kräfte aufgefasst, wobei der zugehörige Meißner-Ochsenfeld-Effekt die Verdrängung von Massentransport aus dem Volumen des Festkörpers ist. Bei dieser Analogie erscheint der Spröd-duktil-Übergang als Übergang von einem Supraleiter erster Art, der durch Spaltbruch versagt, zu einem Supraleiter der zweiten Art, der durch duktiles Risswachstum bei starker Deformation versagt. Dies eröffnet völlig neue Zugänge zur Beschreibung von Plastizität und Bruchverhalten, weil sie dann im Gegensatz zum bisherigen elastischen Zugang, der eher der klassischen Maxwell-Theorie des Elektromagnetismus entspricht, mit modernen Mitteln analog zur makroskopischen (zeitabhängigen) Ginzburg-Landau-Theorie oder mikroskopischen BCS-Theorie behandelt werden sollte. Diese Mittel müssen aber teilweise noch geschaffen werden.
In diesem Zusammenhang gibt es aber vielversprechende Möglichkeiten, da zum Beispiel in diesem Rahmen bereits Arbeiten über den Zusammenhang von quantisierten Wirbelbewegungen und Kavitation erschienen sind, deren Prinzipien eventuell auf die Entstehung von Spaltrissen oder Hohlräumen aus Versetzungen übertragen werden können. Weitere Anwendungen sind die Erklärung von Geometrie- und Größeneffekten durch Längenskalen, die auf natürliche Art in der Theorie der Supraleitung auftreten sowie ein Zugang zu Spannungs-Dehnungskurven als Darstellung des Widerstands eines Körpers gegen mechanische Kraftübertragung, der eine neue Perspektive bei der Beschreibung von Verfestigung und Entfestigung erlaubt.

Conclusions

This thesis is concerned with mathematical modeling of the ductile-brittle-transition based on dislocation dynamics. Qualitative properties of the transition and the dependence of the fracture resistance on temperature in ferritic steels are treated with special emphasis.
Following an introduction through historic developments and the technical significance we give a description of the empirical results to be explained and the basic dislocation theory needed. Then, two models based on the elastic interaction of cracks/ notches and dislocations are considered as well as an analogy to superonductivity.
The first model, which is based on the concept of stress intensity, allows to derive the temperature dependence of the fracture toughness and an explicit criterion for the ductile-brittle-transition. The scatter of the empirical data of the fracture toughness in the transition regime is explained for the first time by the intrinsic dynamics of the model and therefore becomes understandable in pure single crystal materials like silicon. The difference of the magnitude of the scatter between the transition regime and lower temperatures is explained as well as the occurence of cleavage in the presence of considerable plastic flow. The model can not be applied to steels, though, as, among other things, it relies solely on the description of the stress intensity at the crack tip.
The second model compares the dislocation velocity to the velocity of levels of constant stress at a given loading rate to infer the increase of fracture resistance with increasing temperature. Fracture need not be initiated at the crack tip anymore. We show the applicability of the approach to a wide range of possible stress fields and thereafter treat an explicit example in detail. Using this model, we can explain the strong scatter in the transition regime based on fluctuations of the local fracture stress and why the scatter is much smaller outside of the transition regime even if those fluctuations are present. The model predicts a temperature dependence of the fracture initiation sites. Local plasticity, ductile crack growth and cleavage crack growth do not exclude each other. We give a physical justification of the Master curve approach for the temperature dependence of the fracture resistance under irradiation, which is based directly on the dislocation velocity for the first time. The Master curve approach is approximately correct, if the thermal energy is sufficiently small compared to the effective energy barrier for dislocation motion and the irradiation dose is not too large. The model explains, why the shift of the transition regime to higher temperatures correlates to an increase of the yield stress as functions of irradiation, while the correlation is much weaker as functions of temperature. There is no explicit transition

criterion independent of the specimen geometry in the second model anymore. This is not to be seen to be a disadvantage when compared to the first model, though, but rather as a necessary consequence of the more general approach. Some results show the necessity to account for ductile fracture and plasticity-induced cleavage fracture explicitly, to get a more precise description of the transition regime.
Instead of a more detailed analysis of the given models, the final chapter discusses an analogy between solid state mechanics and superconductivity, because it opens a completely new perspective on the problem. The solid state is perceived as superconductor for mechanical forces, where the corresponding Meissner effect is the explusion of mass transport from the solid body. Considering this analogy, the ductile-brittle-transition is a transition from a superconductor of the second kind for mechanical forces, corresponding to ductile fracture and large deformations, to a superconductor of the first kind for mechanical forces, which fails by rapid cleavage fracture. This suggests completely new approaches to the description of plasticity and fracture behavior, because one should not treat the problem based on elasticity theory, which corresponds rather to the classical Maxwell-theory of electromagnetism, but by analogs of the macroscopic time-dependent Ginzburg-Landau-theory of superconductivity or the microscopic BCS-theory. The necessary means have still to be created at least partly, though.
There are promising possibilities of such an approach: Work has been done on the connection of quantized vortices and cavitation, which could be applied to the creation of cleavage cracks or voids by dislocations. Size and geometry effects can possibly be explained by the length scales, which enter the modern theories of superconductivity in a natural way. Furthermore, the analogy suggests an approach to stress-strain-curves as describing the resistance to mechanical force conduction, shedding new light on hardening and softening.

Contents

Chapter 1

Motivation

This work is concerned with the description of the fracture behavior of steels used in certain engineering applications, specifically the construction of nuclear reactor pressure vessels. Before describing the engineering problem in more detail in section 1.2, we will give a short survey of some aspects of fracture as the cause of mechanical failure, which were relevant to the development and shaped the current understanding of the subject. We distinguish between fracture and failure, because the latter can have many reasons not related to fracture, which influence design decisions and hence the risk of fracture.
By mechanical failure of a structure we understand a change in its form or load bearing capacity, rendering it unsuitable for its intended purpose. This may be due to abrasion or deformation in the case of a cogwheel, which will no longer operate properly in a gear, or fracture of an airfoil, destroying an aircraft.
Understanding mechanical failure of structures is a ubiquitous challenge in engineering: Whether the consequences of failure are limited to the structure under consideration, merely necessitating its replacement, or constitute a serious threat to health and life of people, like the collapse of a bridge or fracture of a pressure vessel, preventing such failures is important. But a proper understanding of failure not only allows its prevention but also to confidently extend and modify known designs of objects to achieve a save operation under a wider variety of conditions, enhanced durability, easier handling or other desired characteristics. For such a purpose a comprehensive understanding of possible mechanisms leading to failure is mandatory. Therefore engineering has ever been concerned with the comprehension of failure processes, whether by systematic investigation or simple trial and error.

1.1 Historic research related to fracture

This section contains some historical examples which elucidate important developments in the understanding of fracture and the incentives that led to the related research efforts, which need not at all be directly connected with the problem of brittle fracture. The transition to brittle fracture of usually ductile steel structures, the so-called ductile-brittle-transition (DBT), is the topic of this thesis and the examples chosen here represent some parts of the development, which were of special relevance to the understanding of the DBT by the present author. The position of this thesis in the general research effort and some contributions are discussed at the end of section 1.2. Only a minimal part of the field is discussed in this section and the reader is referred to the vast body of literature. The references provide a number of possibilities to begin the study of the subject, where many different points of view are proposed. We begin with a short discussion of the phenomenology of fracture.

The phenomenological processes leading to failure of steel structures with which we are concerned are irreversible deformation and fracture on a time-scale which is very short with respect to the intended operating time, we exclude creep and fatigue. Phenomenologically, fracture can be classified as brittle or ductile. Brittle fracture is accompanied by little or virtually no prior deformation beyond the linear elastic regime and minimal energy dissipation. This process is often unstable and results in rapid mechanical failure. Ductile fracture goes along with strong irreversible deformation and correspondingly strong energy dissipation during the fracture process. Because of the significant deformation before fracture, it is usually possible to take appropriate countermeasures. Due to these different characteristics, it is a major concern of engineering to ensure operating conditions leading to a ductile response of the materials in use. At the fourth international conference on fundamentals of fracture in 1993, Robb Thomson, coauthor of [175], called the competition between ductility and brittleness "the 'first fundamental problem' of fracture", [216, p. 2], while the problem had been intensively studied for several decades.

Before steel became an affordable construction material for large structures during industrialization, available materials like brick were brittle and unsuitable to carry tensile loads. Therefore construction of cathedrals and bridges relied on appropriate arches, transmitting the load of the construction material by compressive stresses, [5]. Even then, an improved empirical understanding of the load-bearing capacity of structures led to a radical change in the designs of cathedrals between the romanesque style, where the thick

outer walls carry the load, and the gothic style, where pillars and flying buttresses do the same, allowing for large areas of figured glass in the walls.
During the 19th century, steel became a predominant material and it was therefore possible to construct buildings carrying significant tensile loads, such as the Tower Bridge of London. The increasing use of tensile loads as well as the demand for cheap construction and saving of material led to brittle fractures unexplanable by the simple approximations for the stress distribution in structures then used by engineers, [151]. Therefore the theory of elasticity was used to solve the boundary value problems arising in the analysis of stress and strain in deformable objects more accurately. This motivation is apparent from the titles of a number of research articles using mathematical methods around the beginning of the previous century, [75, 95, 105, 123, 124, 240, 241]. By then the method of stress functions to compute the stress distribution in a two dimensional linear elastic solid had been introduced by Airy, [3], to investigate the influence of the stresses and deformations on the optical properties of instruments used in astronomy. Due to Maxwell, [138, 139] and Ibbetson, [94], the connection to the biharmonic equation was established and these and related works on statics and elasticity attracted the attention of Felix Klein in Göttingen. His students Anton Aloys Timpe and Karl Wieghardt, who submitted his fundamental article [240] while working in Braunschweig, see [243] for an english translation, received their PhD's with theses on these subjects and continued to publish in the area, [106, 219, 220, 221, 222, 239, 242]. The method of stress functions was extended to three dimensions by Papkovitch and Neuber, [150, 151], and the requirements of engineering and lack of the necessary computing power for effective numerical methods led to the development of experimental methods to solve the basic equations, [73, 239].
Stress functions for general continua are treated in [224], which contains copious references to the earlier literature. The author found [141, 184] especially helpful for details on the history of the biharmonic equation and early approaches to fracture, while [218] is a general reference on the history of strength of materials.
One of the main insights gained during the early period of research in fracture before the second world war was the identification of the crucial role of notches and cracks for the integrity of a component. While the earliest designs focussed on a supposedly sufficient area cross-section to carry loads, the influence of (rapid) changes of this cross-section was noticed, [151]. This influence is exemplified by the stress concentration at the tip of notches and cracks, which is reported already in [95, 240] and shows the characteristic asymptotic behavior $1/\sqrt{r}$ near the notch tip, where r is the curvature radius of the notch in question. Griffith used [95] in the most influential early

paper [71] on brittle fracture to give a theory based on the existence of cracks of a critical size, where he compared the change of surface energy and elastic energy due to the elongation of a crack to decide, whether it propagates or not. This paper, containing an error corrected by Griffith in [72], immediately aroused interest in Germany, [244], and is still cited frequently, while [240] was almost forgotten, [183].
One major incentive for research on brittle fracture were the catastrophic fractures sustained by the so-called Liberty Ships produced in the USA during the second world war. Due to the urgent need to supply the British isles and replace merchant vessels lost in the war, mass production of freighters and tankers was initiated. In order to speed up construction a number of measures that led to subsequent problems were taken: Amongst others were the employment of a large workforce with substandard training, using steel of low quality especially with respect to impact testing and replacing riveting by welding. While this allowed to build ships in numbers previously unknown, a significant number sustained serious failures during service afterwards, which is discussed in many places, [5, 99, 202, 215]. A thorough and readable account is given in [24], a major source of information for the author about investigations of brittle fracture before 1960.
From the perspective of physics, an interplay between several factors was the cause of those unexpected brittle fractures. One was the stress concentration due to notches or other geometric discontinuities, another was the tendency of notch-brittleness in steels: Under certain conditions a tensile specimen, see Figure 2.1 in chapter 2, fails in a ductile manner, while a notched specimen may exhibit brittle fracture. Furthermore low temperatures and triaxial loading make a structure more prone to brittle fracture. In this context, welding is detrimental to the overall structure in two respects compared to riveting: Firstly, improperly fabricated welds can act as crack initiators. Secondly, while an extending crack in a riveted plate is stopped at its boundary and has to be reinitiated in the next, a welded structure has no such discontinuities to prevent a crack from traversing the whole structure. Prevention of brittle fracture has ever since been a major research topic for engineering branches particularly concerned with its risks, like aerospace and nuclear engineering.
The main object of this thesis is to improve the theoretical knowledge about the transition from ductile to brittle fracture behavior and the influence that geometry, temperature, strain rate, irradiation and other factors have on it. We discuss materials with a heterogeneous microstructure, because ferritic steel, a standard construction material of a reactor pressure vessel (RPV), is of special interest.
The salient point in understanding the DBT is its connection to the defor-

mation of the given structure. In a tensile test of a ductile material we can distinguish reversible elastic deformation at low external load and irreversible plastic deformation at high external load. Elastic deformation in metals is adequately modeled by linear elasticity theory based on Hooke's law. Its microscopic origin and the determination of effective elastic constants of a polycrystal given its constituents are not of interest here. On the contrary, plastic deformation plays an essential role for fracture and the DBT, warranting a more detailed description of its nature.

A major research problem in mechanics of materials during the end of the 1920th was the discrepancy between the theoretical shear strength of crystals as investigated by Frenkel, [65], and the stress necessary to observe plastic deformation, which was found to be lower by orders of magnitude. The microscopic explanation for this curious behavior was given in 1934 independently by Orowan, Polanyi and Taylor, [158, 170, 210, 211]. In his analysis Frenkel had assumed that two parts of a crystal were sliding relative to each other along a crystallographic plane, where each part moved as a whole. Orowan, Polanyi and Taylor introduced line defects, the so-called dislocations, which could glide far easier through a crystal than two surfaces along each other. This explained the discrepancy and led to significant work on dislocations before they were even observed in experiments, [35, 36, 116, 212]. Dislocations had already been introduced in the mathematical theory of elasticity before and they are discussed in [134, Appendix to chapters VIII and IX], where references to the early work of e. g. Timpe and Volterra can be found. With the help of dislocations the permanent nature of plastic deformation is readily understood. As defects in the crystal structure, dislocations carry deformation fields. They are created and move during straining and do not vanish again, except by leaving steps on the surface of a crystal, thus producing deformation which does not disappear during unloading. Furthermore dislocations are useful in understanding crystal growth, which was discussed in 1953 in [172, Chapter 10].

Even though they are helpful to elucidate a number of phenomena in solid state physics and their existence was proved by direct observation, [4], the investigation of dislocations raised objections early on. The preface of [172] by one of the then principal investigators in the field contains the often quoted statement: "Finally, it became apparent that dislocations could explain not only any actual result but virtually any conceivable result, usually in several different ways." He then advocated a careful combination of the development of a theory based on accepted first principles and meaningful experimental verification. Fitzgerald's critique in the first two paragraphs of the introduction of [63] was far more radical: "A variation in the degree of sophistication may exist in these 'dislocation theories,' but they all have one feature in com-

mon, viz., an attempt is made to describe a *non-elastic phenomenon* (plastic slip) entirely in terms of *linear elastic concepts*. In my opinion, this is an illogical and ill-fated enterprise. After almost thirty years, this approach has led to no numerical calculation in agreement with measured values of any mechanical quantity - except through the arbitrary assignment of values to several 'constants.'" Fitzgerald accepts the existence of dislocations as proven by experiments, but does disapprove of their description in terms of elasticity to explain the mechanical properties of crystals. He goes on to develop a theory of particle waves in crystals, which has not been accepted. Still, we think of deformation as expressing mass transport, where Fitzgerald described momentum transfer and will also refrain from an analysis of the stress field in terms of the equilibrium equations of linear elasticity when expedient, compare the discussion in section 2.2.

Early attempts to incorporate the effects of plastic deformation and dislocations in the quantitative description of fracture in metals were published in [101] by Zener, [253], and Irwin, [96]. As both introduce concepts, which are still applied in modeling fracture, the DBT and its connection to plastic deformation, we give a short discussion. Zener reviews experimental work on fracture of metals, where it is demonstrated, that surface defects causing the low fracture resistance in glass according to Griffith, [71], are not the reason for premature failure in metals. He goes on to describe how grain boundary sliding may cause stress concentrations at corners where three grains meet, and how dislocations gliding in shear bands may concentrate stresses at obstacles sufficiently to induce local cracks. Then he cites experimental evidence, that deformation precedes fracture in metals, but emphasizes that the micro-mechanisms are understood only in very special cases. The idea of dislocations inducing cracks or coalescing to form a crack was taken up by Stroh, [200, 201, 202], and a number of other investigators. The book [237] gives plenty of examples of cracks described by dislocations. The main conclusion of Zener's paper is that localized plastic deformation is an important cause of fracture in metals.

Irwin's contribution of interest seems to contradict this assertion at first. In discussing dynamics of fracture of metals he is also obliged to modify Griffith's original approach, but in the other direction: He introduced an additional contribution to the energy balance equation by incorporating the plastic work and claimed that the contribution of the surface tension is generally not significant, but that their relative contributions change with changing crack contour. Essentially, the usual surface energy of a material is replaced by an effective energy, which may be orders of magnitude larger, [160]. This approach is still found in introductory texts on fracture mechanics, [74, 99]. Another contribution of Irwin, which had a major impact on fracture research

is the concept of stress intensity factors, [97], to be discussed in section 3.1. The contradiction between these two viewpoints on the influence of plastic deformation on fracture may be resolved by considering an analogy to electrostatics. Dislocations take the role of mechanical charge carriers, which form a type of incomplete Faraday cage around a crack. Inside the plastic zone around a crack the stresses are relieved by plastic deformation, but at or near its boundary the dislocations may cause a strong stress concentration able to induce cracking, if their local density is large enough.
We will model the DBT based on stress relief, known as shielding in the literature. This allows to describe the increase of fracture toughness with increasing temperature in the transition regime, an effect whose modeling by induced cracking due to increasing plasticity is meaningless.
Another analogy with electrodynamics will be very helpful to understand the phenomenon: We think of solid structures as superconductors for mechanical forces. The change in the fracture behavior during the DBT is then regarded as analog to the transition between an electromagnetic superconductor of the first kind (corresponding to brittle fracture) and the second kind (corresponding to ductile fracture). While certain analogies between the stress fields of dislocations and magnetic fields of wires conducting an electric current are well-known and the discussion of them began already during the 1950s, when the research on dislocations progressed rapidly, [147, Chapter 2.6 and 8.1], the attempt to explain the DBT based on the conception of the rigid body as superconductor for mechanical forces seems to be new. It has interesting consequences also for other subjects in the mechanics of materials, which will be discussed in chapter 4.
The next section is concerned with the engineering background of this thesis.

1.2 The service life of a nuclear reactor

A major technical problem where brittle fracture prevention plays a decisive role is the accurate prediction of the service life of commercial nuclear reactors. While nuclear reactors are an expensive investment, they produce a large amount of electricity practically independent of environmental conditions. Therefore there are strong economic incentives to operate them as long as possible. The main inherent obstacle is the increasing embrittlement of the reactor pressure vessel (RPV) during service due to neutron irradiation. Because of the disastrous consequences of a brittle failure of an RPV during service, it must remain an incredible event, [126]. This conflict between the economic objective and the *condicio sine qua non* of safe operation results in strong efforts by the nuclear industry to investigate the effect of irradiation

embrittlement on the reliability of the RPV.
The safety assessment with respect to fracture of RPVs during the design life has hitherto been based on empirical approaches, an example of which is described in [53]. These empirical approaches are often found to be rather conservative in their prescriptions, [126], therefore modifications incorporating the results of extensive test programs of relevant physical quantities are suggested by the nuclear industry. These can serve to extend the lifetime of existing reactors and as a basis to design nuclear power plants with a longer initial design life.
When trying to improve on the margins of the empirical approaches, there are numerous problems of widely different types the investigators have to adress. These may be due to the mechanics and geometry of the components or due to the properties of the materials in use.
To name but two examples of research conducted within the Fifth Framework Programme of EURATOM, the shared cost action project VOCALIST (validation of constraint-based methodology in structural integrity), [127], assessed possible benefits to be gained by the so-called loss of constraint related to the stress state of a shallow fatigue crack in an RPV as compared to the usual deep crack fracture toughness test specimens. The basic problem is thus one of the relative length of a sizeable flaw and thus of geometry on the macroscopic scale (or a little below). It is argued that due to the resulting different stress state around the crack in an RPV, higher values of the apparent toughness compared to the plane strain values obtained by valid fracture mechanics tests can be assumed.
On the other hand during the project FRAME (fracture mechanics based embrittlement), [227], approximately 700 fracture toughness specimens were tested by several institutions to obtain a data basis for irradiation embrittlement monitoring based on the so-called Master curve, see subsection 3.2.4. During these tests the effect of copper, nickel and phosphorus on the fracture toughness of the irradiated specimens was investigated. Copper and nickel are known to form precipitates under irradiation, which act as barriers to dislocation motion, thus raising the yield stress and lowering the ductility of the material, making it more prone to brittle fracture. This is called hardening embrittlement, [53]. Phosphorus segregates to grain boundaries under irradiation, and is suspected to weaken these, such that they may fail in a brittle manner, [53], which is called non-hardening embrittlement. The length scales of both processes are below the grain size and thus far removed from the macroscopic size of the component, but still their influence on macroscopic toughness can be considerable.
These examples show the relevance of modeling physics and mechanics over a wide range of length scales and with completely different methods as re-

gards the theoretical approach as well as its experimental verification. This challenge is well-recognized within the nuclear community and during the Sixth Framework Programme of EURATOM a major effort has been made to integrate the different parts of the investigations in one common tool:
The Integrated Project PERFECT (Prediction of Irradiation Damage Effect in reactor Components) was established with the objective to develop tools that simulate the consequences of irradiation damage across all length scales from the atomistic to that of test specimens and even reactor components, [1]. These tools were to be distributed among the european nuclear industry and used in a collective european exercise of component analysis relying on simulation to assess material behavior. Furthermore the project served to educate young researchers in the degradation of materials. The project was planned for 4 years beginning in January 2004 and was extended until the end of June 2008. The consortium initially consisted of 12 institutions and 16 universities from 11 countries in Europe. It was coordinated by EDF (France).
The present thesis was supported within PERFECT under the grant F16O-CT-2003-508840. It contributed to the work package 3, RPV mechanics. Its initial objective was to model dislocations with the help of partial differential equations derived from conservation laws for the Burgers vector, compare section 2.2. Thus it was to provide a link between the atomistic scale, where irradiation induced precipitation influences the dislocation mobility, and the macroscopic scale, where dislocation based plasticity affects the stress state in front of a crack, influencing the fracture behavior of the component. More precisely a quantitative description of the increase of fracture toughness with increasing temperature in the transition regime and a criterion for the DBT and the ductile-to-brittle transition temperature T_{DBT} applicable to ferritic steel were sought.
These objectives were met at least in part, though the picture that emerged is rather different from the usual elasticity based analysis and what was originally envisaged. In chapter 2 we first discuss the problem of fracture testing to obtain the framework to understand the following developments and describe the phenomena which can be discussed with the aid of the present models. We also give an overview of other approaches to the fracture problem. Then we introduce basic concepts from the theory of dislocations and discuss the standard elastic analysis of the stress fields of dislocations with respect to its applicability to the fracture problem. In chapter 3 we introduce two models describing the DBT. In the first section we describe cleavage fracture starting from a crack tip and influenced by a strongly simplified approximation of the dislocation dynamics around the crack. The resulting model gives an explicit criterion for the DBT and the temperature

dependence of cleavage toughness. It explains the different levels of scatter found in the fracture toughness data in different temperature regimes. The model can be justified with a stress intensity based approach due to Hart [80], but the qualitative conclusions following from it are actually valid more generally and therefore more relevant than the derivation. We discuss the problems when trying to apply our first model to the DBT in steel. Due to the shortcomings of this first approach, the second section contains a model that can also deal with fracture processes starting in the strongly loaded zone close to the main crack tip but not directly at the main crack. We introduce a method to account for dislocation shielding in an approximate manner, which can be applied to crack or notch stress fields of very general kinds and compute the relevant functions explicitly for a tractable example.
Again we obtain the temperature dependence of fracture toughness, but there is no specific criterion for the DBT based on properties of the material, while a criterion based on the geometry of the material can be given. This is not entirely unexpected, as effects like notch-brittleness are known from experiments. Additionally, we can incorporate failure processes starting at arbitrary sites close to the main crack. As in the first model we find different levels of scatter at different temperatures to be expected in the toughness data. A number of qualitative features from the experiments, which are puzzling from a conventional perspective can be explained by our model. A particular example of its usefulness is the nontrivial discussion of the so-called Master curve hypothesis for the temperature dependence of fracture toughness under irradiation. According to the present author's knowledge this is the first place, where a direct connection between dislocation dynamics and this hypothesis is established. Furthermore we can derive expressions for the correlation of yield stress increase and the temperature shift of the transition regime under irradiation, while explaining at the same time, that these properties need not correlate as functions of temperature. Additionally, we describe the rate dependence of the temperature range of the transition and discuss some related issues. Chapter 4 gives an analogy between the physics of the DBT in mechanics and superconductivity, which motivates some of the viewpoints advanced in this thesis.

Chapter 2

Basic facts in fracture and plasticity

In this chapter we shall introduce the framework to understand our contribution to the research on fracture and the DBT. We begin by discussing which phenomena we want to describe in section 2.1. This will be followed by an overview of a number of approaches to these phenomena in the literature. Afterwards we introduce the concepts from the theory of plasticity and dislocations we shall need later on and discuss the usual elastic analysis of the stress and strain fields of dislocations with the application to fracture problems in mind.

2.1 Experimental results about the DBT

This thesis deals with mathematical modeling of mechanical properties of materials applied in large macroscopic structures and we shall discuss their assessment now. The information sought is related to three different types of behavior: In the regime of low stresses the material behaves elastically, which means it deforms reversibly depending on the applied stress. At higher stresses it begins to react irreversibly, either by deformation or fracture.
In order to carry out meaningful modeling, we must discuss relevant experimental results first. The experimental setup is designed according to the intended purpose, which may be an assessment of elasticity, plasticity or fracture. The simplest test of interest here is a uniaxial tensile test at constant strain rate of a dog bone specimen, depicted schematically in Figure 2.1. The applied load and elongation are measured during the test and used in connection with the specimen geometry to determine a stress-strain-curve, see Figure 2.2. This curve often shows the effects of elastic and plastic defor-

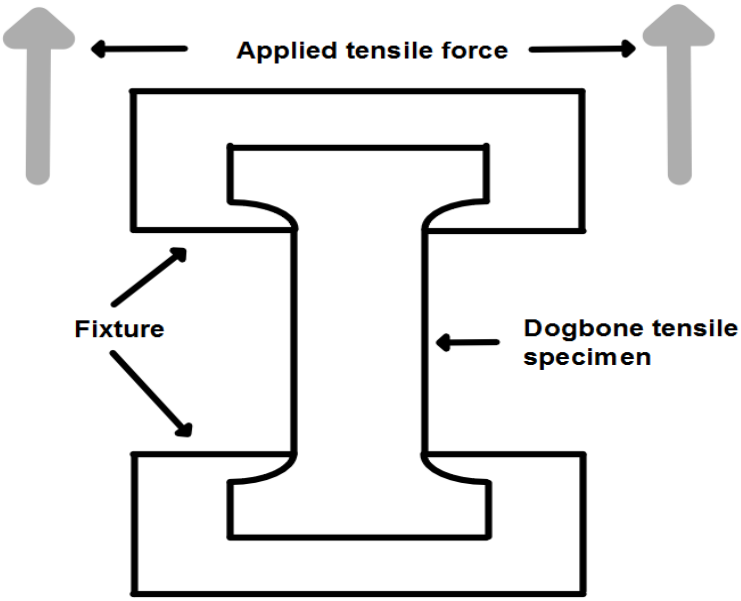

Figure 2.1: Schematic drawing of a uniaxial tensile test using a dog bone specimen.

mation before final failure at room temperature for the relevant types of steel. From the stress-strain curve one obtains the elastic modulus by the initial slope of the curve. One important quantity to describe the plastic behavior is the yield stress, which characterizes the onset of plasticity. Its definition depends of the particular kind of deformation behavior of the specimen. If the initial plastic deformation in the specimen is localized in Lüders bands, one may take the level of the corresponding stress plateau. If the plateau is absent, one usually takes the stress at a specified small amount of plastic strain, i.e. a small but significant deviation from the initial linear behavior. Furthermore one might wish to determine the ultimate tensile strength, i.e. the maximum value of stress when necking sets in, corresponding to the maximum in the stress-strain-curve, or the strain hardening exponent in the plastic part of the true stress-true strain curve. We will only utilize elastic properties and the yield stress, so we will not discuss these quantities here, though we will return to the interpretation of plastic deformation in chapter 4.

It is difficult to obtain quantitative fracture data from such a simple tensile test due to several related factors. First of all, if the material is ductile, it will deform plastically and the final failure sets in by necking, a plastic instability leading to local thinning of the specimen. The notch due to neck-

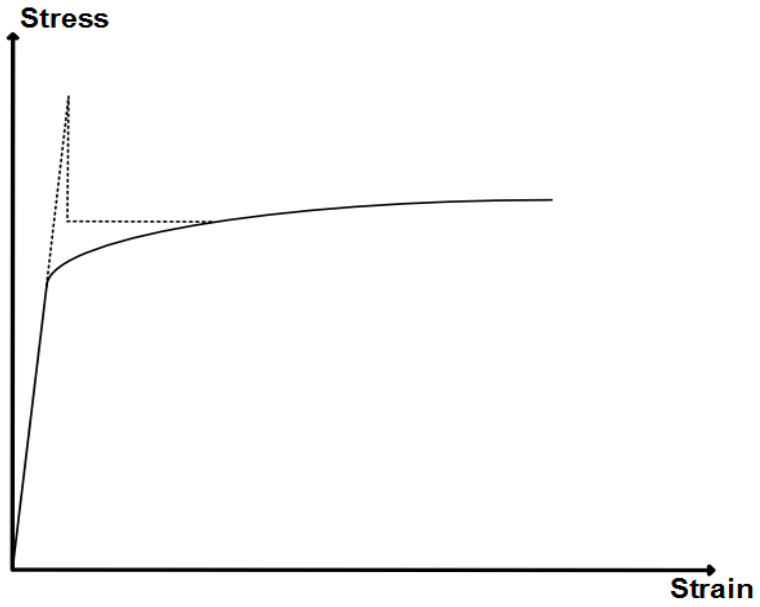

Figure 2.2: Schematic representation of a stress-strain-curve. The solid line corresponds to homogeneous deformation throughout the specimen, while the plateau in the dashed line is typically observed while waves of localized deformation, so-called Lüders bands, travel through the specimen.

ing causes an inhomogeneous stress state close to the neck, which can not be controlled or determined during the test, so it is not possible to relate the load at failure/fracture to a well-defined stress at the notch. Also the specimen might be so ductile, that no (brittle) fracture is observed at all. Furthermore brittle fracture is strongly influenced by defects, so the worst defects in a specimen must be known before a test. The solution to both problems when determining the brittle fracture strength by some measure is to introduce the major defect in a specimen beforehand by some sort of pre-cracking. If the pre-crack is severe enough it will be the worst flaw in the specimen and careful procedures allow to control its length and shape.
The influence of the length and shape of the defect is due to the increasing stress concentration associated with a longer and sharper crack. Some approaches have already been pointed out in chapter 1. The method of stress intensity factors will be discussed at the beginning of section 3.1. Stress intensity factors are one of the major concepts in fracture mechanics and were introduced by Irwin, [97], as relevant to fracture analysis. They form the basis of a large part of linear elastic fracture mechanics (LEFM), which is covered in many textbooks on the subject, [5, 33, 66, 74, 99, 122]. As already

remarked in chapter 1, the book of Neuber, [151], covers the analysis of general notches. It is interesting for its critique of the simplifications inherent in the use of stress intensity factors and fracture mechanics. On the other hand, there have been recent advances in the mathematical analysis of the boundary value problems for the equations of linear elasticity to be discussed in section 3.1, which justify the use of stress intensity factors for sharp cracks, [199]. We shall keep in mind, that notches or cracks can influence fracture behavior in two ways: They can reduce the fracture resistance and they can lead to brittle behavior even if unnotched samples of a certain material show ductile fracture.

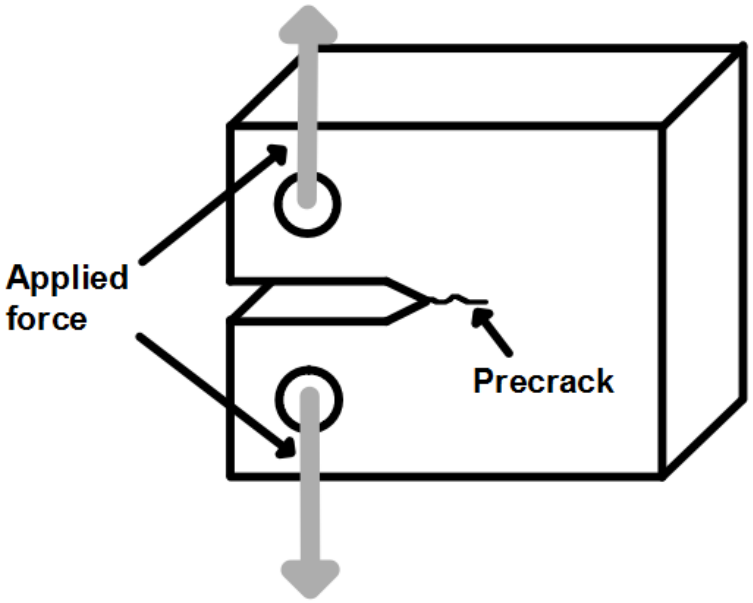

Figure 2.3: Schematic drawing of a fracture toughness test using a compact tension specimen.

The two most important types of test for brittle fracture are the traditional Charpy-V-notch test, and the modern fracture toughness test based on fracture mechanics. In the Charpy test, [13], a heavy pendulum dropped from a specified height hits a notched bar specimen and the energy absorbed is determined from the height the pendulum achieves after collision. It is known that the results from Charpy and fracture toughness tests are difficult to correlate, [40, 169], still a number of general characteristics are similar. We will refer mainly to fracture toughness tests, but in the literature on the DBT one often finds impact energies determined by Charpy tests. A schematic

drawing of a fracture toughness test is shown in Figure 2.3. Fracture toughness testing has been standardized in the USA during the 60th and 70th of the preceding century and the ASTM (American Society for Testing and Materials) has issued a number of standards on toughness testing under different conditions. These standards, such as E 399-90 and E 1820-01 and more specifically E 1921-97, [2], are constantly revised and updated. Standard E 1921-97 is about the reference temperature T_0 which is determined in connection with the so-called Master curve approach, [232, 234], to cleavage fracture in the transition regime to be discussed later on. Details about fracture toughness testing can also be found in the textbooks [5] and [99].
The most important relation we will describe in this thesis is the relation between the so-called fracture toughness K_{exp} measuring the resistance of a material to cleavage fracture and the temperature T. We will discuss its dependence on the external strain rate, geometry and plastic properties.
Fracture toughness versus temperature data are documented in numerous sources, see [43, 61, 137, 161, 167, 168, 169, 234] to name just a few. Mostly though, the data displayed has already been processed using a particular model, as in Figure 2.4, where the Master Curve procedure was used to determine T_0, see section 3.2.4. As the horizontal axis displays $T - T_0$ instead of T itself, the temperature shift in the data from irradiated specimens is not directly visible. The curves in Figure 2.4 were determined in [34] using the Master Curve approach, they are not of interest for our own model. The data points are representative of the general behavior of toughness versus temperature in steel though, and its reproduction is authorized, therefore it was chosen here. The source of the data shown in Figure 2.4 is [34, p. 148, Figure 3] in [61].
The main characteristics of general toughness versus temperature data displaying a DBT are the following:

1. At low temperatures, the toughness is comparatively low, almost constant and the scatter in the data is small. In this temperature range fracture occurs solely by cleavage.

2. In a certain temperature range the toughness values as well as their scatter increase strongly. In this regime the fracture mode changes from cleavage to ductile fracture.

3. Depending on the material and the conditions, cleavage and ductile crack extension may both occur in the same specimen in the transition regime.

4. At higher temperatures ductile fracture occurs exclusively. The scatter in the data as well as the temperature change are smaller.

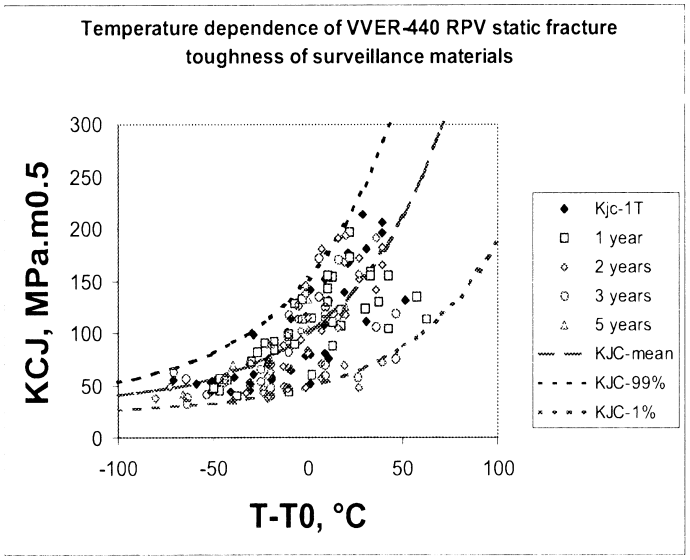

Figure 2.4: Toughness versus temperature data for different states of irradiation of reactor pressure vessel surveillance material processed by the Master Curve approach, taken from [34, p. 148, Figure 3].

5. The transition range shifts to higher temperatures when increasing the external strain rate, [233].

6. Larger specimens tend to be more prone to cleavage, [5, 167].

7. A specimen may embrittle due to notches and cracks.

8. A strong triaxiality of the stress state at a notch tip may induce brittle behavior.

9. The transition regime shifts to higher temperatures under neutron irradiation, [232].

10. The shape of the Toughness-temperature relationship is claimed to be universal for different states of irradiation (Master curve, [232]).

11. There is a correlation between the irradiation-induced increase of the yield stress and shift of the transition regime, while the correlation between yield stress decrease and toughness increase as functions of temperature is not as clear, [26, 43, 104, 153, 154, 187].

12. The fracture initiation sites are temperature dependent, [5, 182].
13. The upper shelf toughness in the ductile regime decreases under irradiation.

We will not discuss ductile fracture in this thesis, so the fourth and last point will not receive much attention, but we will offer at least qualitative explanations for all the others. As the DBT has been an issue in science and technology for several decades, numerous attempts to describe and understand it have been made and the literature on the subject is vast. Any attempt at a comprehensive literature survey here is bound to be incomplete and misleading, so we will focus on the sources relevant to the authors understanding of the subject and those which may help to clarify the choices made by the author when modeling the DBT.
A paper about the DBT and embrittlement in fusion reactor alloys, [155], summarizes the understanding of the problem in 2003 as follows: "... The BDT models also vary greatly in what they assume and the underlying physics they treat. Differences include static versus propagating cracks, straight versus ledged crack fronts, various sources and configurations of crack tip dislocations, various atomic and dislocation configurations leading to crack trapping, equilibrium versus dynamic dislocation positions, alternative constitutive-velocity laws and ways to couple to continuum plasticity, and a variety of stress field states (et cetera). Thus, the various BDT models predict such a wide range of results so that they can be picked, or adjusted, to be consistent with almost any experimental observation; and there is no clear and obvious basis to choose one over another. There are also a number of unresolved questions that have not even been adressed. ... In summary, there are no rigorous models of $K_\mu(T)$."
The authors of [155] use BDT for our DBT and $K_\mu(T)$ for our $K_{\exp}(T)$. Indeed, we shall assume as little as possible about the underlying physics in chapter 3 to come to some conclusions, which may be applied quite generally. They will necessarily be mostly of a qualitative nature, but some quantitative results about the Master curve approach can be given, see section 3.2. Before turning to dislocation plasticity, we will discuss some topics relevant in research connected with the DBT.
The effect of the microstructure of steels on fracture properties and the DBT will not be investigated in detail, but it can be accounted for in several ways within the model devised for steel, see section 3.2. This approach is due to the generic nature of the DBT, which occurs in a wide range of materials and different microstructures, compare chapter 4 and the problem already mentioned to choose the right model for the microstructure. Information about the influence of the microstructure on mechanical properties of steel

and its metallurgical control can be found in [90] and [145].
When analyzing the toughness of a material one of the major considerations to be made is usually which type of microscopic process governs cleavage fracture. One aspect of this is, whether cleavage occurs by transgranular fracture through the individual grains or intergranular fracture along grain boundaries. Intergranular failure by collapsing grain boundary cohesion may occur due to irradiation-induced migration of contaminating elements like phosphorus to the grain boundaries, [61, 98], and is thus relevant for nuclear applications. Phosphorus segregation leads to non-hardening embrittlement, but can usually be mitigated by controlling the concentration of the contaminent, [145]. It will not be considered here, also because its mechanism is not related to dislocation dynamics.
Transgranular fracture is affected significantly by the grain size, where a smaller grain size leads to a tougher (fracture resistant) as well as stronger (deformation resistant) material. This rare concurrent occurence of both phenomena motivates procedures to refine the grain size in steels, [145]. While these expensive processes significantly improve the mechanical properties, they do not eliminate the DBT, so a true understanding of it must still be found. A main reason not to consider the grain size explicitly later on is that it does not change significantly under irradiation while the macroscopic mechanical properties do, so something else must be responsible for irradiation-induced embrittlement.
Another aspect of micromechanics of crack extension in steels is, whether the mechanism implies fracture to be controlled by usually plasticity-induced nucleation of microcracks, or the propagation of an existing crack into the surrounding material. The governing mechanism is reported to differ for different kinds of steel, [46, 167]. While the early theory of Stroh, [200, 202], implies nucleation control and does not predict an effect of the tensile stress at the notch root on fracture, such an influence was found in experiments, [46, 111]. Following this and reported evidence of cracked carbides, [129, 140], many authors in the engineering literature favored models based on crack extension from cracked carbides governed by some type of tensile stress criterion, [46, 76, 167, 234] or an extension of this, [137], at least for ferritic steels for nuclear applications. This approach is not unanimously accepted, though. Deformation twins were reported in connection with cleavage already in the fifties, [24], and again by [29, 225, 226]. Furthermore [43, 118, 117] object to fractured secondary particles as cleavage initiators.
In section 3.2 we present a model based on a critical tensile stress criterion, but shall leave the operating micromechanism of cleavage open. It is then still possible to derive a number of relevant experimental observations. The range of applicability of these conclusions must remain open for such a simplified

approach, but it is at least useful to show that many qualitative results of the experiments do not necessarily depend on the details of the microstructure. This lends credibility to the approach as such, as sources like [232, 234] claim the applicability of their macroscopic modeling suggestions to a wide class of ferritic steels without considering the microstructure in detail, which is at least partly corroborated by our model of section 3.2. If such an empirical observation holds, the corresponding explanation should also not involve those details, or better yet explain why they are irrelevant under the given circumstances.

One of the main considerations for nuclear applications is modeling the influence of irradiation on the mechanical properties. Non-hardening embrittlement due to phosphorus segregation has already been discussed, we will focus on hardening embrittlement. This term stems from the fact, that neutron irradiation damage goes along with an increase in yield stress and a corresponding decrease in toughness and increase of the T_{DBT}. Especially in old pressure vessels, copper is a major cause of concern, as it forms precipitates under irradiation, which act as obstacles to dislocation motion and thereby inhibit plastic flow, leading to hardening as well as embrittlement, [61]. If these obstacles are incoherent, they do not carry a long-range stress field and can therefore be surmounted by thermal activation. Therefore there is a straightforward approach to modeling this type of irradiation damage by an increase in the effective energy barrier of an Arrhenius-law used to describe the temperature dependence of the dislocation velocity, see equation (3.28). This will indeed allow to explain significant observations, so we will be content with it. Further details about the DBT in steel will be discussed in the corresponding sections of the following chapters.

Up to now the literature discussed in this section deals with fracture in steel. But the DBT is a phenomenon observed in many different materials, see [69, 87, 177, 178, 180]. Furthermore steel is unsuited to understand the connection between the microscopic processes and macroscopic observations as its microstructure is too complicated for simple connections between them. Therefore physicists investigating this connection often use single crystals of pure materials for their experiments. Thus it is no surprise, that systematic experimental investigations concerning the microscopic origin of the DBT began with silicon, [198], which was already then obtainable in nearly perfect single crystals and in which the dislocation dynamics was well understood, [32]. While the decisive influence of plastic deformation due to dislocations on the DBT is taken for granted in these researches, there has been a long debate, whether dislocation nucleation or mobility controles the DBT and about the suitability of various models, [6, 8, 68, 86, 143, 180]. The model introduced in Section 3.2 is based on mobility, but it is not the aim of the

author to contribute to this debate. Indeed the evidence discussed at the end of section 3.1 seems to indicate, that no general answer applicable to all materials nor even to a single material arises, as geometry and deformation history have an influence on the outcome of experiments.

2.2 Elements of dislocations and plasticity

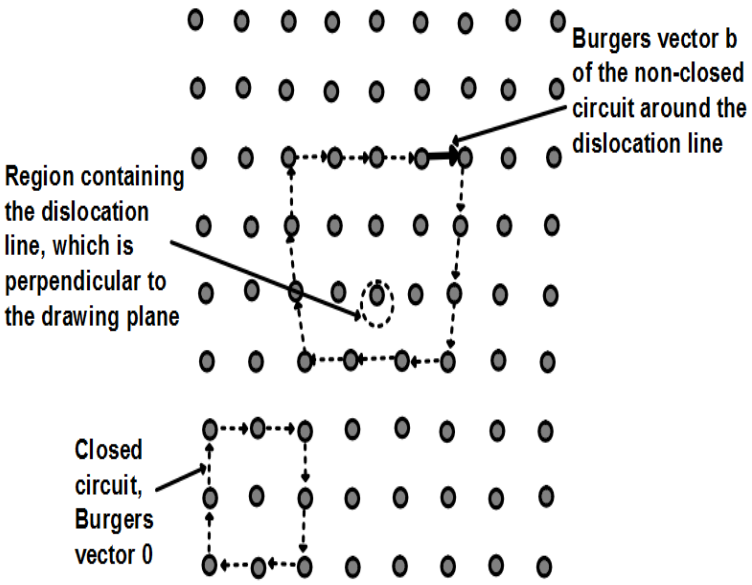

Figure 2.5: An edge dislocation inside a crystal structure. The dislocation line is at the end of the extra half-plane in the crystal. The geometric meaning of the Burgers vector is depicted.

As the experimental results on mechanical failure of metals and other materials indicate, the absence of cleavage is concurrent with strong irreversible deformation, known as plasticity. This section introduces dislocations, the line-defects in crystal structures which cause plasticity. They have already been mentioned in section 1.1 and their introduction to explain the substancial discrepancy between theoretical and observed strength was discussed. We will have no need to use the specific structure of dislocations, so we shall keep their discussion short and refer the readers to the textbooks and monographs on the subject such as [44, 88, 93, 116, 147, 172, 238, 257].
Figure 2.5 contains a 2-d drawing of an edge dislocation in a crystal structure. The edge dislocation can be envisaged as insertion of an extra half

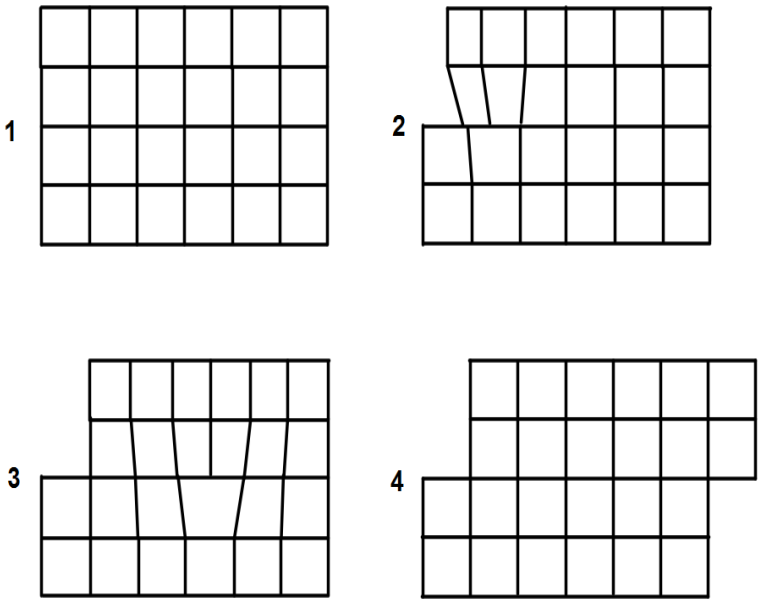

Figure 2.6: The effect of an edge dislocation moving through a crystal from left to right.

plane into the crystal. The boundary of this half plane constitutes the dislocation line, in its vicinity the strain due to the extra half plane is strongest. The dislocation is characterized by its line vector, specifying the direction of the dislocation line and the so-called Burgers vector $\mathbf{b}$, named for the author of [35, 36]. For a dislocation in a crystal lattice the Burgers vector is defined as the segment between the starting point and endpoint of a loop around the dislocation line, which would be closed if the dislocation line were absent, see Figure 2.5. It is a measure of the strength of the dislocation, the displacement it causes for the atoms surrounding it. Dislocations may also be defined in a continuous medium, in which case the Burgers vector is the integral of the strain along a closed circuit around the dislocation line, again measuring the displacement due to the line. Dislocation line vector and Burgers vector are perpendicular for an edge dislocation. Figure 2.6 is a sketch of the effect of moving an edge of the type shown in Figure 2.5 through a crystal from left to right. It shows how the material above the glide plane containing line vector and Burgers vector of the edge is displaced during the movement of the dislocation with respect to the material below. This visualizes the irreversible deformation associated with a moving dislocation, the source of plasticity.

The screw dislocation is another type of dislocation, which looks like a spi-

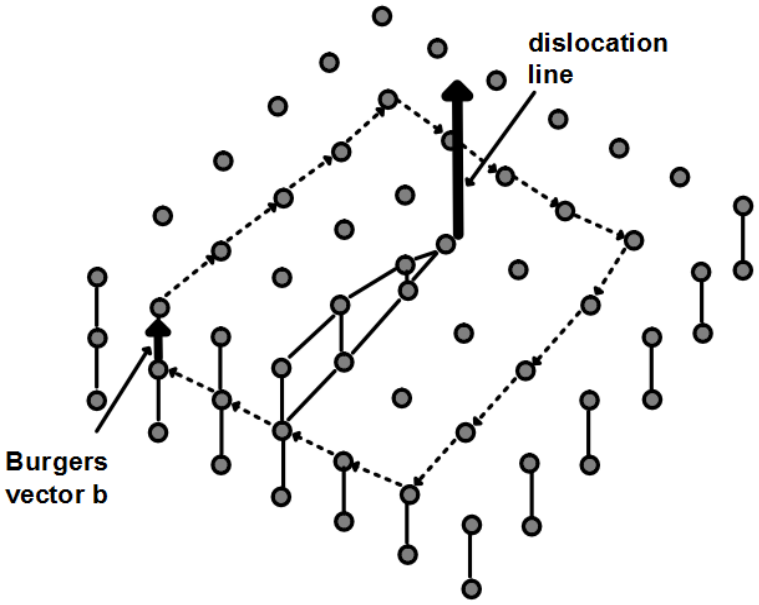

Figure 2.7: A screw dislocation in a crystal.

ral staircase. Its line vector and Burgers vector are parallel, see Figure 2.7. There are also mixed forms of the two and a comprehensive discussion of related defects in crystals and continua is contained in [147] amongst others. For the model of section 2.3 it is of major importance, that a dislocation can not end in the crystal, but only on its surface. Its Burgers vector is conserved, and if it does not touch a surface, then it forms a closed loop. A proof of this well-known fact is given for example in [147, section 1.2.2]. The conservation of the Burgers vector allows to establish corresponding conservation laws for the density of moving dislocations, see section 2.3.

As a crystal containing a dislocation is deformed, dislocations carry stress and strain fields. We shall cite the result of the usual elastic analysis from [147] for the purpose of illustration:

Dislocations are treated as lines of singularity in an otherwise perfectly elastic medium. The first problem to be solved is usually that of the stress and strain field surrounding a straight dislocation. Take the edge dislocation from Figure 2.5 and introduce cylindrical coordinates, such that the dislocation line coincides with the z-axis, while the Burgers vector is directed along the x-axis: $\mathbf{b} = (b, 0, 0)$. Then the plane strain elastic equilibrium equations in the plane orthogonal to the dislocation line can be solved using the stress

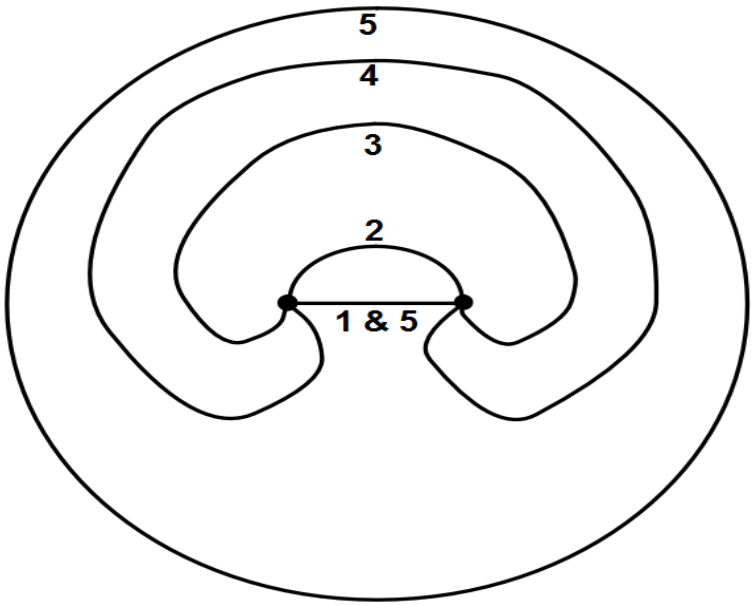

Figure 2.8: Drawing of the Frank-Read-mechanism of dislocation multiplication. If an external stress is applied, the initially straight dislocation line pinned between two obstacles, 1, begins to bow out, 2. This process continues while the external stress is strong enough, 3, 4, until a situation is reached, where different parts of the dislocation unite, forming a circle and a new pinned straight line, 5, which may serve as source for another dislocation.

function

$$\chi_e \;=\; -\,\frac{b\mu}{2\pi(1-\nu)}\, r \sin\varphi \ln\left(\frac{r}{b}\right), \tag{2.1}$$

which obeys the biharmonic equation except for the singular line $r = 0$ in the absence of body forces. Here (r, φ, z) are the usual cylindrical coordinates, μ is the shear modulus and ν the Poisson ratio of lateral contraction. From the stress function, which fulfills a role similar to the potential in electrostatics, the components of stress in the plane orthogonal to z may be derived by differentiating twice, the formulas are given in cylindrical coordinates by

$$\sigma_{rr} \;=\; \frac{1}{r}\,\partial_r\chi_e \;+\; \frac{1}{r^2}\partial_{\varphi\varphi}\chi_e\,;\; \sigma_{r\varphi} \;=\; -\partial_r\left(\frac{1}{r}\partial_\varphi\chi_e\right)\;;\; \sigma_{\varphi\varphi} \;=\; \partial_{rr}\chi_e\,, \tag{2.2}$$

and lead to

$$\begin{aligned} \sigma_{rr} &= \frac{-b\mu}{2\pi(1-\nu)}\frac{\sin\varphi}{r}, \\ \sigma_{r\varphi} &= \frac{b\mu}{2\pi(1-\nu)}\frac{\cos\varphi}{r}, \\ \sigma_{\varphi\varphi} &= \frac{-b\mu}{2\pi(1-\nu)}\frac{\sin\varphi}{r}, \end{aligned} \tag{2.3}$$

for the stresses and

$$\begin{aligned} e_{rr} &= \frac{-b(1-2\nu)}{4\pi(1-\nu)}\frac{\sin\varphi}{r}, \\ e_{r\varphi} &= \frac{b}{4\pi(1-\nu)}\frac{\cos\varphi}{r}, \\ e_{\varphi\varphi} &= \frac{-b(1-2\nu)}{4\pi(1-\nu)}\frac{\sin\varphi}{r}, \end{aligned} \tag{2.4}$$

for the strains. The theory of the screw dislocation is simpler, as it involves only pure shear strains, [147]. For a straight screw along the z-axis the only non-vanishing components of stress and strain are given by:

$$\begin{aligned} \sigma_{\varphi z} &= \frac{b\mu}{2\pi r}, \\ e_{\varphi z} &= \frac{b}{4\pi r}. \end{aligned} \tag{2.5}$$

The main characteristic of these solutions we wish to point out is the proportionality of stresses and strains to the reciprocal of the distance from the dislocation line in the case of edge dislocations as well as screw dislocations. Any text on dislocations usually starts the elastic analysis with those examples, while Burgers's more sophisticated solution of a rectangular dislocation in an infinite three-dimensional solid, [35, 36] is treated only in more comprehensive texts like [88, 147], though not as detailed. Still, there is one point in Burgers's analysis, which is not prominently discussed in the standard treatments and this absence has a strong bearing on the understanding of the subject by the author:
Dislocations in actual crystals often stem from so-called Frank-Read-sources or similar objects, see Figure 2.8 and the cited monographs. Therefore real-world dislocations are often found as loops of different sizes rather than straight dislocations ranging from one end of the crystal to the other. Burgers's solution for the loop shows that stresses and therefore strains surrounding a loop do not have the simple $1/r$-behavior of straight dislocations. This

should not be surprising, as the $1/r$-dependence of the stresses is a consequence of the plane strain stress function χ obeying a biharmonic equation, independent of any structure of dislocations in crystals. This consequence is apparent in cartesian coordinates, where the tensile stress components are obtained from χ by

$$\sigma_{xx} = \partial_{xx}\chi\,;\ \sigma_{yy} = \partial_{yy}\chi\,. \tag{2.6}$$

As χ obeys the biharmonic equation, the sum of the tensile stresses is consequently subject to the Laplace equation, forcing the divergence of the gradient field of the sum of the stress components to vanish. From the rotational symmetry of the configuration, we obtain the $1/r$-dependence of the sum of the tensile stress components, as the circumference of a circle around the dislocation line scales proportional to r. This is the well-known behavior of a point charge in two dimensions, while we may surround any finite dislocation loop in three dimensions by a sphere of finite radius, so one would expect a stronger decrease of the field for such a configuration, which is indeed the case, [35].
This discrepancy shows that the solution to the elastic equations for a straight dislocation (of infinite length!) could be misleading actually. Yet the author has not found a comprehensive discussion of this problem in the literature, so it does not seem to have a significant bearing on the description of macroscopic inelastic behavior in terms of the properties of dislocations. Therefore the author does not rely on a detailed elastic analysis for his explanation of the DBT or even dislocation dynamics itself in chapter 3. We will use some parts of it only when convenient.
Permanent plastic deformation is caused by moving dislocations and in real crystals the crystal structure has a significant influence on the way dislocations move. In polycrystals dislocation motion is impeded by grain boundaries, but the deformation behavior also depends on the crystal structure in single crystals. Dislocation motion is often observed on special crystallographic planes. Edge dislocations can move easily by glide only in their glide plane given by the line vector and Burgers vector. Perpendicular to it they must move by climb, which involves diffusion of vacancies or interstitials and therefore operates only at sufficiently elevated temperatures. Screw dislocations do not have a distinguished glide plane, but in ferritic steels, where iron is in the body centered cubic phase, their movement is impeded by the complicated structure of the dislocation core and thermal activation is needed to move them, see [194] and [7] for details of the theory. Therefore they determine the deformation behavior at low temperatures.

2.3 The influence of plasticity on fracture

As indicated in chapter 1, plasticity influences the fracture behavior and can cause a transition from brittle to ductile behavior. There are many different models for this phenomenon, but the basic idea is the same in most and may be made clear by the analogy to a Faraday-cage from chapter 1: Plastic deformation changes the shape of the specimen in a mechanical test permanently in such a way, that local stress concentrations are reduced, so brittle fracture is impeded. Due to the limited amount of plasticity, this effect is not as complete as in a Faraday-cage, but it can cause the DBT for example, so its influence on fracture is indeed very significant.
Early models for this shielding effect in terms of dislocations were given by Dugdale, [52] and Bilby, Cottrell and Swindon, [25]. The description of shielding is based on the interaction of the stress field of the crack with the fields of dislocations. This drew the attention of applied mathematicians early on, [10, 11] and a detailed equilibrium theory of crack tip shielding by dislocations was developed, [128]. Depending on the sign of the dislocations, i.e. the direction of their Burgers vector, they were termed shielding and anti-shielding, but as simulations, [136] and the analogy to electrodynamics suggest, these names are actually misleading. It depends on the relative position of dislocation and crack, the direction of the applied forces and the position along the crack front, whether a dislocation is shielding or anti-shielding.
Detailed investigations of loaded cracks by electron microscopy were performed already in the early 80th, [156, 157], and confirmed enhanced dislocation activity close to the crack tip. Often a dislocation free zone (DFZ) developed in the immediate vicinity, which is crossed by dislocations instantaneously, which then arrange in an inverse pile up (high dislocation density close to the crack tip, gradually lower density further away). The DFZ is thus due to a kinetic effect. A number of theoretical investigations on crack tip shielding have since been published, but we will only give a short description of the modified version, [82], of the dislocation dynamics equations introduced by Hähner and Stamm in [77], as we will use them in section 3.1.
Consider Figure 3.1, showing a plane structure under the so-called anti-plane shear load. In this configuration dislocations of both signs are assumed to move in glide planes parallel to the crack, so there is no movement in the y-direction. The idea is to use the conservation of the Burgers vector, see section 2.2, to write down balance laws for the dislocation densities of both

signs, ρ^+, ρ^-:

$$\begin{aligned} \partial_t \rho^+ + \partial_x (u\rho^+) &= \frac{q}{2} u\rho - 2hu\rho^+\rho^- \,, \\ \partial_t \rho^- - \partial_x (u\rho^-) &= \frac{q}{2} u\rho - 2hu\rho^+\rho^- \,. \end{aligned} \tag{2.7}$$

On the left hand side we only need to differentiate with respect to x, as the dislocations move only in this direction. The terms have the following meaning: u is the dislocation velocity of one sign, hence the negative sign on the left hand side of the second equation, the first term on the right hand side models dislocation multiplication and the second dislocation annihilation, with corresponding parameters q and h determining the effectiveness of these mechanisms. Multiplication is assumed proportional to the existing total dislocation density $\rho = \rho^+ + \rho^-$ and always contributes to the densities of both signs simultaneously because the Burgers vector has to be conserved. Annihilation carries a negative sign as expected and is proportional to the product of both densities.
As we are interested in local changes of the net dislocation density, because the net density determines the effective long range stress field, we introduce the net dislocation density $\alpha = \rho^+ - \rho^-$ and obtain the following equation by adding and subtracting equations (2.7) from each other:

$$\begin{aligned} \partial_t \rho + \partial_x (u\alpha) &= qu\rho - hu\left(\rho^2 - \alpha^2\right) \,, \\ \partial_t \alpha + \partial_x (u\rho) &= 0 \,. \end{aligned} \tag{2.8}$$

The second equation of this system is used in section 3.1. While the system (2.8) formally looks like an ordinary system of balance laws, there is an important difference to many standard hyperbolic conservation laws known in applied mathematics: The dislocation velocity depends on the local value of the driving stress, which is a quantity determined *non-locally*, so the local dislocation velocity itself cannot be determined from local data only. Indeed, special systems of this type do not develop shocks during simulations, [207, 209], as the backstresses between dislocations keep them apart.

Chapter 3

Two models for the DBT

This chapter contains the author's contributions to modeling the DBT from a rather classical perspective, where we try to understand the DBT by describing the effect of moving dislocations on the stress distribution inside a specimen. We deviate significantly from the numerous similar attempts by shifting the emphasis from the analysis of the elastic stress fields to identifying basic ideas applicable under more general circumstances. This already reflects the insight gained from a completely different perspective discussed in chapter 4.
The emphasis is on the model introduced in section 3.2, but a simpler approach is discussed in the first section, as it allows to understand the typical scatter in experiments in the transition regime in a very simple way. Furthermore it is instructive to discuss its shortcomings to motivate the developments in section 3.2.

3.1 A stress intensity based approach

The model considered in this section is based on the so-called stress intensity, as introduced by Irwin, [97]. Irwin solved a certain boundary value problem for the stresses in a plate containing a crack, see Figure 3.1, by a series expansion around the tip of the crack of the form

$$\sigma(r,\phi) \;=\; \frac{k}{\sqrt{r}} f(\phi) + g(r,\phi)\,, \tag{3.1}$$

where f and g are bounded functions, such that the periodic function f depends only on ϕ, while k is constant. Here (r,ϕ) are polar coordinates, where the origin coincides with the tip of the crack. Irwin argued, that because of the boundedness of g, the behavior of the material close to the crack is governed by the magnitude of k. A certain constant multiple of k is called the

stress intensity at the crack tip. He postulated that unstable cleavage fracture would commence, if a critical value k_{cl} of k would be reached. The value k_{cl} is called the cleavage fracture toughness.
The expansion (3.1) has the advantage, that it can be obtained quite easily in practice, compared to the usually elaborate methods based on the energy method of Griffith, [71]. Therefore it was soon widely used and became the fundamental concept of the then new linear elastic fracture mechanics (LEFM), see section 2.1. The procedures of LEFM were criticized by Neuber, [151], because the expansion (3.1) can not be obtained by analyzing the stresses in the vicinity of a notch tip and then taking the limit of vanishing notch root radius. Neuber finds that the general analysis contains more parameters relevant to the stress state than (3.1), so that (3.1) is an undue simplification of reality. On the other hand the elliptic boundary problems of elasticity for regions containing sharp cracks were rigorously analysed and the validity of an expansion of the form (3.1) established for such regions during the last decades, see [199] and the references cited there.
We shall adopt the stress intensity approach in this section in order to obtain the initial value problem (3.12). We do so mainly to allow a simple motivation, rather than derivation, of this initial value problem. The point about it is not the quantitative result, but its simple structure and the general qualitative conclusions we can draw from it. Quantitative investigations will be given based on the model of the following section.
For simplicity, consider a structure containing a crack which is loaded in anti-plane shear, we assume translational symmetry along the crack front and thereby reduce the problem to the plane x-y-configuration depicted in Figure 3.1. The following treatment of the stress intensity is based on the work of Hart and Wu, [80, 245], and we will adopt their conventions for the numerical factors in the definition of the stress intensity, which differ slightly from (3.1). It is customary to indicate the anti-plane shear loading stress intensity factor by a subscript as K_{III}, but we will suppress this, as we have no need to discuss general loading here. We will describe a fracture test, where a specimen is loaded externally by a constant shear rate, beginning at time $t = 0$, when the external shear stress τ_{ext} is zero. It is assumed, that the crack propagates by cleavage in an unstable manner, if the effective shear stress intensity factor at the crack tip K_{eff} reaches the cleavage toughness K_{cl} of the material. To decide when K_{cl} is reached, we need a model for the stress distribution inside the structure and shall take the simplest relevant one: As discussed in chapter 2, the effect of notches and cracks is of paramount importance for fracture, so in this section we will ignore any contributions to the stress field except for the stress intensity term. The idea is to write down and solve a differential equation for the time evolution of

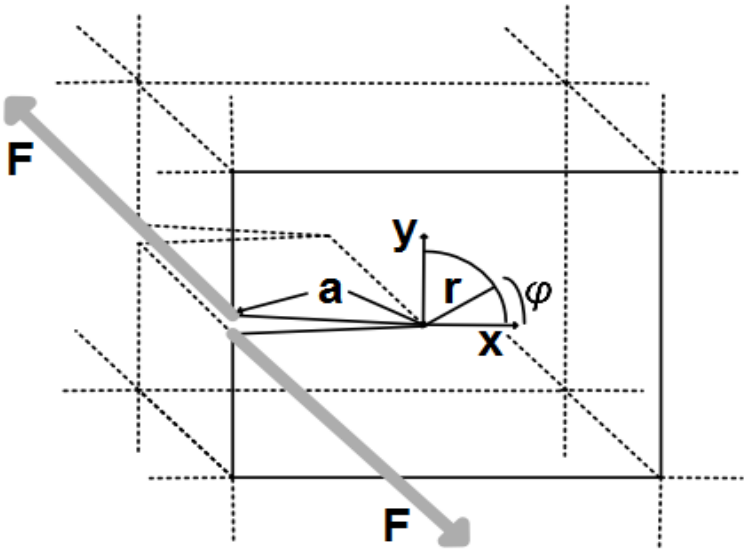

Figure 3.1: A crack in a structure under load by point forces F in anti-plane shear (Mode III) at a distance a from the crack tip. The structure is extended to infinity in all directions.

the effective stress intensity at the crack tip, which governs the fracture behavior. In this section, it is not the aim to derive a valid quantitative model in a rigorous way. We shall be content with a qualitative discussion of our results and discuss implications and shortcomings afterwards.
The effective stress intensity factor K_{eff} contains two contributions. One derives from the external loading. The second contribution is due to local plastic deformation around the crack tip induced by the strongly increasing stress level close to the crack. There are formulas for this internal contribution K_{int} to the stress intensity due to Hart and Wu, [80, 245]. The anti-plane shear case, [80], is chosen for simplicity as the principal conclusions to be drawn in this section remain valid for the other loading modes, too. Except for Hart's basic formula for anti-plane shear loads, we shall not adopt the approach of Hart and Wu.
The effective stress intensity at the crack tip K_{eff} is given by:

$$K_{\text{eff}} \;=\; K_{\text{ext}} + K_{\text{int}} \;\Rightarrow\; \dot{K}_{\text{eff}} \;=\; \dot{K}_{\text{ext}} + \dot{K}_{\text{int}} \tag{3.2}$$

where the dot denotes differentiation with respect to time t, while $\dot{K}_{\text{ext}}$ and $\dot{K}_{\text{int}}$ are to be determined. At a constant external shear rate, the external stress increases linearly according to Hooke's Law, $\tau_{\text{ext}} = \mu\gamma$, where μ is the

shear modulus and γ is the applied shear. From the applied forces the external stress intensity factor K_{ext} is determined, [77], in keeping with equation (3.4) below for a single notch configuration:

$$K_{\text{ext}} \;=\; \sqrt{2\pi a}\tau_{\text{ext}} \;\Rightarrow\; \dot{K}_{\text{ext}} \;=\; \sqrt{2\pi a}\mu\dot{\gamma}\,, \tag{3.3}$$

where a is the distance from the tip of an infinite crack of concentrated forces F applied at the crack faces leading to an external shear stress τ_{ext}, see Figure 3.1. The shear stress is applied at a constant rate $\dot{\gamma}$, we have $\dot{\tau}_{\text{ext}} = \mu\dot{\gamma}$. In the discussion of the internal contribution K_{int} we ignore the finite specimen dimensions by using the equation of Hart, which was derived for an infinite crack. This means we are limited to small-scale yielding, so the size of the plastic zone remains small compared to other relevant dimensions, such as width and depth of the specimen and the crack length. An extensive discussion of small-scale yielding in fracture is given in [33]. The equation for the contribution of plasticity to the stress intensity factor derived by Hart in [80] is

$$K_{\text{int}}(t) \;=\; -\frac{\mu b}{\sqrt{2\pi}}\int_{p.z.} dA\frac{\alpha(z,t)}{\sqrt{z}}\,, \tag{3.4}$$

where μ is the shear modulus already introduced, b is the absolute value of Burgers vector and α the net dislocation density from (2.8). Hart uses the complex quantity $z = x + iy$, even though he is not considering a line integral. The integral is a plane integral taken over the whole specimen, but as significant contributions to α develop only in the plastic zone close to the crack, shortened to p. z. in (3.4) above, the area of integration is effectively finite. We differentiate under the integral sign to obtain

$$\dot{K}_{\text{int}}(t) \;=\; -\frac{\mu b}{\sqrt{2\pi}}\int_{p.z.} dA\frac{\partial_t\alpha(z,t)}{\sqrt{z}}\,. \tag{3.5}$$

The partial time derivative in this expression may be replaced by the spatial derivative of the dislocation flux $u\rho$ according to equation (2.8). Therefore we have to give a reasonable approximation for the dislocation velocity and the total dislocation density to compute $\dot{K}_{\text{int}}(t)$. The evaluation of the resulting integral was given already in [82, 83] and we will not repeat it here, as it is not relevant to our reasoning. We will only explain the physical principles of the approximation and give the results.

To get a simple equation, we assume the following dynamics: Any dislocation close to the crack tip moves with infinite velocity to the position x_p, where the effective stress intensity at the crack tip is assumed to cause the material to flow. Hence x_p is the boundary of the plastic zone, determined by the

yield stress (critical resolved shear stress) τ_y here:

$$\tau = \frac{K_{\text{eff}}}{\sqrt{2\pi r}} \Rightarrow \sqrt{x_p} = \frac{K_{\text{eff}}}{\sqrt{2\pi}\,\tau_y}\,. \tag{3.6}$$

Neglecting the effects of the finite dislocation velocity inside the plastic zone is rationalized by the following conception: There are essentially three different regimes for the dislocation velocity, [112, 148, 195]. At very high stresses dislocations travel at a significant fraction of the velocity of sound, which is an upper bound for the dislocation velocity. The effect is analogous to the well-known relativistic effect of mass increase of objects travelling at a significant fraction of the speed of light. Then there is an intermediate regime of stresses, where the dislocations travel slower but still in a continuous manner and the dependence of the dislocation velocity on the external stress is approximately linear (the so-called dislocation drag regime). If the stresses on the dislocations are too low to surmount the strongest barriers impeding dislocation motion, thermal activation is needed to move dislocations. Dislocation slip becomes discontinuous and a steep gradient of the dislocation velocity as a function of applied stress develops. In the vicinity of a crack in a structure which is loaded externally at a level below the yield stress, all these regimes will be present because of the singular crack tip field and the moderate external load, see Figure 3.2. In this case the dislocations will reach the area near the boundary of the plastic zone almost instantly (meaning in a very short time compared to the time it takes to load the specimen to fracture in a standard quasi-static test), as the diameter of the plastic zone will only be a fraction of a millimeter in lengths, while the velocities in the relativistic and drag regimes are high. The strong velocity gradient in the thermally activated regime means the distance over which a dislocation is essentially stopped is very short, which is a justification to use such a model, at least if interactions between dislocations are ignored. These interactions will cause the area over which the dislocations are stopped to be spread out, but while this will certainly modify the value of the plastic strain rate, the qualitative theory we will develop is not altered at all, therefore we will adopt this approach for now.
Estimates of the plastic zone size based on the external stress intensity and yield stress are common in the literature, [237], our choice of the effective stress intensity is motivated by the interesting equation it leads to. We will comment on this at the end of this section.
Due to the drastic velocity law, we may now evaluate the integral in (3.5) by

$$\frac{\sqrt{x_p}\dot{\gamma}_y}{b}\,, \tag{3.7}$$

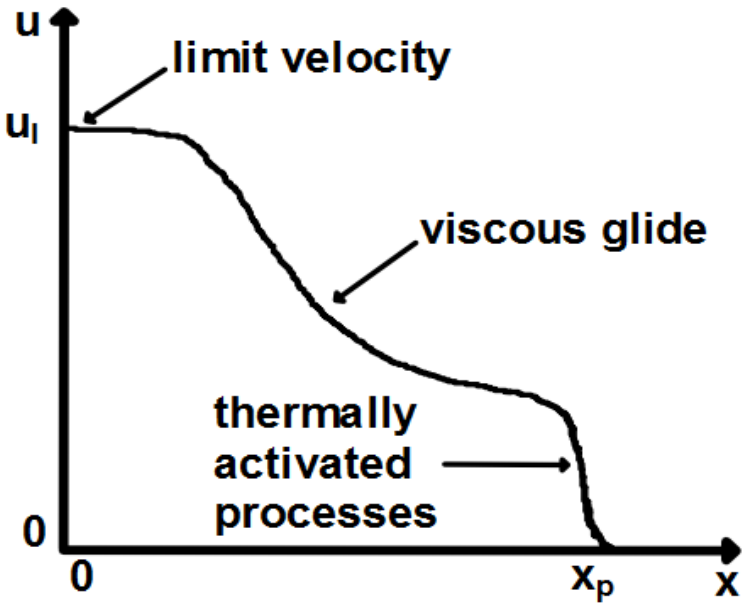

Figure 3.2: Schematic drawing of the different velocity regimes inside the plastic zone. u_l is the limiting velocity, given by the velocity of sound. In a narrow region close to the boundary x_p of the plastic zone thermal activation is needed to drive the dislocations forward and the dislocation velocity drops essentially to zero.

where the plastic strain rate $\dot{\gamma}_y$ is given by

$$\dot{\gamma}_y \;:=\; -\,b \int_{-\pi}^{\pi} \cos\frac{3\theta}{2}\,\partial_r\, u\rho(x_p,\theta)d\theta\,. \tag{3.8}$$

The computations leading from (3.5) to (3.8) are discussed in [82, 83]. The integral in (3.8) has got a simple physical interpretation: It is the product of the absolute value of the Burgers vector and the number of new dislocations arriving at each instant on the boundary of the plastic zone. The radial component of the boundary we have put at x_p, while the contribution of every dislocation to K_{int} is weighted due to the exact geometric position it arrives at this boundary and hence contains the angle θ. It is by no means easy to compute $\dot{\gamma}_y$ exactly, because it will depend on any processes related to dislocation creation and multiplication, which have to be properly accounted for. It is possible to integrate the contribution of crack tip dislocation emission: It will simply enlarge the number of dislocations on the boundary. For our purposes it is enough to think of $\dot{\gamma}_y$ as a time-indepentent increasing function of temperature; the validity of this will be discussed later. From (3.5), (3.6)

and (3.7) we obtain a simple term for the rate of the plastic contribution to the effective stress intensity:

$$\dot{K}_{\text{int}} \;=\; -\frac{\mu\dot{\gamma}_y}{2\pi\tau_y}K_{\text{eff}}\,. \tag{3.9}$$

Equations (3.2), (3.3) and (3.9) are combined to give a very simple equation to model the DBT:

$$\dot{K}_{\text{eff}} \;=\; \sqrt{2\pi a}\mu\dot{\gamma} \;-\; \frac{\mu\dot{\gamma}_y}{2\pi\tau_y}K_{\text{eff}}\,. \tag{3.10}$$

The next step is to introduce relevant non-dimensional variables. As we are interested in the question of K_{eff} reaching the cleavage toughness, we choose:

$$K \;:=\; \frac{K_{\text{eff}}}{K_{\text{cl}}};\; \hat{t} \;:=\; \frac{\sqrt{2\pi a}\mu}{K_{\text{cl}}}\,\dot{\gamma}\,t\,, \tag{3.11}$$

where the new time scale $\hat{t}$ is chosen, such that the cleavage toughness is reached under fully elastic conditions for $\hat{t} \;=\; 1$, if we start loading the specimen at $\hat{t} \;=\; 0$ and $K \;=\; 0$. The corresponding initial value problem in the new variables is

$$\frac{dK}{d\hat{t}} \;=\; 1-\beta K;\; K(0)=0\,, \tag{3.12}$$

where

$$\beta \;=\; \frac{\sqrt{x_{\text{cl}}}\dot{\gamma}_y}{2\pi\sqrt{a}\dot{\gamma}}\,;\; x_{\text{cl}} \;=\; \frac{K_{\text{cl}}^2}{2\pi\tau_y^2}\,, \tag{3.13}$$

so that x_{cl} is the plastic zone size when the cleavage toughness is reached. This is indeed an initial value problem for an inhomogeneous linear first order ordinary differential equation with constant coefficients. We are not interested in the usual form of the solution $K(t)$, but want to know the time t_{cl} it takes to reach the cleavage toughness, given a certain value of the parameter β. We do not use the hat for the new time-scale here anymore. Performing the elementary integration and putting $K \;=\; 1$ afterwards, we obtain $t_{\text{cl}} \;:=\; t(1;\beta)$ as function of β:

$$t_{\text{cl}} \;=\; \frac{-1}{\beta}\ln\left(1-\beta\right). \tag{3.14}$$

The simple computation of $t(1;\beta)$, leading to an elementary function is an important advantage when discussing the implications for fracture, see the discussion following the outline of the quantitative consequences.

Assuming that unstable cleavage commences as soon as the critical condition $K = 1$ is reached, we can relate $t_{\rm cl}$ and the apparent macroscopic fracture toughness in a simple way: For fully elastic conditions $\beta = 0$ holds and so the apparent cleavage fracture toughness equals $K_{\rm cl}$, corresponding to $t_{\rm cl} = t_{el} = 1$. For non-vanishing plasticity, $\beta \neq 0, t_{\rm cl} = t_{\rm pl}$ will be larger according to equation (3.14). The apparent load-displacement curve will remain linear for a longer time, leading to a higher apparent fracture toughness $K_{\rm exp}$, in agreement with the usual procedures to determine the fracture toughness, [5]. Therefore we may take the right hand side of (3.14) as the ratio between the cleavage fracture toughness under fully elastic conditions and the apparent cleavage fracture toughness according to our model as function of β:

$$\frac{K_{\rm exp}}{K_{\rm cl}} = \frac{-1}{\beta} \ln(1-\beta) . \tag{3.15}$$

This function is the solid line plotted in Figure 3.3. The curve has a number of desirable features when trying to understand the DBT, compare section 2.1. First of all, there is a DBT: If $\beta < 1$, cleavage will commence at a

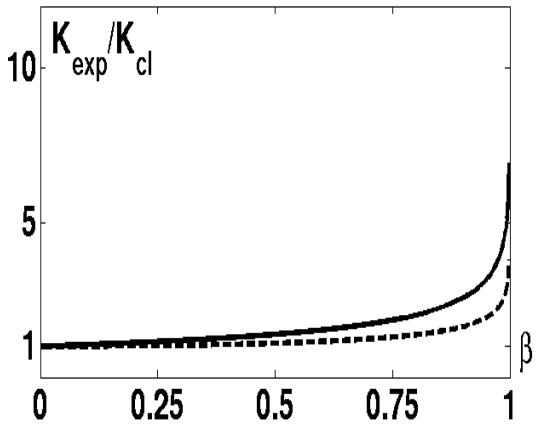

Figure 3.3: The function $K_{\rm exp}/K_{\rm cl}$ of the parameter β. The solid curve corresponds to the right hand side $1 - \beta K$ in (3.12), see (3.15), the dashed curve to $1 - (\beta K)^2$, see (3.20).

certain time $t_{\rm cl}$, which grows with β but remains finite, while for $\beta \geq 1$ there is no cleavage fracture, because the critical condition $K = 1$ is not reached. We can thus write down a criterion for the DBT as $\beta = 1$, which implies

$$\dot{\gamma}_{y,crit} = \frac{\left(\sqrt{2\pi}\right)^3 \sqrt{a}\tau_y \dot{\gamma}}{K_{\rm cl}} \tag{3.16}$$

by equation (3.13). The plastic strain rate $\dot{\gamma}_{y,crit}$ necessary for the DBT shows desirable dependencies on several important quantities: It increases with increasing external strain/loading rate, crack length and yield stress and decreases with increasing elastic cleavage fracture toughness. We will have to discuss the dependency on the yield stress, though. To compute the apparent cleavage toughness as a function of temperature, we need to model the temperature dependence of $\dot{\gamma}_y$ and shall use an Arrhenius-law:

$$\dot{\gamma}_y \;=\; \nu_{pz} \exp\left(-\frac{G}{kT}\right). \tag{3.17}$$

One should keep in mind that we are actually counting dislocations throughout the plastic zone boundary, so the pre-exponential factor ν_{pz} is essentially a free parameter at this point, while k is the Boltzmann-constant and G the activation enthalpy, in which we do not yet account for contributions of irradiation damage or external stress, see section 3.2 for a more general approach. With the help of the Arrhenius-law and equation (3.16) we can compute the ductile-brittle-transition temperature T_{DBT}. It is given by

$$T_{\mathrm{DBT}} \;=\; \frac{G}{k \,\ln\left(\frac{\nu_{pz}}{\nu_{min}}\right)}, \tag{3.18}$$

with ν_{min} being defined in the next inequality (3.19). If the argument of the logarithm is smaller than 1, there is no finite positive transition temperature, reflecting the fact that the pre-exponential factor must fulfill the inequality

$$\nu_{pz} \;>\; \nu_{min} \;:=\; \frac{\left(\sqrt{2\pi}\right)^3 \sqrt{a}\tau_y\dot{\gamma}}{K_{\mathrm{cl}}} \tag{3.19}$$

for a transition to occur at all, corresponding to the DBT criterion (3.16). Figure 3.4 shows the resulting curves of the temperature dependence of $K_{\mathrm{exp}}/K_{\mathrm{cl}}$ for three different strain rates using the parameter values of Table 3.1.

The main reason to discuss the model problem (3.12) is the resulting dependence of K_{exp} on β. It is strongly nonlinear and singular, even though the underlying equation is linear and very simple. This explains the different regimes in the experimental toughness values versus temperature. At low temperatures below the transition regime plastic deformation is strongly impeded and the plastic deformation rate $\dot{\gamma}_y$ is so small, that β is significantly smaller than its critical value. In this case fracture toughness is only slightly dependent on plastic deformation and its value and the scatter in the

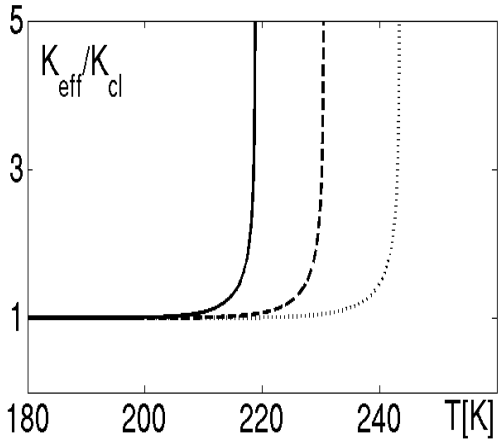

Figure 3.4: The predicted apparent fracture toughness for the data from Table 3.1 and the shear rates $\dot{\gamma} = 10^{-6}\,1/\mathrm{s}$ (solid), $\dot{\gamma} = 10^{-5}\,1/\mathrm{s}$ (dashed) and $\dot{\gamma} = 10^{-4}\,1/\mathrm{s}$ (dotted).

crack length a	10^{-4} m
activation enthalpy G	0.86 eV
pre-exponential factor ν_{pz}	10^{15} 1/s
critical resolved shear stress τ_y	200 MPa
inverse Boltzmann-constant $1/k$	11605 K / eV
cleavage fracture toughness K_{cl}	20 MPa$\sqrt{\mathrm{m}}$

Table 3.1: The parameters used for Figure 3.4.

experimental data remain small and approximately the same over a significant temperature range (corresponding to the lower shelf in experiments). This provides a justification to choose an empirical toughness value from the lower shelf as representative of the elastic cleavage toughness even if some plastic flow is present, which is fortunate as lower shelf values are usually not available for arbitrarily low temperatures. At higher temperatures in the transition regime the contribution of plasticity to the apparent fracture toughness becomes appreciable and the increase in absolute value is accompanied by a strongly increasing sensitivity of the fracture response to changes in β and hence plastic deformation near the critical value $\beta = 1$. Therefore the increasing apparent toughness along with the strong scatter in the transition regime are easily explained as well as the occurence of cleavage in the

presense of considerable plastic flow. Furthermore one can account for the deformation rate by its influence on β, leading to embrittlement for higher strain rates.
To the best of the authors' knowledge, this is the simplest model showing the aforementioned features. After several decades of modeling the DBT there are of course many far more detailed models available and two examples of those with a similar formal approach resulting in $K(t)$-curves are discussed in [30, 132, 133] based on analytical considerations and in [207, 209] based on 2-d simulations. The former model discusses different plastic instabilities in its framework and the latter consists of a simple but carefully implemented model based on stress intensities. Both do not give $t(K;\beta)$-relations or discuss their relevance, but remain with the $K(t;\beta)$-dependence, which is more readily available in those models. Therefore they do not contain a detailed discussion of the nature of scatter in the transition regime and the lower shelf, both of which are straight forward in the model introduced here. The author also knows of no other place, where these issues are discussed with the help of explicit $t(K;\beta)$-relations, though they are certainly available implicitly in any serious DBT-model based on dislocation dynamics. One obstacle might have been, that the $t(K;\beta)$-relations are not always functions as in our simple approach, indeed in both models cited above $t(K;\beta)$ is multi-valued in general.
It is of high relevance to the foregoing analysis, that the qualitative behavior explained is clearly not limited to a model problem like (3.12). The reason for the different regimes of the fracture response to plastic flow is the existence of a zero of the right hand side of the differential equation (3.12), thus a purely qualitative observation not depending on the quantitative details of the derivation. This zero corresponds to a certain critical value of K given by $K = 1/\beta$, so it depends on the parameter β. If the parameter is such that the critical value of K gives a K_{eff} close to the cleavage toughness, small changes in β will have strong effects on the fracture response, while if K_{eff} of the critical point is far removed from K_{cl}, the fracture response to plasticity is negligible. A simple estimation of the resulting integral when separating variables shows these qualitative conclusions to be true for equations whose right hand side is of the type $1 - f(\beta K)$ with $f(1) = 1$ and $f(x) \leq x$ for $x \leq 1$. To illustrate this point, Figure 3.3 depicts the curves $K_{\text{exp}}/K_{\text{cl}}(\beta)$ for the right hand sides $1 - (\beta K)^n, n = 1, 2$ of the initial value problem of type (3.12). For $n = 1$, this solution is given in equation (3.15), while for $n = 2$, the solution is

$$\frac{K_{\text{exp}}}{K_{\text{cl}}} = \frac{1}{\beta} \operatorname{arctanh}(\beta)\,. \tag{3.20}$$

It is clear, that many other models based on differential equations with right hand sides of the type $1-f(\ldots)$, where $f(\ldots)$ depends on a set of parameters to be specified, will show similar behavior, even if their solutions can not be estimated in terms of the right hand side $1-\beta K$.
The conclusions about the qualitative properties of the fracture response to plasticity drawn from the solution of (3.12) will thus remain true for a large class of more realistic models and if we consider the DBT to be caused by plastic deformation and hence dislocation motion, we should expect the experimental observations reported on the toughness properties and their scatter on the lower shelf and in the transition regime. Indeed some comments in [68] show, that there is considerable scatter in the T_{DBT}-data in silicon single crystals. In [68] the authors warn to attribute the characteristics of the DBT in silicon to the mobility of dislocations without careful prior investigation of the origin and nature of this scatter. This points to the relevance of a careful analysis of the fracture response to plastic flow in the transition regime in steels also, without attributing the scatter solely to the distribution of some types of secondary particles or other defects, compare section 3.2.
While the philosophy of the model to describe the transition by a competition of two terms, one from the external load and one from plasticity, seems reasonable, allows to describe the DBT and to understand a number of the salient experimental observations, the simple model introduced suffers from some serious drawbacks. These drawbacks will now be discussed.
The first point of concern regards the approximation chosen for the size of the plastic zone. We have related it to the effective stress intensity at the crack tip, while it is attributed to the external stress intensity in the literature, [237]. The analogy to the Faraday-cage in electrodynamics indeed hints at the external stresses to govern the plastic zone size: The charge carriers always move to the boundary of the electric conductor, even though the field inside is zero, hence it does not constitute the driving force. Because of these concerns we will not base the driving force for plasticity on the stress intensity at the crack tip in the more realistic approach of the next section.
While the expression (3.13) captures many qualitative dependencies of the apparent fracture toughness on other parameters and toughness increases with the size of the plastic zone, the dependence of the critical rate on τ_y is introduced by our approximation of the plastic zone size. The resulting assertion, that an increasing yield stress leads to more brittle behavior is not at variance with the facts, but the correlation between these quantities is not as simple as might be inferred from (3.13), see section 3.2. The more general model in section 3.2 will offer a different viewpoint. A convincing and representative example for the role of an increasing plastic zone size in the DBT is given in [198, Figures 8,9] for silicon.

The second is again due to the relation between the stress intensity factor and the approximation of the plastic zone size. The approximation (3.6) considers only the singular term of the expansion around the crack tip. As the model is adapted to small-scale yielding, the plastic zone size must be small compared to any other relevant specimen dimension. The specimen boundary must be at such a distance, that the contribution of this singular term to the stress level at the boundary is not necessarily dominating. As we have to account for external stresses which are at least a significant fraction of the yield stress of the material, the yield stress may therefore be reached quite far from the crack tip and correspondingly the plastic zone may be of considerable size. Therefore it is not clear, whether the singular term of the expansion of the stress field at the crack tip is the only relevant one to understand the dynamics inside the complete plastic zone. Such considerations are relevant to the comparison of experimental results about the DBT in silicon for two different specimen types, as shown in [31]. Furthermore the simulation [207, 209] indicates the important role of the dislocations throughout the plastic zone, because their backstresses govern the number of dislocations nucleated inside the plastic zone available for further shielding, emphasizing the importance of the dynamics far removed from the crack tip. Hence it is not desirable to base a quantitative analysis solely on the singular term of the expansion of the stress field at the crack tip.

There are reasons, why the applicability of the stress intensity concept as such is doubtful. The first is related to the natural preference of the main crack tip as crack initiation site, because the stresses will always be largest at the tip due to the singularity of the elastic stress field. This is not confirmed by experiments in steel, where the failure sites are distributed throughout a certain area in front of the main crack, with a number of different concepts as to why certain sites are the origin of fracture, [22, 43, 137, 161, 185, 226, 231], compare 2.1. There is no simple justification for any of these failure sites in terms of an analysis based on uniaxial singular stress fields, as they do not give any natural criterion to exclude cleavage starting from the main crack where the stresses are highest due to the singularity.

Another concern about the stress intensity is its definition depending on a sharp crack. In reality the crack flanks open under load, which can be used to identify cracks in structures by only slight loads, [135]. While [12] reasons, that the tips still remain sharp, linear elasticity does not apply to the immediate vicinity of the crack tip anymore. Furthermore crack tips tend to blunt by plastic deformation, so an initially sharp crack develops a non-vanishing and increasing radius of curvature at its tip, diminishing the stress concentration. There are attempts to model blunting while retaining the stress intensity concept, [30, 133], but these did not convince the author.

We rather seek an analysis which can deal with the stress distribution in a structure directly, without introducing concepts related to singularities.
The last point we shall discuss is the meaning of $\dot{\gamma}_y$. We assumed it to depend on the temperature via an Arrhenius-law. While deformation by dislocations increases strongly with temperature in the thermally activated regime where the Arrhenius-law applies, we have to discuss the contribution from the whole plastic zone. Due to the box type velocity law chosen throughout the plastic zone, any dislocations created anywhere within the plastic zone contribute to the density accumulating at the boundary, whether they were already present and moved a certain distance by thermal activation or they were created by multiplication inside the plastic zone and travelled the decisive distance to the boundary during the relativistic or drag type zone. As this contribution by multiplication may be rather strong, [6, 8, 9, 100], the prevailing mechanism contributing to $\dot{\gamma}_y$ might not be described consistently by an Arrhenius-law in this model. Therefore some comments are given on this issue here:
The positive temperature dependence in a thermal activation regime can stem from an increasing size of the plastic zone due to the dislocations at its boundary moving away from the crack tip quickly enough, allowing more dislocations to be stored in the plastic zone. The beneficial effect of a high dislocation mobility controlling the DBT was found in many experimental studies of silicon, see [6, 31, 32, 68, 85, 198] and references given in these, claimed to be of central importance in many cases, [177, 179], and corroborated by recent simulations for iron and tungsten, [207, 209], among many other examples. Our simplified model in this section is inconsistent with this, but in some cases one might argue for the DBT to be controlled by thermally activated dislocation emission from a crack tip, first studied in detail in [175]. Numerous later studies increased the complexity of those models and analyzed many different configurations of homogeneous and heterogeneous nucleation, [15, 16, 42, 62, 173, 174, 189, 190, 191, 192, 193, 204, 205, 249, 250, 251, 256]. But emitted dislocations must still be transported away from the crack tip to enable further nucleation, so it can only be relevant as rate controlling step, if the barrier to dislocation glide is accordingly low. Nucleation at crack tips has been criticized for principle considerations in [181], while [6, 8, 68] argue for its relevance to a true understanding of the DBT. This is particularly interesting as both [6, 68] acknowledge and discuss the experimental investigations cited above, which emphasized the role of dislocation mobility.
Be that as it may, in the temperature regime considered plastic deformation in steels increases with temperature as is evident from a decreasing yield stress for example. The Arrhenius-law can then also be used to fit the experimental data, i.e. essentially as a model including free parameters. This

is all we need here.
The aforementioned analysis shows the need to improve the model leading to equation (3.12) in order to make quantitative predictions and to get rid of some non-desirable qualitative features of the model. While one could try to modify the model in this section to make it more realistic while retaining its salient features, we will adopt a rather different approach in the next section. It will not be based on stress intensities and can be applied to problems under general loading conditions.
One might question the inclusion of section 3.1, because we will adopt another model we claim to be more appropriate for steel and not containing the difficulties with the physical interpretation, but the model equation (3.12) serves its purpose as the presumably simplest in an entire class of models, which explain major qualitative features of the experimental $K_{\exp}(T)$-curves on the lower shelf and in the transition regime. The qualitative features do not depend on the details of the modeling and we can retain three main conclusions:

- The model gives a justification to use the lower shelf value of the experimentally determined fracture toughness as representative of the cleavage toughness in the absence of plasticity.

- The model explains the occurence of cleavage in the presence of significant plastic flow.

- The model explains the different levels of scatter on the lower shelf and in the transition regime and attributes the strong scatter in the transition regime to the cancelation of the competing contributions to the time evolution of the stress state, leading to a strong sensitivity to small disturbances, whatever be their nature.

Therefore it is very helpful to judge more complicated approaches, which should at least reproduce the qualitative conclusions from (3.12) and must furthermore show their superiority when applied to real world problems.

3.2 The DBT in ferritic steel

As mentioned before, there are a number of problems of the stress intensity based approach of the previous section. While some depend on the specific quantitative approximations within the model itself, some are due to the general nature of the stress intensity. Therefore we will develop a model by combining the ideas of Neuber concerning his so-called Mikrostützwirkung,

[151], with the experimental evidence gathered in [32, 142, 207, 209] using a simple but general method based on elementary concepts of dislocation mechanics in this section. First we will discuss the general approach and then treat an analytically solvable model in detail. As in the preceding section, we shall at first describe the approach and its consequences and only later discuss the simplifications inherent in it and their effects on the results.

3.2.1 The concepts underlying the general approach

We shall first discuss the type of information sought by our approach and the implications for reasonable simplifying assumptions.
We aim at a qualitative understanding of the DBT, which should at least explain the increase of toughness with temperature in the transition regime and the transition from brittle to ductile fracture, viewed as function of temperature and stress concentration and describe the scatter in the different regimes. This necessitates the presence of a temperature dependent quantity in our model as well as a prominent position of inhomogeneity of the stress field. Furthermore we wish to apply the model to ferritic steels, whose fracture depends on a critical value of the tensile stress near the notch root or crack tip, [47] and starts not necessarily at the notch root/crack tip itself, see the discussion at the end of section 3.1. We shall now combine these principal considerations with experimental observations to set up as simple a model as possible to assess the effect of moving dislocations on fracture.
For simplicity we will limit ourselves effectively to one dimension. We consider only the tensile stress component acting on a plane which contains the notch or crack. Under tensile load, its stress concentration is highest; see Figure 3.5 for the tensile loading mode. This stress component f is inhomogeneous and has a singularity at a certain position, which is at $x = 0$ in Figure 3.6. The singularity corresponds to a sharp crack, but as cracks under load do not remain infinitely sharp, we may cut it off at the position x_n in the elastic case, which represents the specimen boundary. In an elastic notch stress problem this position will usually be determined beforehand from the geometry to be described and be given in terms of certain shape parameters like length and curvature radius of the notch in question, [151], but as solving concrete notch stress problems is not our main interest, we will keep the discussion qualitative. We focus on the effect of a single notch or crack and therefore assume the stress component to be a function which decreases monotonically with increasing distance from the notch tip to the value at another external boundary. This assumption of monotonicity implies, that the maximum stress present in the elastic case is always at the position x_n and its magnitude is $f(x_n)$. In the elastic case we will thus as-

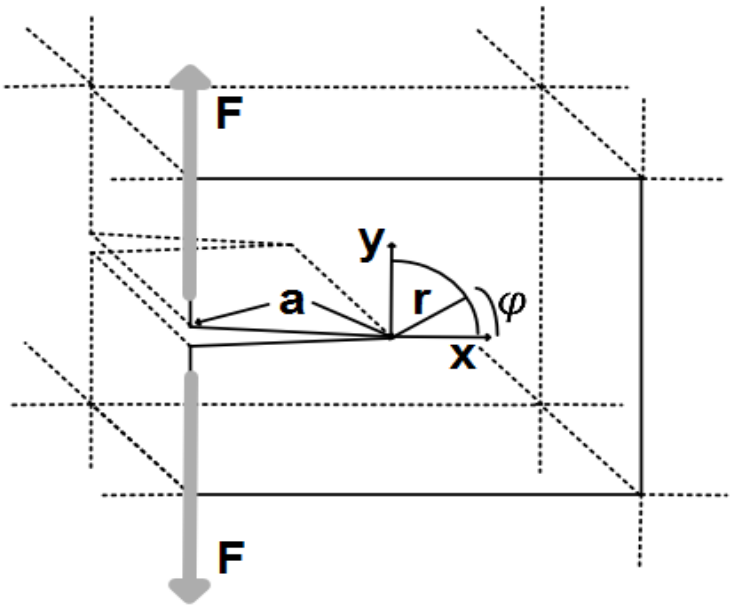

Figure 3.5: A crack in a structure under tensile load (Mode I) by point forces F.

sume, that unstable cleavage fracture commences, if the stress at x_n reaches the value σ_f, which is the case if the external stress in our model reaches the value $\sigma_f/f(x_n)$. In the elastic case in our model, the time until cleavage in a test at constant external strain rate, hence constant external loading rate, is therefore determined solely by the stress concentration factor $f(x_n)$. Effects of secondary stress concentrators practically relevant for example in welding will alter the relation between external stress and stress at the notch tip. This means that the stress level close to the crack tip will not even nearly decrease to the external stress, if only a region near the crack is considered. Due to those considerations, the function f representing the stress component in Figure 3.6 is subject to certain restrictions according to its meaning describing a component of the stress due to a notch or crack, which are given and discussed at the beginning of the following section.
As already mentioned, f and x_n will be affected by the geometry of the specimen. They can not be freely chosen for a concrete problem and are to be determined using elasticity theory. Unfortunately, neither the exact configuration nor a rigorous estimation of the difference between the actual structure and the idealization of the elastic model is usually available in practice. Hence it is essential, that the concepts introduced can be applied to quite general types of external loads and specimen shapes in two as well as

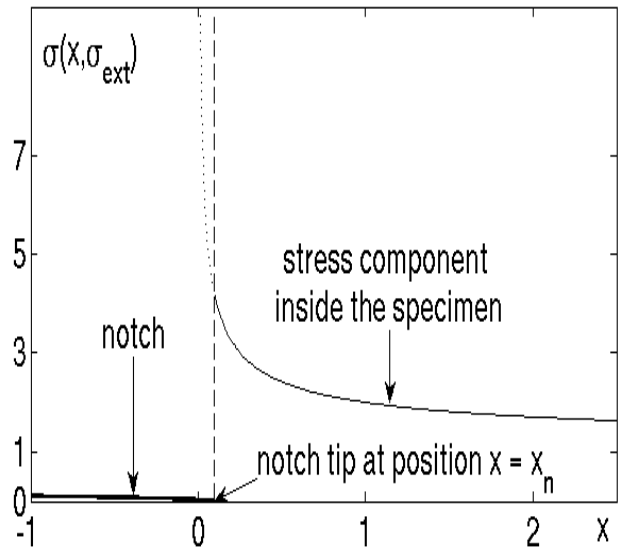

Figure 3.6: The shape of a singular component of the stress state at a notch, $f(x) = \frac{1}{\sqrt{x}} + 1$. The singular point $x = 0$ is outside the specimen, if the crack is not sharp/a notch is considered.

three dimensions. This will be possible, so we will choose our examples not because they correspond exactly to a specific solution of an elastic problem but such that they allow to do the necessary calculations for our approach in closed form, bringing out the salient features without unnecessary and distracting computational detail.
The problem of infinite stresses in linear elastic problems whose boundaries contain corners or cracks is already discussed in [240], where the principle concept which is prominent in Neuber's treatment is also announced: The stress is only defined with respect to a surface element and if we average it over a certain surface of finite extent, we will obtain meaningful values that always remain finite. Accordingly, Neuber introduced his concept of Mikrostützwirkung, which consists of giving a certain magnitude to the minimal surface element over which to average. He postulated this to be a material parameter, but we shall alter this interpretation to describe the effect of plasticity. The idea is that if such an effect exists, it is to be based on a physical mechanism and not to be postulated as material parameter beforehand. The physical mechanism we have in mind is the movement of dislocations under stress inside the specimen. The velocity of the dislocations given a certain stress level will be related to the size of the region in

which such an averaging process due to the stress field of the dislocations is effective.
According to these considerations, we take the dislocation velocity u to be given as a function $u(\sigma, T)$, where σ is the local value of the relevant tensile stress component for cleavage fracture and T is the temperature, thus introducing the relevant temperature dependent quantity in the model. The precise relationship between the dislocation velocity on the actual slip planes of the dislocations and the tensile stress in front of the notch is not of interest at this stage. It may be used to introduce effects of the triaxial stress state at the notch root though.
To fix the relationship between dislocation velocity and region of effective averaging we draw upon two things. Firstly, the experimental observations concerning silicon by [32, 142], which point to the relevance of dislocations following the rising stress level in a coherent manner. An increasing external stress leads to a moving local level of constant stress, see Figure 3.7. As

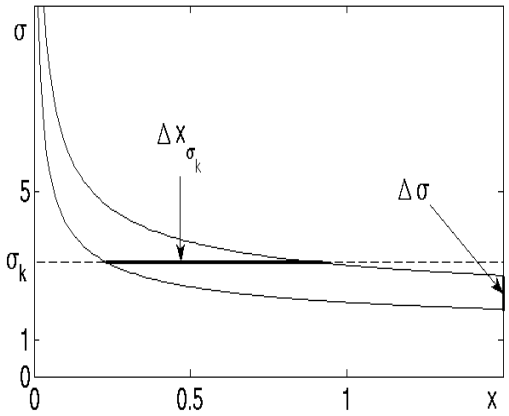

Figure 3.7: The definition of the stress level velocity $\dot{x}_{\sigma_k}$: The level of constant stress moves, if the external stress is changed, leading to the difference Δx_{σ_k} in a certain time interval Δt. We have $\Delta\sigma = \dot{\sigma}_{ext}\Delta t$, $\dot{x}_{\sigma_k} = \lim_{\Delta t \to 0} \Delta x_{\sigma_k}/\Delta t$.

the dislocation velocity is governed by the local stress, dislocations will either follow the level of local constant stress or the local stress will increase. Therefore we shall introduce the concept of stress level velocity, see Figure 3.7.
Secondly, the papers [207, 209] discuss a simple model for dislocation dynamics in the vicinity of a crack accounting for the 2-d interactions of straight

dislocations among themselves and an approximation of the elastic field in a notched bend specimen. In the specimen, which can initially be devoid of dislocations, a single dislocation source emits a dislocation at a certain local stress, which then travels away from the source. The stress at the source increases until the next dislocation is emitted and so on. The salient observation during the simulations for us is that the dislocations align in such a way, that each travels at about the same level of stress, [209, Figure 6a]. This result is intuitively appealing, because if the velocity is governed by the local stress, dislocations which do not move at a velocity that keeps the local stress level constant, will be slowed down by increasing back stresses from preceding dislocations further away from the crack tip if they are too fast, or accelerated by the increasing stress field of the crack tip and following dislocations relative to the preceding ones if they are too slow. This behavior is thus inherently stable and expected to be the rule for quite arbitrary stress-strain laws, as long as the dislocation velocity is governed by the local stress. A similar result on shielding dynamics is found in simulations reported by [31].

We shall use these observations from experiments and simulations to discard the detailed dislocation interactions. Especially in steel we may safely assume, that there are enough dislocations present such that they can keep a certain region at a certain stress level from a further increase of the stress. Furthermore we assume that the size of this region can be accounted for by the relation between dislocation velocity at a certain stress and the corresponding stress level velocity. We will derive a position x_k for each stress level at which those velocities coincide and apply this concept to fracture by postulating, that the stress concentration $f(x_f)$ at the position x_f corresponding to the cleavage fracture stress level σ_f determines the time until fracture in the cleavage regime.

The experimentally observed cleavage fracture resistance as function of temperature is thus related to the stress concentration at the boundary of the specimen $f(x_n)$ relevant in the elastic case and the temperature dependent stress concentration at the boundary of the shielded zone $f(x_f)$ relevant in the plastic case. For a fixed value σ_f of the fracture stress and a constant external loading rate, we use Hooke's law and the constant strain rate to determine the external stress at each instant and to relate the time to fracture t_{el} in the elastic regime and the time to fracture t_{pl} in the plastic regime to the local conditions as in section 3.1:

$$\dot{\sigma}_{ext}\, t_{el}\, f(x_n) \;=\; \sigma_f \;=\; \dot{\sigma}_{ext}\, t_{\mathrm{pl}}\, f(x_f) \tag{3.21}$$

is equivalent to

$$\frac{K_{\exp}}{K_{el}} = \frac{t_{\mathrm{pl}}}{t_{el}} = \frac{f(x_n)}{f(x_f)}. \tag{3.22}$$

Here, $K_{\exp}$ and K_{el} can not be interpreted as the usual fracture toughness, but as the fracture resistance is given in terms of toughness, we do not change the notation. The reader should still be aware of the different physical interpretation of the fracture resistance as given here. Of course the relation (3.22) is valid only, if x_f is inside the specimen. Otherwise the elastic value prevails, so there is no discernible influence of plasticity on fracture at low temperatures, as in section 3.1. The relation (3.22) can be directly generalized to a large class of more refined models.
Within the model there is no way to determine the relation between $f(x_n)$ and the experimental values of the cleavage toughness in the fully elastic regime, therefore this relation is to be determined from fracture tests at very low temperatures, where there is no significant plasticity and the predicted values of the fracture resistance are relative values again, just as in section 3.1. This is in the nature of things.
The criterion (3.22) differs from the one proposed in [84], since the local fracture stress instead of the yield stress is used to bound the region governing t_{pl}. This is more consistent with the expectation that an increasing local resistance to fracture leads to an increasing toughness. Furthermore the effects of plasticity are already accounted for by computing x_f and the introduction of the yield stress at this stage would be redundant. Many conclusions are qualitatively unaltered though, because the criteria in [84] and (3.22) have the same structure.

3.2.2 The general analytic procedure

We introduce the general procedure based on the considerations in the preceding subsection by focusing on the special case of linear elasticity and a constant external strain rate. In this case the introduction of nondimensional variables is particularly simple to follow. After the procedure has been elucidated in this simple case, we will give rigorous conditions for the existence and uniqueness of the key quantities of our approach and discuss some relevant examples.
In linear elasticity, the tensile notch/crack stress component σ_{yy}, see Figures 3.5 and 3.6, will be determined by an equation of the form

$$\sigma_{yy} = f(x)\,\dot{\sigma}_{\mathrm{ext}}\,t^*, \tag{3.23}$$

where $\dot{\sigma}_{ext}$ is the constant external strain rate, t^* is time, y refers to the coordinate system in Figure 3.5, and $f(x)$ is the stress component obtained

by solving the elastic boundary value problem. The equation is defined for all x inside the specimen, which is to the right of x_n in Figure 3.6. As the resulting dimension of the other variables on both sides of equation (3.23) is that of stress, f must already be a dimensionless quantity and x should also be dimensionless. The corresponding length scale of reference depends on the configuration in the problem at hand, see [151]. The proper choice is the crack length a, if the crack is short with respect to the other specimen dimensions, while it is the ligament length for long cracks. We will focus on the case of short cracks, so $x = x^*/a$, where x^* is the length given in meters or any other unit of length. In order to obtain a dimensionless equation we must introduce a reference stress. As we are concerned with fracture, one should choose the fracture stress of the material, if it were well-defined. We consider the fracture stress σ_f actually as only locally defined in steel, but we will simply estimate the material behavior by assigning presumed maxima and minima of the local values, thus computing the interesting quantities for two different values of σ_f. Deviding both sides of equation (3.23) by σ_f and introducing the dimensionless quantities

$$\sigma \;=\; \frac{\sigma_{yy}}{\sigma_f}\,; \qquad t \;=\; \frac{\dot{\sigma}_{\text{ext}}}{\sigma_f}\,t^*\,, \tag{3.24}$$

we obtain

$$\sigma \;=\; f(x)\,t\,. \tag{3.25}$$

Now consider Figures 3.6 and 3.7. If f is strictly monotonically decreasing and differentiable, the position x_{σ_k} of the stress level σ_k and its velocity $\dot{x}_{\sigma_k}$ are well-defined single valued functions of t. While x_{σ_k} is obtained from

$$\sigma_k \;=\; f(x_{\sigma_k})\,t \tag{3.26}$$

by inverting f, $\dot{x}_{\sigma_k}$ can be obtained from the same equation by implicit differentiation:

$$\dot{x}_{\sigma_k}(t) \;=\; -\,\frac{f(x_{\sigma_k}(t))}{f'(x_{\sigma_k}(t))\,t}\,, \tag{3.27}$$

where f' is the derivative of f with respect to its argument, while the dot denotes differentiation with respect to the non-dimensional time scale t here. As it is regularly used in the literature to denote the derivative even if the considered quantity still has a dimension, we will also continue to use it in that case. It will be clear from the context, which case is implied.
As we wish to compare the stress level velocity, especially of the fracture stress level $\sigma_k = 1$, to the dislocation velocity, we need an expression for this velocity. We will again use an Arrhenius-law:

$$u^*(\sigma_{yy}, T) \;=\; l\nu \exp\left(-\frac{G_u + \Delta G - V\sigma_{yy}}{kT}\right), \tag{3.28}$$

where l is an appropriate length scale, ν is an attempt frequency, G_u is the activation energy in the unirradiated state, ΔG is a shift due to irradiation, k is the Boltzmann-constant and V is an effective activation volume.
Indeed, l and V need some qualification. The proper choice of the length scale l depends on the microstruture of the steel and the dislocation ensemble. It is the mean distance between two relevant obstacles, which may be given by defects of the microstructure or related to the interactions of the dislocations themselves, which may accumulate at certain positions and form obstacles for other dislocations.
Concerning V, firstly, the true driving stress on the dislocations is the critical resolved shear stress of the relevant dislocation glide planes, which can be connected to σ_{yy}, but this connection depends on the favoured glide planes and stress triaxiality. One can take those things into account at this stage. We do not go into the details, as they bear only on the quantitative, but not the qualitative conclusions.
Secondly, even for simple base-centered-cubic crystals like the ferritic phase of iron, the effective activation energy depends in a nonlinear way on the applied stress and there are two different temperature regimes, [7, 194]. Therefore one may question equation (3.28), still we do not need the full stress dependence of the activation energy, but only its value for the minimum and maximum local fracture stress values, hence it is always possible to fit V to our needs.
The dislocation velocity u^* does not correspond to the non-dimensional form of our length and time scales. If we introduce them, we obtain

$$u(\sigma, T) \;=\; \frac{l}{a}\,\frac{\nu\,\sigma_f}{\dot{\sigma}_{\text{ext}}}\exp\left(-\frac{G_u + \Delta G - V\sigma_f\,\sigma}{kT}\right). \tag{3.29}$$

for comparison with $\dot{x}_{\sigma_k}$ instead. The function $u(\sigma, T)$ then expresses the amount of crack length travelled by a dislocation while the external stress is increased from zero to the fracture stress σ_f. The main equation for our approximation is therefore

$$u(\sigma_k, T) \;=\; \dot{x}_{\sigma_k}(t_k)\,, \tag{3.30}$$

where a critical time t_k corresponding to the stress level σ_k is defined by this equation. Under certain circumstances it may itself define a region in the material bounded by

$$x_k \;:=\; x_{\sigma_k}(t_k)\,, \tag{3.31}$$

which is save from a rising stress level, because $u(\sigma_k, T) \;\geq\; \dot{x}_{\sigma_k}$ is fulfilled inside this region and so the dislocations will align themselves to inhibit a further increase of the stress. If we take $\sigma_k = 1$, corresponding to $\sigma_{yy} = \sigma_f$,

conditions which ensure this region includes the vicinity of the notch/crack tip will give a criterion for an increasing apparent fracture toughness in the sense of equation (3.22). Define t_f by

$$u(1,T) \;=\; \dot{x}_1(t_f)\,, \tag{3.32}$$

compare (3.30) and x_f by

$$x_f \;:=\; x_1(t_f)\,, \tag{3.33}$$

compare (3.31), then $\sigma_k = 1$ and equation (3.26) imply $f(x_f) = 1/t_f$ and therefore

$$\frac{K_{\exp}}{K_{el}} \;=\; \frac{t_f}{t_{el}} \;=\; f(x_n)\,t_f\,, \tag{3.34}$$

using equation (3.22), which is valid for $t_f \geq t_{el}$, see the discussion of (3.22). Equation (3.34) allows to determine the toughness-temperature-relation even without the explicit computation of x_f.
Our next task is thus to identify conditions, which fit the case of a component of a notch stress field and (rigorously) ensure the existence of a region at the notch/crack tip, where $u(\sigma_k,T) \;\geq\; \dot{x}_{\sigma_k}$. This will be done also for nonlinear elasticity and a not necessarily constant loading rate, as there are no additional obstacles of interest.
In the general case, the relevant notch stress component σ inside the specimen is given by an equation of the form

$$\sigma \;=\; g(x,\sigma_{ext})\,, \tag{3.35}$$

where g must fulfill certain requirements to be a reasonable candidate for a notch stress function, which are summarized in the following definition:

Definition 3.2.1. *A function*

$$g : (0,\infty)\times[0,\infty)\to[0,\infty)\,,\;\; (x,y)\;\mapsto\; g(x,y)$$

is called a candidate notch stress function (CNSF), if it is at least twice continuously differentiable on $(\varepsilon,\infty)\times[0,\infty)$ for any positive ε and has the following properties:

$$\lim_{\substack{x\to 0\\ y>0}} g(x,y) = \;\infty\,, \tag{3.36}$$

$$\lim_{x\to\infty} g(x,y) = \;y\,, \tag{3.37}$$

$$g(x,0) = \;0\,, \tag{3.38}$$

$$\partial_x g(x,y) < \;0\,, \tag{3.39}$$

$$\partial_y g(x,y) > \;0\,. \tag{3.40}$$

The relations in the last two lines are understood as valid for all (x, y) for which they make sense according to the domain of g and its differentiability properties. It is understood in (3.36), that $y > 0$ is arbitrary but fixed while x tends to zero.
The physical meaning of the conditions in definition 3.2.1 is the following: Without loss of generality, we have put the stress singularity of the crack at $x = 0$, see (3.36). The other specimen boundary has been put at infinity, (3.37), so we limit ourselves to local considerations close to the notch/crack tip. Different positions of the boundaries and singularities will be convenient depending on the geometry of the specimen and notch under consideration but such changes will not alter the salient properties discussed below.
The position $x_n > 0$ mentioned before has deliberately been left unaccounted for, as it is of no relevance to the considerations connected to the determination of possible solutions of (3.30). It enters only at a later stage. The structure is assumed to be free of other relevant sources of internal stress, resulting in the conditions (3.37), (3.38) and (3.39). If an additional geometric structure changes the stress distribution inside the specimen, it will influence (3.37), if it is so far from the crack under consideration, that we do not include it explicitly in the configuration. If it is very close to the crack, (3.39) will usually not be tenable any more. If permanent internal stresses are present, a function of the given type may still be enough to analyze the behavior close to the crack/notch tip, but then conditions (3.37) and (3.38) must be modified to include the additional source of stress. Condition (3.40) means that the local stress increases, if the external stress does.
We will always assume that the external stress $\sigma_{ext}(t)$ is an at least twice continuously differentiable function of t with strictly positive loading rate $\dot{\sigma}_{ext}(t)$ bounded from below by a positive constant

$$\sigma_{ext} : [0, \infty] \to [0, \infty], \; t \mapsto \sigma_{ext}(t)\,, \tag{3.41}$$

such that

$$\sigma_{ext}(0) \;=\; 0\,. \tag{3.42}$$

The position of each stress level x_{σ_k} is defined by

$$\sigma_k \;=\; g(x_{\sigma_k}(t), \sigma_{ext}(t))\,, \tag{3.43}$$

for an arbitrary but fixed $\sigma_k > 0$. As the external stress $\sigma_{ext}(t)$ and g are twice continuously differentiable and their partial derivatives do not vanish, we can use the implicit function theorem to show, that $x_{\sigma_k}(t)$ is itself a twice continuously differentiable function of t. From (3.43) we can compute the stress level velocity $\dot{x}_{\sigma_k}$ by implicit differentiation, as in the linear case above,

see Figure 3.7. The result is

$$\dot{x}_{\sigma_k}(t) \;=\; -\frac{\partial_y g(x_{\sigma_k}(t),\sigma_{ext}(t))}{\partial_x g(x_{\sigma_k}(t),\sigma_{ext}(t))}\,\dot{\sigma}_{ext}(t)\,. \tag{3.44}$$

As g and its partial derivatives will always be evaluated at $(x = x_{\sigma_k}(t), y = \sigma_{ext}(t))$ in the following, we will not mention this explicitly, because some of the expressions become difficult to read otherwise. It is always understood, that g and its partial derivatives are to be evaluated at this point, though. The external loading rate is positive, hence (3.39) and (3.40) imply the stress level velocity to be positive, so $x_{\sigma_k}(t)$ is strictly monotonically increasing, as expected.

At each position $x > 0$ the stress $g(x, \sigma_{ext}(t))$ is a strictly monotonically increasing function of t due to property (3.40) and the strictly positive loading rate. The properties (3.36) and (3.39) of g imply the existence of a single position $x_{\sigma_k} > 0$ for each value $\sigma_k > \sigma_{ext}$ and each positive time, while they show the non-existence of such a (finite) position if $\sigma_k \leq \sigma_{ext}$. The question, whether $x_{\sigma_k} > x_n$, so it is inside the specimen and therefore of potential relevance to toughness is discussed in connection with the example in the following subsection 3.2.3 only.

We will now investigate, whether the dislocations can follow a certain stress level σ_k close to the notch/crack, so this driving stress σ_k is sufficient to keep $u_k = u(\sigma_k, T)$ at least as large as the stress level velocity $\dot{x}_{\sigma_k}$. This will be done by giving sufficient conditions for the existence and uniqueness of solutions of

$$u_k \;=\; \dot{x}_{\sigma_k}(t)\,, \tag{3.45}$$

and a consideration of the monotonicity of $\dot{x}_{\sigma_k}$. The findings are summarized in

Theorem 3.2.1. *Let u_k be a positive constant, t be the time and let $g(x, y)$ be a CNSF according to definition 3.2.1. If $\sigma_{ext}(t)$ is a twice continuously differentiable function with $\dot{\sigma}_{ext}(t) \geq d > 0$ and $\sigma_k = g(x_{\sigma_k}(t), \sigma_{ext}(t))$, such that*

$$\frac{\ddot{\sigma}_{ext}}{(\dot{\sigma}_{ext})^2} \;>\; 2\,\frac{\partial^2_{xy} g}{\partial_x g} \;-\; \frac{(\partial_x g)^2\partial^2_{yy} g + (\partial_y g)^2\partial^2_{xx} g}{(\partial_x g)^2\partial_y g}\,, \tag{3.46}$$

is fulfilled for all t, where the derivatives of g are to be evaluated at $(x = x_{\sigma_k}(t), y = \sigma_{ext}(t))$, then there exists a unique positive t_k such that

$$\begin{aligned} t < \; t_k \;&\Rightarrow u_k > \; \dot{x}_{\sigma_k}(t)\,;\\ t = \; t_k \;&\Rightarrow u_k = \; \dot{x}_{\sigma_k}(t)\,;\\ t > \; t_k \;&\Rightarrow u_k < \; \dot{x}_{\sigma_k}(t)\,, \end{aligned}$$

if

$$\lim_{t\to 0} \dot{x}_{\sigma_k}(t) \;<\; u_k\,.$$

If furthermore

$$\partial_y g(x_{\sigma_k}(t), \sigma_{ext}(t)) \;=\; o(\,\partial_x g(x_{\sigma_k}(t), \sigma_{ext}(t))\,)\,,\; t\to 0\,, \tag{3.47}$$

where $o(x)$ denotes the small Landau symbol, then such a t_k exists for each positive u_k.

As $x_{\sigma_k}(t)$ is a strictly monotonically increasing function under the given conditions, we infer from the Theorem, that close to the singularity at $x = 0$ we have $u_k > \dot{x}_{\sigma_k}(t)$, if the conditions of the Theorem are fulfilled, so there is a shielded region close to the crack/notch tip in this case.

Proof. The idea of the proof is straightforward: As already shown, $x_{\sigma_k}(t)$ is a twice continuously differentiable function, so we can investigate $\ddot{x}_{\sigma_k}(t)$ to give a condition for $\dot{x}_{\sigma_k}(t)$ to be strictly monotonically increasing, which turns out to be (3.46). As $\dot{x}_{\sigma_k}(t)$ is bounded from below by zero, $\lim_{t\to 0} \dot{x}_{\sigma_k}(t)$ exists in this case, so we have a unique t_k by the intermediate value theorem for sufficiently large u_k, as furthermore

$$\lim_{t\to t^*} \dot{x}_{\sigma_k}(t) \;=\; \infty\,,$$

because of (3.37) and (3.39): x_{σ_k} exists only for $\sigma_k > \sigma_{ext}$, so equation (3.45) can only have a solution in this case and x_{σ_k} must monotonically travel to infinity in the finite time t^*, defined by

$$\sigma_k \;=\; \sigma_{ext}(t^*)\,.$$

The quantity t^* is indeed finite, as the external loading rate is positive and bounded away from zero. The final condition on the partial derivatives is necessary to ensure

$$\lim_{t\to 0} \dot{x}_{\sigma_k}(t) \;=\; 0\,.$$

This is guaranteed by equation (3.44), as the loading rate is bounded away from zero. Therefore we only need to investigate the positivity of $\ddot{x}_{\sigma_k}$:

$$\begin{aligned}\ddot{x}_{\sigma_k} &= -\left(\ddot{\sigma}_{ext}\,\frac{\partial_y g}{\partial_x g} + \dot{\sigma}_{ext}\left(\frac{\dot{\partial_y g}}{\partial_x g}\right)\right) \\ &= -\ddot{\sigma}_{ext}\,\frac{\partial_y g}{\partial_x g} - \frac{\dot{\sigma}_{ext}}{(\partial_x g)^2} \\ &\quad \left(\partial_x g\left(\partial^2_{yy} g\,\dot{\sigma}_{ext} + \partial^2_{xy} g\,\dot{x}_{\sigma_k}\right) - \partial_y g\left(\partial^2_{xx} g\,\dot{x}_{\sigma_k} + \partial^2_{xy} g\,\dot{\sigma}_{ext}\right)\right)\,.\end{aligned} \tag{3.48}$$

From this equation $\dot{x}_{\sigma_k}$ can be eliminated with the help of (3.44) and after a short computation we obtain

$$\ddot{x}_{\sigma_k} = -\frac{1}{(\partial_x g)^3} \tag{3.49}$$
$$\left(\ddot{\sigma}_{ext}(\partial_x g)^2 \partial_y g + (\dot{\sigma}_{ext})^2 \left((\partial_x g)^2 \partial^2_{yy} g + (\partial_y g)^2 \partial^2_{xx} g - 2\,\partial_y g\,\partial_x g\,\partial^2_{xy} g\right)\right) .$$

For $\ddot{x}_{\sigma_k}$ to be positive the term in brackets must be positive, because $\partial_x g$ is negative. From this we get the inequality

$$\frac{\ddot{\sigma}_{ext}}{(\dot{\sigma}_{ext})^2} \;>\; 2\,\frac{\partial^2_{xy} g}{\partial_x g} \;-\; \frac{(\partial_x g)^2 \partial^2_{yy} g + (\partial_y g)^2 \partial^2_{xx} g}{(\partial_x g)^2 \partial_y g} ,$$

after some rearrangements. The reader is reminded, that this inequality does not constitute a partial differential inequality, because it is only to be valid for g evaluated at $(x = x_{\sigma_k}(t), y = \sigma_{ext}(t))$, while the derivatives of σ_{ext} are just functions of t. The arguments were left out of the expression to make it simpler to read. □

While it is of interest to characterize the conditions for the validity of (3.47), such an investigation is besides the point here, because the Theorem helps us only in situations in which $x_{\sigma_k}(t_k)$ is already inside the specimen, meaning $x_{\sigma_k}(t_k) \geq x_n > 0$. This has to be figured out anew for each application anyway. The Example 3.2.1 shows, that any limit for (3.47) and the corresponding $\dot{x}_{\sigma_k}(0)$ may occur even if the function under consideration fulfills the monotonicity conditions of a CNSF.
The Theorem was given to show the potential existence of a safe region close to a notch/crack tip under rather general circumstances, which can be computed from the knowledge of the stress function and external load alone. Indeed, two main advantages of our approximation to the shielding dynamics of dislocations are its applicability to rather arbitrary notch stress fields and its simplicity. It does neither depend on a special quantitative ansatz for the notch stress field, nor on the theory used to compute the stresses, whether linear or nonlinear. This is especially advantageous, as the real stress distribution inside a specimen made of steel with its complicated microstructure is not precisely known. The only things needed to use the approach are some general qualitative properties of notch stress fields and a reasonable guess of the stress distribution close to the crack/notch tip in question. The examples below show, that it will give reasonable results especially for notch stress fields, while this is not the case, if the ideas are applied to arbitrary functions not fulfilling all requirements of a CNSF. The approach is comparatively simple, as we do not compute the true dislocation dynamics explicitly,

which would necessitate extensive numerical calculations.
We shall not investigate the general nonlinear case further, but give the special form of (3.46) in linear elasticity. Then we have

$$g(x, \sigma_{ext}) \;=\; f(x)\sigma_{ext}$$

and by specialization from (3.46) or an analogous computation we obtain the inequality

$$\frac{\ddot{\sigma}_{ext}(t)\,\sigma_{ext}(t)}{(\dot{\sigma}_{ext}(t))^2} \;>\; 2 \;-\; \frac{f''(x_{\sigma_k}(t))\,f(x_{\sigma_k}(t))}{(f'(x_{\sigma_k}(t)))^2} \tag{3.50}$$

for $\ddot{x}_{\sigma_k}$ to be positive. In the usual case of a constant external strain rate, this condition simplifies further to

$$f''(x_{\sigma_k}(t)) \;>\; \frac{2\,(f'(x_{\sigma_k}(t)))^2}{f(x_{\sigma_k}(t))}\,. \tag{3.51}$$

Inequality (3.51) can be elucidated expediently by $f(x) = x^{-\beta}$, though $f(x)$ is not a CNSF according to our definition. The main considerations for the stress level velocity still apply.

Example 3.2.1. *Let the positive constants c and β be given and consider*

$$\sigma \;=\; c\,x^{-\beta}\,t\,.$$

Then

$$x_{\sigma_k}(t) = \left(\frac{c\,t}{\sigma_k}\right)^{1/\beta}, \tag{3.52}$$

$$\dot{x}_{\sigma_k}(t) = \frac{1}{\beta}\left(\frac{c}{\sigma_k}\right)^{1/\beta} t^{(1-\beta)/\beta}, \tag{3.53}$$

$$t_k = \left(\frac{\sigma_k}{c}\,(\beta\,u_k)^{\beta}\right)^{1/(1-\beta)}, \tag{3.54}$$

$$x_k = \left(\frac{\sigma_k\,\beta\,u_k}{c}\right)^{1/(1-\beta)}, \tag{3.55}$$

if $\beta \neq 1$. If $\beta = 1$, then $\dot{x}_{\sigma_k} = c/\sigma_k$, independent of t. Hence no well-defined t_k and x_k exist.

Indeed, $1/x$ solves the differential equation $f''\,f \;=\; 2\,(f')^2$ for positive and negative x. The equality corresponding to (3.51) therefore separates power laws with monotonically decreasing stress level velocities ($\beta > 1$) from those with monotonically increasing stress level velocities ($\beta < 1$).

While the latter fulfill the limiting condition (3.47), the former do not even possess a corresponding finite limiting value. The condition (3.37) of a CNSF is violated by the power laws considered here and we find, that there need not be a diverging stress level velocity at all, while divergence for small times and close to the singularity is also possible.
Because of the asymptotic $1/\sqrt{r}$-behavior of the crack stress fields of linear elasticity, this case is of special interest to us and yields particularly simple expressions:

Example 3.2.2. *Consider*

$$\sigma \;=\; c\,x^{-1/2}\,t\,,$$

where c is a positive constant. Then

$$x_{\sigma_k}(t) = \left(\frac{c\,t}{\sigma_k}\right)^2, \tag{3.56}$$

$$t_k = \frac{\sigma_k^2}{2\,c^2}\,u_k\,, \tag{3.57}$$

$$x_k = \frac{\sigma_k^2}{4\,c^2}\,u_k^2\,. \tag{3.58}$$

The asymptotic crack field example thus belongs to those, where the stress level σ_k is shielded at small times and close to the crack tip, while the situation will become unstable later and further away from the tip. This was expected, because such characteristics lead to predictions in accordance with experimental facts. As there is also some "distance" between the asymptotic notch stress solution and the exponents with diverging stress level velocities for positions close to the singularity, we may suppose with some confidence, that there is a shielded area close to the crack/notch tip for the stress fields from applications. Equation (3.57) implies the asymptotic validity of a linear relationship between the apparent fracture toughness and the dislocation velocity, a strange coincidence.
We now have a model to describe an increase of the apparent fracture toughness but not yet fixed a criterion for the transition between ductile and brittle fracture itself. The theory as given here suggests only one option by itself. This is to account for the finite size of the specimen. If x_f grows so large, that it reaches the other end of the specimen, we may expect brittle fracture to be inhibited. Such a criterion seems especially reasonable as there are effects due to the geometry like notch-brittleness. The occurence of the DBT in many different materials also suggestes, that there is maybe no material depend criterion of general validity. The criterion in section 3.1 is not convincing from this perspective, as it depends on the stress intensity alone and

so is limited to a consideration of a crack tip.
Still, the situation is unsatisfactory, as ductile fracture *does* commence in practice and was not described here. It will cut the curves of fracture resistance versus temperature in Figure 3.9 short somewhere, and as we described neither plasticity-induced fracture nor ductile void grow, we can not fix that position. Material properties will surely enter there. We will discuss some evidence about this situation in subsection 3.2.5.

3.2.3 A detailed example

The simple power law example of the preceding section is not a CNSF and does not allow to connect the stress state at the crack tip directly to the applied stress, as long as no additional finite boundary is introduced. It turns out, that we obtain a CNSF for which all computations can be done explicitly if we simply add a constant. The asymptotic inverse square root dependence of the stress on the distance to the crack tip suggests to choose this specific value of the exponent for the stress function component. Hence we shall focus on the following function:

$$\sigma \;=\; \left(\frac{k}{\sqrt{x}} + 1\right) t\,, \tag{3.59}$$

where k is constant and $x > 0$. Then the right hand side fulfills the conditions for a CNSF. To complete the configuration, we have to fix a suitable x_n. As has been discussed before, x_n depends on the solution of a boundary value problem, usually from linear elasticity theory fitted to a specific geometry, it can not be placed at will. Still we choose a slightly different viewpoint. As we will usually not know the exact shape of a pre-crack in practice and also wish to understand regularities in the data, for which this information is not available anyway, we do not solve an elastic problem. We will simply assume, that x_n depends on the notch length a and the curvature radius of the tip r as a function of r/a, which is common for short cracks in specimen, [151], and though this function can be rather intricate for a complicated geometry, we will be pragmatic and take

$$x_n \;=\; c^2\,\frac{r}{a}\,, \tag{3.60}$$

where c is constant. This gives the following elastic stress concentration at x_n:

$$f(x_n) \;=\; \frac{k}{\sqrt{x_n}} + 1 \;=\; \frac{k}{\sqrt{c^2\,\frac{r}{a}}} + 1 \;=\; \frac{k}{c}\sqrt{\frac{a}{r}} + 1\,. \tag{3.61}$$

The position x_n and hence the constant c are unrelated to the comparison of dislocation velocity and stress-level-velocity, so they will be of minor significance for the qualitative behavior of the toughness-temperature curves. For accurate quantitative predictions in applications, more precise expressions than (3.59) and (3.60) should be found, though.
We will now apply the procedure of the preceding subsection 3.2.2 to equation (3.59). From the start we will consider only the stress level $\sigma_k = 1$, corresponding to $\sigma_{yy} = \sigma_f$, relevant to fracture. The corresponding quantities t_f, x_f and x_{σ_f} have been defined in equations (3.31), (3.32) and (3.33). The development starts with

$$1 \;=\; \left(\frac{k}{\sqrt{x_{\sigma_f}}} + 1 \right) t \,, \tag{3.62}$$

defining x_{σ_f}, which implies

$$x_{\sigma_f}(t) \;=\; \left(\frac{kt}{t-1} \right)^2 . \tag{3.63}$$

As we have obtained $x_{\sigma_f}(t)$ explicitly, we can compute

$$\dot{x}_{\sigma_f}(t) \;=\; 2\,k^2\,\frac{t}{(1-t)^3} \tag{3.64}$$

directly, without implicit differentiation. Because

$$\lim_{t \to 0} \dot{x}_{\sigma_f}(t) \;=\; 0$$

is obvious from (3.64) and the other prerequisites of Theorem 3.2.1 are also fulfilled, we know that there exists a unique $1 > t_f > 0$ solving

$$u_f \;=\; \dot{x}_{\sigma_f}(t_f) \;=\; 2\,k^2\,\frac{t_f}{(1-t_f)^3} \tag{3.65}$$

for an arbitrary positive constant $u_f := u(1,T)$, where the non-dimensional dislocation velocity $u(\sigma,T)$ is given by equation (3.29).
Equation (3.65) is equivalent to the third degree polynomial equation

$$t_f^3 - 3t_f^2 + \left(3 + \frac{2k^2}{u_f} \right) t_f - 1 \;=\; 0 \,, \tag{3.66}$$

which may be simplified by substituting $w = t_f - 1$ to get

$$w^3 + \frac{2k^2}{u_f} w + \frac{2k^2}{u_f} \;=\; 0 \,. \tag{3.67}$$

By evaluating the left hand side at $w = -1$ and $w = 0$ and considering its derivative we can again prove the existence of a unique solution w_f in the interval $(-1, 0)$, as expected.
It is known since the sixteenth century, that polynomials of at most fourth degree can be solved by radicals and the solution for third degree polynomials is explained in [152] and can be found in any elementary algebra text. Therefore we can give the closed form of t_f and $x_f = x_{\sigma_f}(t_f)$:

$$t_f = 1 - \left(\frac{k^2}{u_f}\right)^{1/3} \left(\sum_{i=0}^{1} \sqrt[3]{1 + (-1)^i \sqrt{1 + \frac{8\,k^2}{27\,u_f}}} \right) , \tag{3.68}$$

$$x_f = k^2 \left(1 - \frac{\left(\frac{u_f}{k^2}\right)^{1/3}}{\left(\sum_{i=0}^{1} \sqrt[3]{1 + (-1)^i \sqrt{1 + \frac{8\,k^2}{27\,u_f}}} \right)} \right)^2 . \tag{3.69}$$

Even though it is not apparent at first, $t_f(u_f)$ is differentiable at $u_f = 0$

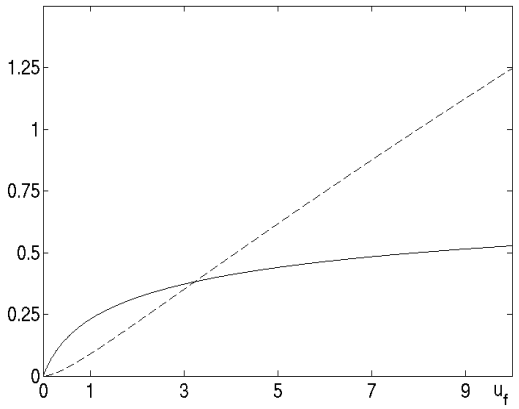

Figure 3.8: The functions $t_f(u_f)$ (solid line) and $x_f(u_f)$ (dashed line) for $k = 1$, see (3.59), the units are dimensionless; $t_f(u_f)$ is bounded by and asymptotically approaches 1, because it always remains smaller than the time it takes the external load to reach the fracture stress, which is the reference-timescale; $x_f(u_f) = t_f^2(u_f)/(t_f^2(u_f) - 1)$ becomes unbounded when passing to the limit $u_f \to \infty$. This means, that the size of the shielded zone at the crack tip grows arbitrarily, if the dislocation velocity grows without bound.

and can be obtained as ordinary power series from (3.66) or (3.67) by the method of undetermined coefficients.
From (3.66) we have

$$t_f(u_f) \;=\; \frac{1}{2\,k^2}\,u_f \;-\; \frac{3}{4\,k^4}\,u_f^2 \;+\; \frac{9}{4\,k^6}\,u_f^3 \;+\; O(u_f^4)\,, \tag{3.70}$$

while we can obtain all higher order terms from the recursion relation

$$t_{i+1} \;=\; \frac{-3\,t_i \;+\; 3\sum\limits_{j+k=i} t_j t_k \;-\; \sum\limits_{l+m+n=i} t_l t_m t_n}{2\,k^2}\,, \tag{3.71}$$

valid if $i \geq 3$ for the coefficients t_i of the ansatz

$$t_f(u_f) \;=\; \sum_{i=1}^{\infty} t_i u_f^i\,,$$

which is inserted into (3.66). Here $j,k,l,m,n \in \{1,2,\ldots\}$ and the first three coefficients are taken from (3.70).
A small value of k leads to a steep increase of $t_f(u_f)$ near the origin, so a weak singularity is shielded particularly effectively for small velocities. The approach of t_f to 1 and x_f to ∞ for arbitrary large dislocation velocities u_f are only of a low algebraic order. The functions t_f and x_f are plotted in Figure 3.8 for the value $k = 1$ of the parameter in (3.59).
From equations (3.34) and (3.61) we can now obtain the fracture toughness - temperature relationship in this example:

$$\frac{K_{\exp}}{K_{\mathrm{el}}}(T) \;=\; \begin{cases} 1 & \text{if } f(x_n)t_f \;\leq\; 1 \\ \left(\frac{k}{c}\sqrt{\frac{a}{r}} \;+\; 1\right)\, t_f(u_f(T)) & \text{if } f(x_n)t_f \;>\; 1\,, \end{cases} \tag{3.72}$$

where t_f is taken from (3.68) and $u_f(T)$ from equation (3.29). As announced before, we have a closed form solution, but already in this example it is rather complicated. In general, numerical methods will be unavoidable to compute $K_{\exp}(T)$, but substantial qualitative and quantitative information can be obtained without the precise knowledge of this function. This is the objective of the next subsection.

3.2.4 The cleavage fracture toughness in the transition regime

Let us now describe the implications of the model for the fracture behavior in the transition regime. First, we use equation (3.72) to create Figure 3.9.

mean free path l	10^{-5} m
crack length a	10^{-4} m
attack frequency ν	10^{13} 1/s
external loading rate $\dot{\sigma}_{ext}$	7 MPa/s
local fracture stress σ_f	700/750 MPa
activation enthalpy G_u	1.68 eV
activation volume V	$2.5 \times 10^{-28}\mathrm{m}^3$
crack tip radius r	10^{-7} m
inverse Boltzmann-constant $1/k$	11605 K / eV
stress function constants c, k	1

Table 3.2: The parameters used to create the graphs of Figures 3.9, 3.10, 3.11 and 3.12, unless specified otherwise.

All Figures to be presented were created with the parameters given in Table 3.2, unless specified otherwise. We will comment on the data in subsection 3.2.5.

Figure 3.9 is a plot of the predicted apparent fracture toughness versus the temperature according to (3.72) for two different local fracture stresses σ_f in the unirradiated state $\Delta G = 0$ (solids lines) and irradiated state for an energy shift of $\Delta G = 0.125\,\mathrm{eV}$ (dashed lines) and $\Delta G = 0.25\,\mathrm{eV}$ (dotted lines). The different fracture stresses correspond to a lower and upper estimate of the local fracture stress. We have chosen a difference of about 8 percent between these values. This is rather small, as [171] gives a mean value of $4.56\,\mathrm{MPa}\sqrt{\mathrm{m}}$ and a standard deviation of $0.32\,\mathrm{MPa}\sqrt{\mathrm{m}}$ even for a reference material for testing ceramics. In steel with its complicated microstructure and several different microscopic fracture mechanisms discussed, see references in section 2.1, the scatter in low temperature cleavage toughness will not be much smaller, though the sources cited by the author give no thorough discussion of the accuracy of these values. A slight temperature dependence of σ_f can also be accounted for by adjusting the upper and lower bound for σ_f. This will lead to a less precise estimate of the apparent toughness, but this is not a problem for applications, if it is not too conservative.
Figure 3.9 shows the same effect as in section 3.1: At low temperatures there is comparatively low toughness and scatter, while in the transition regime both increase strongly. Due to the strong increase of the scatter in the tran-

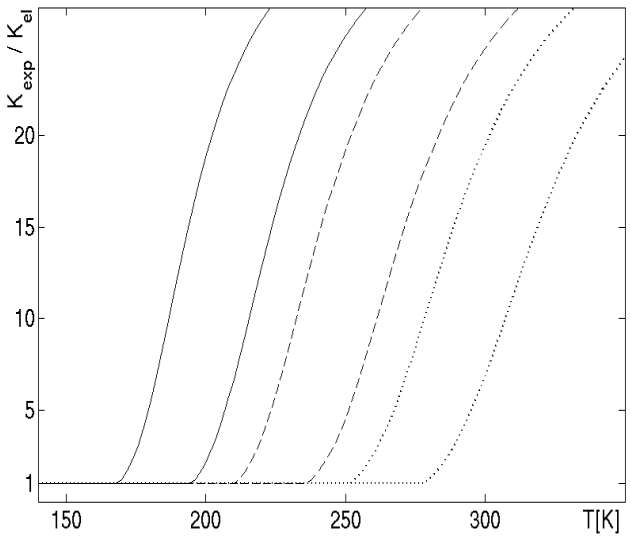

Figure 3.9: Curves of the apparent fracture toughness versus temperature are displayed. The data for the solid lines (unirradiated state) are given in Table 3.2. For the other curves, showing effects of irradiation, $\Delta G = 0.125\,\mathrm{eV}$ (dashed) and $\Delta G = 0.25\,\mathrm{eV}$ (dotted).

sition regime, the scatter at low temperatures seems to be negligible, while it is not. The effect of irradiation damage is clearly visible. The higher energy barrier results in substantial embrittlement, leading to a shift of the transition regime to higher temperatures. Apparently, there is no significant change of the shape of the toughness curves. This observation, utilized in the Master curve approach, will be discussed later in this section. As we have not given a criterion for ductile fracture, the curves make no prediction about the true fracture resistance for very high temperatures, but the apparent toughness increases indeed by about an order of magnitude in the transition regime, compare Figure 2.4. The scatter predicted on the lower shelf is higher than apparent in Figure 3.10, because the bounding curves give the relative increase related to their specific local fracture stress level. However, the cut-off effect due to the position x_n can also be seen. This artifact of the simplifications of the model does not affect the general conclusions, though.

In between both curves there is no prediction made by the model as long as the details of the local fracture resistance σ_f are not specified. Indeed anything conceivable concerning fracture might happen. If a crack is initiated in

an area of low toughness or the main crack advances, it may be arrested in an area of higher toughness or traverse the whole specimen, because the stress intensity increases as it advances. On the other hand an initially stable and ductile fracture process near the main crack can result in unstable cleavage either because the stress intensity increases sufficiently or because a growing crack reaches an area of low toughness and becomes unstable. Hence we will expect local cleavage and ductile crack extension in the same specimen in the transition regime as well as the observed scatter. Significant plasticity can also be present alongside cleavage fracture.
In [84] simple examples of the computation of the apparent toughness based on a definite function $\sigma_f(x)$ of position are given, but they can not be made without some assumptions about the local fracture characteristics, which are always somewhat arbitrary. Therefore we refrain from doing so here and consider only upper and lower boundaries, which we consider as the appropriate approach by now. As we do not describe ductile failure, we have no description of the so-called upper shelf toughness and it is not prescribed in Figure 3.9, see [55] for experimental data. Further discussion and corresponding references on other approaches to this problem are mentioned in subsection 3.2.5.
Figures 3.10 and 3.11 are especially convenient for a discussion of the transition region. Figure 3.10 shows a plot of the necessary local fracture stress as function of the apparent fracture resistance for four different temperatures again based on equation (3.72), while Figure 3.11 shows the corresponding shielded region in front of the notch/crack tip. The Figures are of special interest due to the shape of the curves depicted. The curves are extremely on the left and rather shallow on the right. The levels of upper and lower fracture stress are also indicated.
At the lowest temperature, the shallow part of the curve lies above the fracture stress level. This means, that the local stress necessary to attain a higher apparent fracture resistance is above the local fracture stress, so cleavage at a constantly low level of toughness and low scatter is observed. The stress singularity of the notch/crack dominates the fracture behavior and failure will start in its immediate vicinity.
If the temperature is raised, local shielding near the stress singularity becomes effective in an area in front of the notch tip. The singularity is then partly shielded, and the apparent fracture toughness increases according to equation (3.72). The failure process is still governed by cleavage but may start at a certain distance from the main crack and the scatter increases. This behavior corresponds to the second curve from above in Figures 3.10 and 3.11, which is not vertical in the complete fracture stress range any more. As the stress singularity is notable mainly for very small x_f, the effect

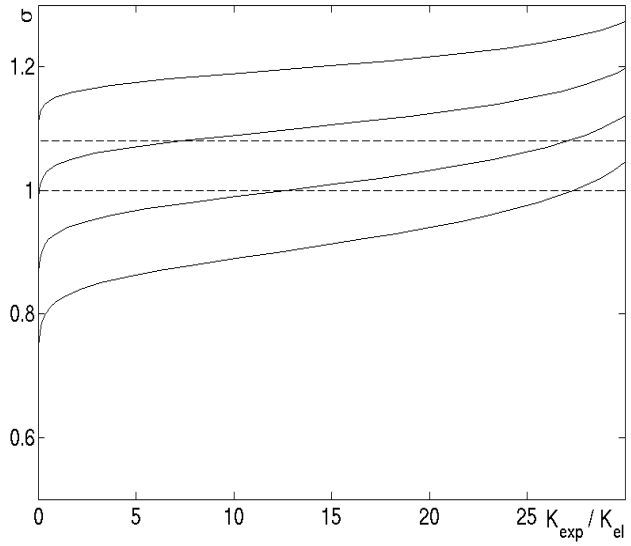

Figure 3.10: The four curves show the necessary stress $\sigma = \sigma_{yy}/\sigma_f$ to reach a certain apparent relative fracture resistance increase for four different temperatures, $T = 140\text{K}$: top, $T = 180\text{K}$, $T = 220\text{K}$, $T = 260\text{K}$: bottom, as functions of this fracture resistance increase. The horizontal lines give the minimal and maximal values of the local fracture stress σ_f.

is barely visible in Figure 3.11.
The third curve from above represents a temperature, where the necessary stress for additional shielding is below the lower fracture stress. Now every measurement of toughness will show a certain increase compared to the low temperature value. Furthermore the region of the fracture stresses is traversed by the shallow part of the curve, so in this part of the curve a slight change in local fracture resistance will have a large effect on the apparent toughness, explaining the increase as well as the scatter in the toughness data within the transition regime. Ductility will be observed during some tests in certain areas of the fracture surfaces of a specimen, because the maximum fracture stress level is not reached there anymore due to the shielding effect of plasticity. The failure initiation sites move further away from the crack tip.
At the highest temperature depicted, corresponding to the lowest curve, the shielding effect is so strong, that the lowest local cleavage stress level is not reached anymore in Figure 3.11. There will be no cleavage in that area anymore. If ductile failure sets in throughout the complete specimen in such a

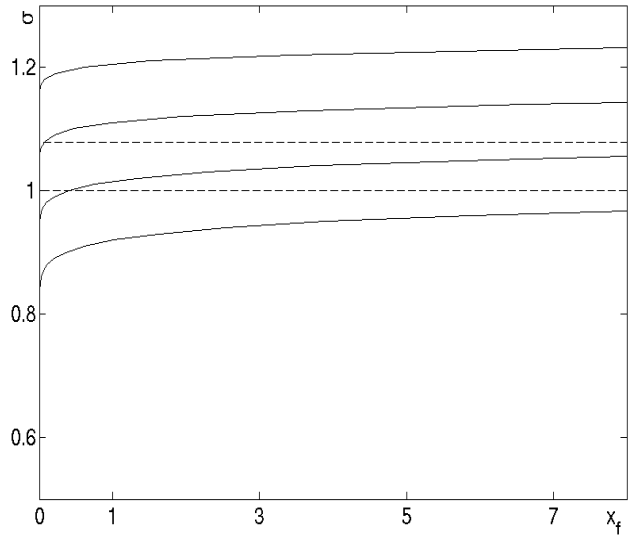

Figure 3.11: The four curves show the necessary stress to shield a certain distance in front of the crack for four different temperatures as function of this distance. The data are the same as in Figure 3.10.

situation, the transition will be complete and the fracture process be entirely ductile. We can still see the lowest curve entering the fracture stress range in Figure 3.10, but such a high cleavage fracture resistance need not be visible in experiments, because ductile fracture may set in beforehand. We will return to this point in subsection 3.2.5.
In this discussion, no macroscopic plastic properties of the material, like the yield stress, are involved. Therefore yield stress and fracture resistance need not correlate with each other. The interesting consequences will be discussed later in more detail.
In general, an increase in apparent fracture toughness can go along with a change of the prevailing failure initiation sites. Such a correlation is reported for example in [5, section 5.3]. The sources cited there attribute this to a certain amount of stable crack growth before an initiation site for unstable cleavage failure is found. The variability of the failure initiation sites is well-known and usually attributed to weakest link statistics of the distribution of secondary particles, in particular carbides in an RPV steel, given local fracture criteria, see for example [22, 137, 162, 235].
While such an approach is not inconsistent with the present model, the viewpoint held here is different. As has been reported in the introductory sec-

tion 2.1, there is still enough doubt about the prevailing microscopic failure mechanisms, that the inclusion of details of certain types of mechanisms may rather be an obstacle than a benefit to understanding. In the author's opinion it is rather likely, that a number of different processes lead to the same macroscopic fracture characteristics in the transition regime and may even happen concurrently in the same specimen. If we leave the effects of stable crack growth, secondary particles and grain boundaries out of consideration, this can indeed influence the prediction we make about the apparent toughness of any single specimen. But we may still expect that we can reasonably estimate the bounds within which these processes happen and the curves in Figure 3.9 are to be understood in this way.

We emphasize the role temperature plays in this connection. While the role of temperature is not immediately apparent if one favors a carbid-based statistical model, our model predicts the correlation between apparent toughness and failure initiation sites reported in [5, section 5.3], as caused by the increase of the temperature dependent shielded region close to the notch/crack tip. According to our model the Mikrostützwirkung of Neuber, [151], which is based on the minimum size of a region over which to average the stresses, is therefore not a material property but inherently temperature dependent. The temperature dependence of initiation sites is not often discussed in the literature, but a connection is reported for example in [182], while [161] contradicts this.

Another important aspect concerns the Master curve behavior, as suggested in [232], for the shape of the fracture toughness versus temperature functions. In our notion, toughness versus temperature data shows Master Curve behavior, if it is possible to fit the empirical data of toughness versus temperature in different states of irradiation by a universal curve of the same shape, which is shifted as a whole towards higher temperatures, if the material is irradiated. If applicable, this concept is very useful, because it allows to fix the complete temperature dependence for each different irradiation condition by determining a single parameter, called T_0 in the literature pertaining to the Master curve approach. T_0 is a single value on the temperature axis, whose determination is possible with comparatively few measurements. This specific value T_0 corresponds to a certain point on the graph of the relationship between temperature and toughness, which is fixed in the complete cleavage regime including the crucial part of the transition regime, because the shape of the curve is fixed. Our interpretation of the Master curve concept is less strict than at other places in the literature, [104, 232], where a specific function for this dependence is proposed. As we do not assume the existence of such a function and doubt a physical basis for it, we only bound the range in which the toughness increases and hence we will discuss the shift of the

bounding curves.
The applicability of the Master curve approach, which has been discussed extensively in the literature, see for example [104, 154, 161], is widely but not unanimously accepted, [137]. To assess the validity of Master curve behavior under irradiation within the present model, we consider the temperature T_c at which a certain relative toughness level c is reached as a function of the irradiation induced shift of the activation energy, see the Arrhenius-law (3.29). The defining equation is obtained from (3.72) as follows:

$$\begin{aligned} c \;=\; \frac{K_{\text{eff}}}{K_{\text{el}}} \;&=\; f(x_n)\, t_f(T_{cu}, G_u) \;=\; f(x_n)\, t_f(T_{cu} + \Delta T_c, G_u + \Delta G) \\ &=\; f(x_n)\, t_f(T_c, G)\,. \end{aligned} \tag{3.73}$$

The quantities T_c, T_{cu} and ΔT_c are defined by this equation. By definition we then have

$$\Delta T_c \;=\; \int_{G_u}^{G_u+\Delta G} \frac{dT_c}{dG}\, dG\,.$$

From this we get

$$\Delta T_c \;=\; \int_{G_u}^{G_u+\Delta G} \frac{dT_c}{dG}\, dG \;=\; -\int_{G_u}^{G_u+\Delta G} \frac{\partial_G\, t_f}{\partial_{T_c}\, t_f}\, dG \;=\; -\int_{G_u}^{G_u+\Delta G} \frac{\partial_G\, u_f}{\partial_{T_c}\, u_f}\, dG \tag{3.74}$$

by implicitly differentiating (3.73) and applying the chain rule to differentiate $t_f(u_f(T_c, G))$. Computing the partial derivatives results in

$$\Delta T_c \;=\; \int_{G_u}^{G_u+\Delta G} \frac{T_c}{G - V\sigma_f}\, dG\,. \tag{3.75}$$

But by the definition of T_c, the fraction in the integral must remain constant while changing G, because otherwise c would not be constant: Changing the fraction changes u_f and $K_{\text{eff}}/K_{\text{el}}$ is a strictly monotonically increasing function of u_f. Therefore we can pick a fixed value of the fraction, here by taking $G = G_u$ and hence $T_{cu} := T_c(G = G_u)$ and evaluate the integral trivially, so the result is:

$$\Delta T_c \;=\; \frac{T_{cu}}{G_u - V\sigma_f}\, \Delta G\,. \tag{3.76}$$

In order to assess the validity of the Master curve concept, we must now compare the shifts ΔT_c for different values of c. If these are exactly equal,

the Master curve concept is exactly valid in our model. If they are not, the magnitude of the deviations is to be assessed. Any differences between the ΔT_c must be due to the fraction on the right hand side of equation (3.76). We will consider it as a function s of $u_c := u_f(1, T_c)$:

$$s(u_c) \;:=\; \frac{T_{cu}}{G_u - V\sigma_f}(u_c)\,, \tag{3.77}$$

called s for shift. As function of u_c, s is obtained by solving the Arrhenius-law for s:

$$s(u_c) \;=\; \frac{1}{k}\,\frac{1}{\ln\left(\frac{\sigma_f\, l\, \nu}{a\,\dot\sigma_{ext}}\right) - \ln u_c}\,. \tag{3.78}$$

Therefore $s(u_c)$ is a solution of the differential equation

$$y' \;=\; \frac{ky^2}{u_c}\,,$$

which is easily solved by separation of variables. Following some standard manipulations we have:

$$\frac{s_{c_1}}{s_{c_0}} \;=\; \frac{1}{1 - \frac{kT_{uc0}}{G_u - V\sigma_f}\ln\frac{u_{c_1}}{u_{c_0}}}\,, \tag{3.79}$$

where $s_{c_1} = s(u_{c_1})$, $s_{c_0} = s(u_{c_0}) = T_{uc0}/(G_u - V\sigma_f)$, so we obtain

$$\frac{\Delta T_{c_1}}{\Delta T_{c_0}} \;=\; \frac{1}{1 - \frac{kT_{uc0}}{G_u - V\sigma_f}\ln\frac{u_{c_1}}{u_{c_0}}}\,, \tag{3.80}$$

valid for arbitrary values of u_{c_1} and u_{c_0}. Equations (3.26) for $\sigma_k = 1$, (3.27) and (3.30) allow to write

$$u_f \;=\; -\,\frac{f^2(x_f)}{f'(x_f)}\,, \tag{3.81}$$

which can be used to replace the logarithm of the velocities by data directly related to the specimen geometry:

$$\frac{\Delta T_{c_1}}{\Delta T_{c_0}} \;=\; \frac{1}{1 - \frac{kT_{uc0}}{G_u - V\sigma_f}\ln\left(\frac{f^2(x_{c_0})\,f'(x_{c_1})}{f^2(x_{c_1})\,f'(x_{c_0})}\right)}\,. \tag{3.82}$$

If we consider only the asymptotic approximation corresponding to Example 3.2.2, and thus take only the inverse square root stress function, this result

can be expressed by the ratio of the arbitrary apparent toughness levels K_{c_1} and K_{c_0} and the particularly simple and suggestive expression

$$\frac{\Delta T_{c_1}}{\Delta T_{c_0}} = \frac{1}{1 - \frac{kT_{uc_0}}{G_u - V\sigma_f} \ln \frac{K_{c_1}}{K_{c_0}}} \tag{3.83}$$

follows. We want to emphasize that these results are exact within their respective models. It is apparent in all expressions, that the Master curve is not exactly valid, because in this case the denominator on the right hand side would have to be 1, which is not the case for two distinct levels c_1 and c_0. This follows clearly from (3.80), because the velocities in the logarithm are different. Still the concept can be rather useful in practice as the errors committed are remarkably small under circumstances applying to steel.
Especially the last of the three expressions allows a simple estimate of the error to be expected when using the Master curve approach. The increase of the apparent fracture toughness as function of temperature before completely ductile fracture occurs can usually be estimated by a factor of 20. Therefore the corresponding logarithm does not exceed 3. The energy barrier $G_u - V\sigma_f$ is of the order of 1 eV, but depending on the material and loading conditions can be higher or lower. The steels considered here have a transition temperature far below room temperature in the unirradiated state, so we may estimate $k\,T_{uc_0}$ by 1/50 eV or a still smaller value. The correction in the denominator is thus mostly smaller than 1/10 even in the most severe case of taking the apparent toughness levels as far apart as conceivable (and hence maximizing the logarithmic term). If the levels are closer together, the relative error will decrease and be almost zero for neighboring levels. Furthermore the relative error does not depend sensitively on the fracture stress σ_f as well, as long as the relative size of the energy barrier remains large compared to $k\,T_{uc_0}$. Therefore this result does not depend strongly on the bounds for σ_f as well.
The preceding estimation exhibits rather small relative errors when applying the Master curve concept in the transition region for steel. On the other hand, the absolute errors grow with increasing ΔG, hence increasing irradiation dose. Indeed, the deviations from the Master curve behavior claimed in [137] relate especially to strongly irradiated materials, while for low irradiation doses the predictions made with the model proposed in [137] essentially agree with Master curve behavior.
Based on our model, this type of behavior is expected for any material, which fails by cleavage based on a maximum principle stress criterion and shows a transition in a temperature range, where the thermal energy available to drive dislocations is sufficiently small compared to the effective energy barrier to be surmounted by them. The meaning of "sufficiently" derives from

the logarithmic factor in the denominator of the formulas and is therefore connected to the stress function, hence the geometry of the specimen in the vicinity of the notch. This type of explanation of Master curve behavior is indeed sufficiently general to be applicable to the whole class of ferritic steels and gives the sought explanation of the phenomenon, which is not connected to particular microscopic details. The analysis can at least be carried over to any model, which uses one microscopic variable, here u_f, as essential to explain the phenomenon. To the best of the authors knowledge, this is the first direct connection of Master curve behavior to general properties of dislocation dynamics (here the height of the energy barrier) and hence it constitutes a major result of this thesis. It is not the first attempt to explain Master curve behavior by microscopic properties of ferritic steels, though.
The model discussed in [154] was found to be consistent with a Master curve approach only if the local critical stress was subjected to temperature dependence without a quantitative model for its physical origin, though it was attributed to local dislocation activity to be analyzed based on elaborations of the Rice-Thomson approach, [175]. Ortner discusses Master curve behavior, [161], based on the Ortner-Hippsley approach, [162], and concludes that only a combined change of more than one parameter involved in this model can explain a constant slope.
The only model the author knows of, in which a connection to dislocation dynamics via the consequences of Orowan's equation, [159], on constitutive laws in macroscopic plasticity is attempted, is described in [104]. In [104] the Master curve behavior is attributed to the properties of the lattice resistance in body centered cubic (BCC) crystals, see [7, 194] for a discussion of the theory of dislocation glide in BCC crystals and [37, 38] for a corresponding investigation of pure iron. It is argued in [104], that only short-range obstacles to dislocation glide can be surmounted by thermal activation, so only these influence the temperature dependence of the flow properties and via the flow properties the fracture resistance-temperature relation. While we also propose to consider thermal activation only for short range obstacles, we do not fully agree with the assertion of [104], that only the lattice-resistance can be described as a short-range obstacle. Furthermore we do not describe the relationship between dislocation dynamics and fracture resistance indirectly by using flow properties like the yield stress. Based on their analysis, the authors of [104] use the constitutive model of Zerilli and Armstrong, [254], for plastic flow and the modified Griffith criterion of [235], incorporating the plastic flow into the effective surface energy, to discuss the effect of plastic flow on the apparent fracture toughness. They conclude, that there are three quantities, which may influence the temperature dependence of fracture toughness: Young's modulus E, the critical strain at crack initiation ϵ_{crit} and

the variation of the yield stress as given by the Zerilli-Armstrong constitutive model. They mention the consistent temperature dependence of Young's modulus of all ferritic steels, take ϵ_{crit} to be given by the Zerilli-Armstrong model without further justification and take the temperature dependence of the flow stress therefore as the only variable, which will distinguish the temperature dependence of fracture toughness for different ferritic steels and apparently different irradiation conditions, [104, Figure 2]. As they attribute the temperature dependence of the yield stress solely to the BCC-lattice resistance, they conclude that all steels with a BCC-lattice should show Master curve behavior, too.

From our perspective, there are the following comments on this: First of all, it seams not clear, whether ϵ_{crit} is a well-defined quantity in the typically inhomogeneous microstructure of steels and whether we are allowed to take the Zerilli-Armstrong value, especially as the authors cite experimental evidence of an exponential dependence on temperature, which should be checked to be consistent with the Zerilli-Armstrong value. Second, the strongest temperature decrease of the yield stress reported in [104, Figure 1] occurs in a temperature range, where the temperature dependence of the fracture toughness reported in [104, Figure 2] is comparatively weak. Indeed, according to our model, the validity of the Master curve hypothesis is not directly connected to the yield stress at all, so it would be desirable to have a more precise analysis of the relationship between yield stress and fracture toughness in the model of [104]. Third, if the temperature dependence of fracture toughness is attributed solely to the lattice resistance of iron, the embrittleling effect of copper and nickel forming precipitates on the nanoscale, see [54] and references therein, becomes difficult to understand, because the precipitates will in general not carry long range stress fields and should therefore be surmountable by thermal activation. Our model can be regarded to give a more general analysis in this context: If the effective energy barrier becomes arbitrarily large, the relative deviation from Master Curve behavior becomes arbitrarily small, so in the athermal limit there is no shape change in accordance with [104], while our theory predicts, that the relative and absolute deviations remain small, if the effective energy barrier is sufficiently large with respect to a certain scale set by the crack geometry and the irradiation dose is not too high.

We will now discuss the relations between temperature and irradiation condition on the one hand and yield stress and fracture resistance on the other hand in more detail. Just as in [104], the values of fracture toughness and yield stress as functions of temperature reported in [43] show no particularly strong correlation. In both cases the yield stress drops rather steeply in the low temperature range, where fracture is still brittle and the toughness

increases only slightly, if at all. On the other hand the yield stress drops far less and only in some part of the transition regime, where the toughness increases strongly. This is surprising at first, especially as there is a clear experimental correlation reported between the increase in the yield stress and decrease in fracture toughness as functions of irradiation, though there is also considerable scatter in the data, [26, 153, 154, 187].
Our model can explain this discrepancy. The absence of a direct correlation of yield stress and fracture resistance as functions of temperature is easy to understand: The description of the transition regime does not involve the macroscopic yield stress, so there is no indication of a particular correlation, though the model does not contradict that. In our model a certain *local* plastic strain rate at the local fracture stress is required for ductile fracture, which may not be connected to the overall plastic strain rate at which general yielding is observed, so temperature-dependent changes of both magnitudes need not correlate at all.
But if irradiation damage leads to an increased glide resistance, modelled by a contribution ΔG in equation (3.29), the yield stress will increase and fracture resistance decrease for a given temperature. It is apparent from Figure 3.10, that any change in the thermal glide resistance will immediately affect the apparent fracture resistance versus temperature behavior, since this is governed by the shallow parts of the curves in Figure 3.10, which shift as soon as the thermal glide resistance is changed. Equation (3.29) induces a correlation between the yield stress increase and a shift of a given toughness value to higher temperatures to be discussed now.
In [154] an empirical relation of $\Delta T = c\,\Delta\sigma$ is reported, where $\Delta\sigma$ is the yield stress shift and $c = 0.68\,\mathrm{K/MPa}$, but considerable scatter is present. This trend is corroborated by the data in [26, 153, 187], of which some relate to Charpy tests rather than to fracture toughness.
Before the derivation of such a correlation within our model, some remarks are in order: As long as there is no definite transition temperature for the comparison of yield strength shift and DBT, a precise correlation can not be established, so if there is no ubiquitous microscopic mechanism behind the DBT in steel, no strictly well-defined correlation is expected to emerge and any empirical data should show scatter, as they do in [154] and elsewhere. In the Master curve framework, the definite temperature T_0 is used for the comparison to the yield stress, so the limits of the validity of any correlation in the corresponding literature are given within our framework by the analysis of (3.80), the relative difference of the shift of two different fracture resistance levels. The correlation below depends in fact on a specific fracture resistance level through the corresponding temperature T_u in the unirradiated state, so its significance for other levels is limited by deviations from Master curve

behavior and this applies to any other corresponding correlation.
To derive the stated correlation, we assume the (average) macroscopic plastic strain rate $\dot{\epsilon}_{pl}$ at yielding as well as the mobile dislocation density ρ to be equal in the unirradiated and irradiated state. In this case any changes of the yield stress and fracture resistance will derive from the exponent of the Arrhenius-law (3.29). This direct connection to the dislocation velocity corresponds exactly to the discussion of the Master curve. We take a temperature T_u corresponding to a specific apparent fracture resistance level in the unirradiated state, where the energy barrier without the stress-induced contribution is G_u and $T_u + \Delta T$ as the transition temperature due to an irradiation induced shift of the energy barrier by ΔG. Correspondingly, we consider the yield stress σ_y at the constant temperature T_u and its shift $\Delta\sigma$ due to ΔG at the constant temperature T_u.
The assumptions of equal plastic strain rates and mobile dislocation densities imply

$$u(\Delta G = 0) = u(\Delta G \neq 0) \tag{3.84}$$

by the Orowan equation $\dot{\epsilon}_{pl} = b\rho u$, [159], where b is the length of Burgers's vector and the value of the dislocation velocity u is immaterial for the derivation. We combine this and the Arrhenius-law (3.29) to get

$$\frac{G_u + \Delta G - V(\sigma_y + \Delta\sigma)}{kT_u} = \frac{G_u - V\sigma_y}{kT_u}\,, \tag{3.85}$$

and therefore we have

$$\Delta G = V\,\Delta\sigma\,. \tag{3.86}$$

On the other hand the shift of the transition region is also due to the exponent in the Arrhenius-law and we obtain

$$\frac{G_u + \Delta G - V\sigma_f}{k(T_u + \Delta T)} = \frac{G_u - V\sigma_f}{kT_u}\,, \tag{3.87}$$

which implies

$$\frac{\Delta T}{T_u} = \frac{\Delta G}{G_u - V\sigma_f}\,. \tag{3.88}$$

We thus get the same equation as (3.76), which originates from the starting point (3.84) having a corresponding part in the derivation of the temperature shift for a specific level in the discussion of the Master curve. Inserting equation (3.86) into equation (3.88) finally gives the sought correlation between ΔT and $\Delta\sigma$:

$$\Delta T = \frac{T_u}{\sigma_y}\,\frac{V(\sigma_y + \sigma_f) - V\sigma_f}{G_u - V\sigma_f}\,\Delta\sigma\,, \tag{3.89}$$

where $V\sigma_f$ was inserted in the numerator for comparison purposes only. The effect of irradation in our model can be observed in Figure 3.9. The value T_u/σ_y is a natural estimate of the slope of the linear correlation, but usually a little to low. Therefore the second factor on the right hand side of (3.89) should be larger than 1, which is only possible, if $V(\sigma_y + \sigma_f)$ is larger than G_u. As the general yield stress can not exceed a reasonable fracture stress value in the transition regime, $V\sigma_f$ should be a significant fraction of G_u and $V\sigma_y$ can not be much smaller than $V\sigma_f$ in this case. This is roughly consistent with the empirical value of 0.68 for the product of the factors on the right hand side of (3.89), the factor according to our data in Table 3.2 for $T_u = 220K$ is in between 0.52 and 0.60, if we take 460 MPa as yield stress, corresponding to data from [104, Figure 2]. The difference in the values corresponds to the difference between the lower and upper boundary for the local fracture stress and can at least partly explain the scatter in the observed data. We stress again, that the shift depends on the chosen temperature level in our theory, which is apparent particularly in equations (3.88) and (3.89), and that the validity of a single factor is subject to restrictions just like the Master curve concept. The correlation warrants further discussion, which is given in subsection 3.2.5.
Another aspect of interest is the strain rate or loading rate dependence of fracture behavior, which we assess using the equation $u_c(T, \dot{\sigma}_{ext}) = u_c(T + \Delta T, \dot{\sigma}_{ext} + \Delta\dot{\sigma})$, keeping the other parameters fixed, compare the derivations concerning the Master curve behavior. This is equivalent to

$$\frac{\Delta T}{T} = \frac{kT \ln\left(1 + \frac{\Delta\dot{\sigma}}{\dot{\sigma}_{ext}}\right)}{G_u + \Delta G - V\sigma_f - kT \ln\left(1 + \frac{\Delta\dot{\sigma}}{\dot{\sigma}_{ext}}\right)}. \tag{3.90}$$

As the effective energy barrier is expected to be large compared to kT, just as in the case of the Master curve, the fraction on the right hand side of (3.90) will be small, unless the compared loading rates are orders of magnitude apart. Furthermore we note that a lower energy barrier, which will be associated with a tougher material, leads to a stronger rate dependence, so tougher materials are expected to be more rate sensitive. The effect of an increasing rate is nonlinear and increases the stronger the further the two compared rates are apart. There is apparently a critical rate, at which the value of u_c used to set up equation (3.90) can not be reached anymore, corresponding to a vanishing denominator on the right hand side of (3.90), but due to the relatively large energy barrier this is far beyond the range of concern.
In Figure 3.12, some curves for different loading rates at a single fracture

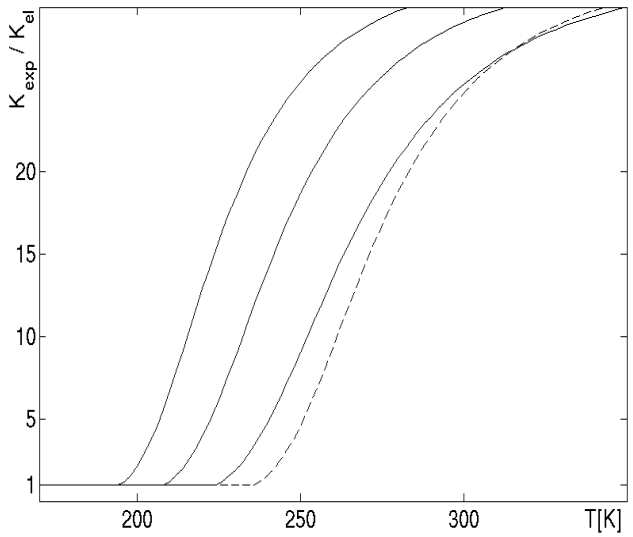

Figure 3.12: The apparent fracture resistance versus temperature for σ_f = 700 MPa is shown for three different strain rates in the unirradiated state (solid lines). The lowest strain rate (left curve) corresponds to the loading rate from Table 3.2, the other rates are increased by the factors 10 and 100. The dashed line corresponds to the same fracture stress and lowest strain rate, but an irradiated state in Figure 3.9, where it is dashed too.

stress value are compared to one of the curves from Figure 3.9. Each time, the rate has been increased by an order of magnitude, the lowest rate corresponding to the data from Table 3.2. Considering that the rates are two orders of magnitude apart, the effect is not very pronounced: The curve for the irradiated state corresponds to a shift of the yield stress of about 80 MPa, if we take the value of 460 MPa for the initial yield stress as above. Indeed, in [233] it was sometimes found difficult to determine a shift of T_0 caused by the strain rate, because the differences in the data for different strain rates were small compared to the general scatter. Apparently, the deviations from the Master curve concept for different strain rates are more significant than those for irradiation in the parameter range, as there is an intersection of two of the curves. We will assess this in the next subsection.

3.2.5 Discussion

The analysis of the dislocation dynamics model introduced here offers some explanation for fundamental observations in the fracture behavior of alloys exhibiting a DBT. The model allows the incorporation of different types of failure initiation sites and it is applicable to rather arbitrary notch/crack stress field. In this subsection we will first discuss its capabilities to explain the list in section 2.1 of experimental observations about the DBT, compare them also to the model of section 3.1 and then come back to certain circumstances we mentioned shortly in the preceding subsection.

- Item 1 and 2; the toughness increase and DBT: Both models we have proposed can explain a practically constant low temperature fracture toughness and a strong increase of toughness in the transition regime. According to both, plasticity influences the fracture behavior significantly only, if it is sufficiently strong. This explains the existence of different temperature regimes, the occurance of cleavage while there is significant plasticity and allows to take experimental toughness values at low temperatures as representative of the elastic toughness. The models explain the increasing toughness by an increasing shielding effect due to moving dislocations near the notch/crack tip.
  While the model of section 3.1 also gave a straight forward transition criterion, this is not at all easy for the second model, as there is no obvious material length scale for the fracture transition to compare the shielded region to. The only directly available length scale of interest is the size of the specimen.
  It is indeed reasonable to take a geometrically given length scale into account, as the geometry of the specimen influences the test results due to notch brittleness and size effects. It is known, that the question of ductility or brittleness is not answered by the material alone. This is corroborated by the insight, that the final chapter offers. Therefore we refrain from giving any other criterion, especially because we have not discussed ductile failure and plasticity-induced fracture.
  In the second model, the increase of the fracture resistance is explicitly connected to the dislocation velocity, but only because creation of dislocations was deliberately left out of consideration. The model can thus not contribute to the decision, whether creation or velocity of dislocations governs the DBT and in the author's opinion, there is no general answer to that question, so we will not contribute more to this debate.

- Item 1 and 2; the scatter in the toughness data: Both models can

explain the different levels of scatter in the toughness data at different temperatures and the strong scatter in the transition regime. In section 3.1 the scatter was explained by the sensitivity to parameter changes near to the point where apparent loading rate and plastic stress shielding rate compensate each other at a single crucial point (the crack tip). The explanation in section 3.2 depends on the heterogeneous microstructure leading to a certain but maybe small scatter in the local fracture stress levels. The small differences of local fracture stresses may cause large scatter in apparent toughness data, because the apparent toughness curves for different local fracture stresses are different and the whole area in between the curves represents possible results of toughness tests, see Figure 3.9. Combining those two explanations, we are lead to the conclusion, that there is probably no physical basis for the description of the apparent toughness in the transition regime as a single curve, as plasticity and local heterogenity will interact to make any single apparent toughness measurement virtually unpredictable in the transition regime.

- Item 3: Both models can explain the coexistence of plasticity and cleavage in the low temperature and transition regime. Only the model of section 3.2 can explain the coexistence of brittle and ductile crack extension in the transition regime. It does so by relating ductile fracture to a high local fracture stress and brittle fracture to a low local fracture stress.

- Item 4: Ductile fracture was not discussed within the models presented here, see [18, 19, 20, 246, 247, 248] for some recent contributions.

- Item 5: An expression for the rate dependence of any level of the apparent fracture toughness is given in equation (3.90). From this expression it is expected, that a relatively large effective energy barrier (compared to the thermal energy available), which implies approximate Master curve behavior, will also imply a relatively weak rate dependence.
  The Master curve behavior is notably violated in the parameter range chosen, compare Figure 3.12. Higher loading rates lead to shallower curves in our approach. While the experimental evidence is difficult to evaluate, [233], this result is not in line with some of the evidence available. While [233] claims the applicability of the Master curve concept under rather general circumstances, researchers from SCK/CEN (personal communication) found the opposite trend from the one predicted here: The toughness increase becomes steeper for higher loading rates. Furthermore the maximum toughness value increases. All investigators

agree on the decrease of fracture resistance and embrittlement due to an increasing strain rate in a non-corrosive environment, though.
The findings at SCK/CEN can not be explained within the present framework, because the loading rate enters in both models in a similar way, which can not explain a steeper fracture resistance increase. Therefore the reasons for such a behavior are probably to be found in detrimental effects of plasticity on fracture properties, that have been mentioned: Plasticity-induced cleavage might account for a steeper increase at higher loading rates, while a higher maximum toughness may be observed, because ductile void growth leading to failure is relatively slower at higher loading rates. The author can not offer definite explanations, though.

- Item 6: A major concern in fracture toughness testing is the validity of results obtained from small specimens when applied to large components for construction. The problem is the tendency of larger specimens to fail at lower loads and by cleavage instead of ductile rupture. This size effect in geometrically similar specimens is at variance with classical elasticity, which contains no intrinsic length scale to explain it. Therefore, models based on the microstructure of the material are necessary to obtain reasonable safety margins for design.
  The standard explanation for this effect in the engineering literature is, that the probability of finding a brittle carbide particle of the necessary size to initiate overall brittle fracture increases in larger specimens, as the absolute size of the highly stressed volume close to the crack tip increases, [230, 231]. This explanation is based on the assumption of a particular micromechanism for fracture, which is still not generally accepted, see [43] and references therein, so it is advisable to investigate alternatives. For Charpy V-notch tests, [21] and [50] discuss two different effects: For relatively small specimens, numerical simulations in [21] conform to the experimental results showing a higher transition temperature and therefore more brittle behavior, if the size increases. The reason is a material dependent and size independent length scale for the cleavage process included in the model of [21]: A certain fixed length over which a sufficient stress for cleavage must be reached, similar to [176].
  Our model predicts decreasing toughness and embrittlement at a fixed temperature for increasing specimen size in a fracture toughness test, because the absolute distance the dislocations travel in a certain time remains fixed, while the crack length increases, decreasing the relative size of the shielded region close to the crack tip. Hence, our model

also contains a material dependent and size independent length scale, but here it is the distance dislocations travel in a certain time given a certain driving stress.
In [50], the influence of material inertia in an elastic-viscoplastic macroscopic model is modelled, while scaling the cleavage length scale according to specimen size as opposed to [21]. In such a configuration, the investigators find only a negligible size effect for very small specimens and a beneficial effect of increasing size for sufficiently large specimens. This effect is not related to material properties, though. Size effects in plasticity have been a very active research field in the past decade, see the review [70].

- Item 7: Another type of geometry effect is associated with a changing crack depth or length-to-width ratio. We will focus on the crack depth. The effect of increasing crack length for short cracks according to classical elasticity is to increase the stress concentration and to cause stronger stress triaxiality at the crack tip, causing lower toughness and embrittlement. For a recent description of the elastic-plastic stress state close to the crack tip and analysis of this effect from the continuum perspective, see [41] and the references therein as well as [127].
  Stress concentration is also accounted for in our model, there is the same effect as above, the smaller ratio of dislocation velocity to crack length leads to a smaller shielded zone close to the crack tip, hence a higher transition temperature, a lower toughness and embrittlement.

- Item 8: Stress triaxiality influences the interrelation between the relevant tensile stress component for cleavage fracture and the resolved shear stress on the dislocation glide planes. A fully triaxial stress state has the relatively lowest shear stress driving the dislocations. This leads to a decreasing size of the zone of effective dislocation shielding, causing embrittlement and decreasing toughness. Triaxiality at the crack tip is caused by the presence of the crack itself, but can be imposed additionally by the applied stress through biaxial and triaxial loading. Within our framework, it can be accounted for by working out the relationship between the tensile stress causing fracture and the shear stress driving the dislocations explicitly.

- Item 9, 10 and 11: As has already been discussed extensively in the preceding subsection, the influence of irradiation on the fracture resistance-temperature relation is often described by shifting a single curve shape along the temperature axis, the so-called Master curve. There is also

some correlation between this shift and the increase of the yield stress due to irradiation. Both can be described within our model and their limitations be assessed by (3.82) and (3.89) and related relations given in the preceding subsection. The Master curve approach is valid within our model, if the thermal energy available during the transition is sufficiently small compared to the effective energy barrier to be surmounted. We want to discuss some further details here. The correlations reported in the literature are of the type cited from [154], linear functions through the origin, the slope is in between about 0.3 and 0.8 and considerable scatter is present. While we can explain the scatter by (3.89), because it shows the dependence of a certain temperature level, we obtain a value close to that reported in [154] only, if yield stress and fracture stress are not to far apart and their influence on the effective energy barrier is considerable. This is at variance with the values of the local fracture stress obtained from experiments by a Beremin-type approach, [22], based on equilibrium elasticity, which are usually much larger. While our result is influenced by the simplified effective energy barrier, the discrepancy is not explained by this. It seems more likely that a connection between cleavage fracture and plasticity due to crack nucleation by dislocations in a *dynamic* manner should be accounted for, equilibrium dislocation pile-ups are probably not enough to understand plasticity-induced cleavage. The equation (3.89) seems to hint at a specific need to modify our approach.
We have also analyzed the basic equation (3.84) used to derive the correlation. If one takes a different ratio of the dislocation velocities in the irradiated and unirradiated state, one obtains a linear function as well, which does not pass through the origin. As all the data available to the author points to a linear function through the origin, this alternative has been discarded.

- Item 12: Temperature dependent initiation sites for cleavage fracture are a consequence of the increasing size of the effectively shielded region close to the crack tip in our model. A temperature dependence of fracture initiation sites will thus be accompanied by an increasing plastic zone size. This effect can be at least partly be obscured by the influence of a heterogeneuos microstructure on the local fracture stress, explaining the negative result in [161].

- Item 13: The fracture resistance in the upper shelf at temperatures above the transition regime is determined by ductile fracture, which is

not described in this thesis, for the description of ductile fracture see the references mentioned under Item 4.

Additionally, we wish to expound some points connected to the choice of data in Table 3.2, the DBT and the appearance of the fracture resistance versus temperature curves in Figure 3.9.
Concerning the choice of data, the most important ones relate to the exponent of the Arrhenius-law and the constants determining the stress concentration. We have chosen a crack length short with respect to a macroscopic specimen but long with respect to the microstructure, with a tip radius which was much larger than an atomically sharp crack, as the crack faces are usually significantly separated before the crack starts to grow even if the material is quite brittle. The ratio of those magnitudes determines the stress concentration factor, which has a strong influence on the shape of the fracture resistance versus temperature curves here, because it determines, which part of the Arrhenius-function is visible in the transition regime.
The curves in Figure 3.9 are quite steep compared to the data shown in Figure 2.4 and in [104], but by some rather slight changes to the stress concentration factor much steeper or shallower curves could have been obtained. The obvious kink in the curves in Figure 3.9 for low temperatures, due to the effect of x_n could also have been made less prominent in this way. This hints at the role of geometry when trying to extract values of the apparent fracture toughness and the interpretation of fracture resistance data in general. Fracture properties are structural properties, not strictly determined by the material. Another hint at this are the very different maximum values of the fracture toughness (which is supposed to be a material property in the literature!) in Figure 2.4, [104] and elsewhere using CT-specimens and [43] using four-point bend specimens. While the data in [43] are always well below 100 MPa$\sqrt{\mathrm{m}}$, those in the other sources reach 200 MPa$\sqrt{\mathrm{m}}$ and more. The maximum values given are determined by ductile failure processes. If these involve a fixed material dependent length scale, like the distance dislocations travel in a certain amount of time, this could also relate this phenomenon to size and geometry. Figure 3.9 shows the K_{exp}(T)-curves up to a relative increase of more than 25, which is not observed in experiments because of ductile fracture. The onset of this is influenced by irradiation, which causes the maximum values of the apparent fracture resistance to decrease. This can also be understood only by a description of ductile fracture, and a rigorous explanation is not known to the author.
The most important choice for the temperature range of the transition regime is clearly the size of the energy barrier. The barrier is in the expected range of about 1 eV, the effective barrier for the unirradiated state in Figure 3.9

is 0.51 eV for the higher value of the local fracture stress and 0.59 eV for the higher value. It is reassuring, that these values and reasonable choices for the attempt frequency and the other data give a transition in the correct temperature range and a corresponding agreement of the shift due to irradiation, when compared to the cited macroscopic data from [104] for toughness and yield stress, which were used as orientation.
There were no data of the dislocation velocity in ferritic steels available, that could have been used instead. The apparent agreement with [104] could have been improved, but that is not the point of our investigation and would have involved some rather arbitrary choices. As we have not resolved any details of the actual dislocation dynamics, a better quantitative result could barely have been expected.
While the findings were outlined using a strongly simplified example, the methodology is applicable to quite general notch stress problems, as the qualitative results are independent of quantitative details. Effects of crack size and shape as well as loading rate are accounted for. The main goal of the approach, however, lies in establishing a connection between general qualitative macroscopic findings, like independence of fracture behavior on the lower shelf from plasticity, increase of cleavage toughness in the transition regime, scatter in the transition regime, temperature dependence of prevailing failure sites and Master curve behavior on the one hand, and the dislocation dynamics on the other hand with the possibility of refining the quantitative predictions by more detailed modeling. In the simplified setting discussed here, the dislocation velocity u_f at the fracture stress level plays the crucial role, whereas initial distribution of dislocations as well as their creation and annihilation kinetics were not considered. This will become necessary in a detailed analysis, if actual dislocation shielding rates at each point within the plastic zone are to be computed and compared to the local loading rate induced by the increasing external load, noting that for any real specimen, the predictive capabilities will also depend on a comprehensive knowledge of the microstructure.
We conclude this chapter with the discussion of some simplifications and aspects of general interest, pointing readers to recent literature along the way. First of all, we already noted the practical impossibility to predict a definite value of the fracture toughness in the transition regime. This is especially relevant for steel, where the sensitivity to changes in the local plastic flux is aggravated by complicated interactions with the microstructure. This effect, amply observed in experiments, is also found in [146, 196], where a crack moving by different mechanisms is considered. For a recent contribution to the usual engineering approach to scatter in the transition regime see [206]. From our perspective, it does not make much sense to try to fix a definite

transition temperature for a particular steel, because there is no basis to claim a simple criterion for a maximum temperature, above which cleavage is impossible. Just as in the case of toughness, we should be content with the estimation of a certain temperature regime in which the transition takes place, which can still depend on the loading history. From the point of view of engineering this corroborates the assertion that the only really safe way of designing a structure is to choose materials which assuredly operate out of the transition regime in any environmental conditions expected.
While our simple models can explain the qualitative features of the fracture toughness versus temperature data, they also force us to realize their insufficiency for a safe estimation of the extent of the transition region. As an example, due to the sensitivity of the results to slight changes in microstructure and plasticity, we should expect a significant influence of a moving crack, as it will affect plasticity around it. While this is not a vital consideration on the lower shelf, where the load-displacement-curve is practically linear up to the final instability due to cleavage, there can be a significant amount of stable crack growth in the transition region close to the upper shelf. This is also visible in the load-displacement-curves, which are classified into different types, [5, Figure 7.13]. There, load drops before final fracture are supposed to indicate stable crack growth. We do not consider moving cracks, so any influence they have on the quantitative prediction are beyond the models discussed here. On the other hand, there is no principle obstacle preventing the extension of the models to include moving cracks. Some references to the literature and description of static versus dynamic cracks may be found in [77, 78], a recent simulation of crack propagation in BCC iron is given in [228]. Brittle crack propagation may be advanced by the nucleation of microvoids, as reported in [118] documenting experimental findings. Simulations in [208] point to the relevance of "vacancy injection" into the material in front of blunted cracks for brittle behavior. The role of plasticity in these processes should be thoroughly investigated, as has been done since Cottrell, Stroh and Zener, [45, 202, 253], for crack nucleation. The role of plasticity-induced fracture in steel has not been discussed in this thesis at all, but certain results of the thesis hint at the importance of this phenomenon. According to chapter 4, we suggest an approach different from the usual ones in the literature, though.
The recent references mentioned above discuss the role of anisotropy and crack blunting for fracture. Again we have to be content to give further references: Effects of anisotropy are considered for example in [103, 228] and blunting in [15] and [81]. The only role of blunting in our model is by defining the maximum stress concentration at the crack/notch tip, as we describe the effect of plasticity on the stress state in front of the crack/notch tip by

shielding and ignore the mechanisms of crack advance. But blunting may influence the crack propagation mechanisms as well, so it may play an important role for a running crack. This becomes important, if there is some stable crack growth before rapid fracture, hence in the description of fracture in the transition regime. Furthermore we did not discuss the influence of the grain structure due to grain boundaries, [214], and grain size, [255]. We used the local tensile stress at a certain position as criterion for the onset of cleavage fracture instead of the classical approach of Ritchie, Knott and Rice, [176], where the critical stress is to be reached in a certain area or length for a two-dimensional model, see [27] for a more recent contribution in that direction.
As is obvious, there are a number of complicating factors left out of consideration, so the prediction of the toughness of any single specimen or even the actual width of the transition regime, especially its threshold at higher temperatures, can not be done with certainty. Still, we shall offer no excuse for that, as the situation is already summarized by Odette et al., [155], cited in section 2.1: There is no commonly accepted rigorous theory of the DBT and even our simple models clearly indicate that it is unlikely to be found if we continue to base the principal investigations on classical elasticity and introduce the material behavior at the microscale only by introducing some supposed to be well-defined parameters into a classical continuum mechanics analysis. The author expects true progress only by changing the paradigm of fracture research to more modern theories in physics, available to mechanics by an analogy between the solid state and electric superconductors discussed in the next chapter. Therefore we stopped the development of our models in the current state because:

- The models explain the basic qualitative features of the DBT of special interest.
- The second model rationalizes the Master curve concept and its limitations.
- Both models indicate that quantitative predictions of fracture toughness in the transition regime without extremely precise knowledge of geometry, microstructure, deformation history and composition and control of loading rate, temperature, etc. is basically impossible and none of the experimentally identified contributions across all relevant length scales may be left out of consideration.
- The developments in the next chapter offer a completely different view point about ductile versus brittle behavior of materials and the DBT, which is more in line with modern physics.

Finally, we shortly mention miscellaneous topics which may be of interest to some readers: The state of the art of modeling and simulation for crystal plasticity of polycrystalline bainitic steel structures under complex loading conditions in the transition regime can be assessed by consulting [125]. Our predictions for the fracture resistance versus temperature apply to toughness. The results of Charpy tests are modeled in [28] and critically discussed in [40]. One effect we have not discussed is warm prestressing. This means loading the material at high temperatures to a level that would cause cleavage at low temperatures. If the material is cooled afterwards, it will not fail by cleavage in the low temperature regime even if the load is kept fixed. This effect is easy to understand based on dislocation dynamics, as the permanent deformation caused by loading at high temperatures shields the external stress, which is not reversed by cooling. Yuritzinn et al., [252], describe it in a study of semielliptic cracks, while [236] observe detrimental effects of warm prestressing due to void damage, an expected problem when loading the specimens to strongly. The DBT is also an issue in polymers, [114], and geology, [14, 51]. On the smallest relevant length scales, the results in [49] relate electron densities to ductile versus brittle behavior in BCC metals, while on the macroscopic side [130, 131] and [121] offer considerations of some interest concerning plasticity and fracture and [149] applies neural networks to the DBT.

Chapter 4

An analogy to superconductivity

This short chapter is concerned with an unorthodox though not entirely new viewpoint concerning solid state mechanics, which allows to put the DBT into perspective in general physics by analogy with the well-known phenomenon of superconductivity. This viewpoint is unorthodox insofar as it is not generally adopted at this moment in order to understand solid state mechanics and especially not to solve concrete problems by researchers in this field. Nevertheless, the analogy between the magnetic field of a current carrying wire and the elastic field of a dislocation line has long been recognized, see [79, 115, 166] and, as mentioned in the introduction, [147, Chapter 2.6 and 8.1] contains a discussion with reference to basic works of Eshelby, [56, 57, 58], which can conveniently be found in [59].
The above mentioned analogy is between classical elasticity as applied to dislocations and the Maxwell theory of electromagnetism, thus two classical field theories. Up to now, there has been no mention of concepts from quantum mechanics in this work except for the ill-fated attempt to bring it to bear on solid state mechanics by Fitzgerald, [63]. The aim of this chapter is to discuss the analogy between the solid state in mechanics and the macroscopic quantum state of superconductivity and to demonstrate that useful conclusions can be drawn from this analogy. Furthermore it may allow to establish a connection between microscopic and macroscopic descriptions in mechanics that can be exploited to give explanations of phenomena (size effects for example) beyond the usual continuum treatments and which enables researchers to apply entirely different methods than have hitherto been used to understand solid state mechanics. We will not try any quantitative modeling but shall be content to point the reader to some of the literature relevant to such an endeavor.

4.1 The rigid body as superconductor

Superconductivity is the loss of practically any electrical resistance in many different materials below a certain critical temperature T_c. This loss may happen practically discontinuously or in a temperature range depending on the composition and purity of the material. The author took information about early works on superconductivity from the book [229], which is otherwise outdated, as it was published before the creation of the phenomenological Ginzburg-Landau-theory (1950), GL-theory in the following, as well as the microscopic theory of Bardeen, Cooper and Schrieffer (BCS-theory, 1957). Any textbook dealing with electric properties of solids usually contains a chapter about this topic, but the author will refer to the following more specialized treatises: The book [223] is a well-known introduction, the state of the art in classical superconductivity as of 1969 is documented in the comprehensive two-volume set [164, 165] edited by Parks and the magnetic flux structures, which are of special relevance in the following, are discussed in [92]. We will discuss the analogy to the classical (in the sense of older, not as opposed to quantum mechanics) theory of superconductivity, the more modern developments of high temperature superconductors beginning in 1986 are not needed, though it is interesting to observe differences between the classical superconductors and their high temperature counterparts. The book [17] was envisaged to give a comprehensive picture of superconductivity in 2008, but it seems already outdated, as a new class of iron-based superconductors was discovered that year and immediately incited the next surge of research activity in the area, [163].
Superconductivity was first discovered in 1911 by Kammerlingh-Onnes, who found that the electric resistance of mercury vanished practically discontinuously at a critical temperature of about 4,2 K. At that time no explanation of this phenomenon was known. A very important step towards understanding the classical superconductors was made in 1933, when Meißner and Ochsenfeld discovered the effect known in Germany as Meißner-Ochsenfeld-Effekt and Meissner effect abroad: An applied magnetic field is expelled from a specimen if superconductivity sets in. This was not expected for a perfect conductor based on Maxwell's theory and showed, that superconductivity was indeed an extra phase of the material in the sense of thermodynamics, [229]. As described in [120, chapter 6], the Meissner effect is more fundamental to physics than the loss of resistivity, as the Meissner effect implies perfect conductivity.
Before continuing the discussion of superconductivity we will now establish the basic analogy between superconductivity implied by the expulsion of a

magnetic field from a material and condensed matter mechanics. The role of the electric current in electromagnetism is the one of mechanical forces in mechanics, while the magnetic field corresponds to mass transport. In an ideal gas, the interactions between the constituents (molecules) are limited to collisions and mass transport is not restricted in any way. Indeed, it is impossible to conduct a mechanical force from one point to another, if there is a significant space filled with an ideal gas in between, as is obvious from everyday experience. This changes if there is a phase transition, which changes the compressible fluid (gas) to an incompressible fluid (liquid). In the liquid, mass transport that changes the volume occupied by the liquid is forbidden. In this case it becomes possible to conduct a force (pressure) from one point to another by containing the liquid in a tube, which prevents the liquid from changing its shape arbitrarily. This principle is utilized in hydraulics. If a material is in the solid state, idealized as rigid body, it is also impossible to change its shape, so any relative mass transport within the volume occupied by the material is forbidden, it may only move as a whole. Any such structure is known from experience as perfect conductor for mechanical forces, which is also evident from Newton's third law. Therefore the mechanical Meissner effect of blocking mass transport in a certain volume allows mechanical superconductivity of forces. Strange though it seems, up to now the author has not found a discussion of this simple analogy in the literature in this form.

In order to relate deformable solids to superconductivity, we must extend its discussion first. Ginzburg and Landau originally dealt with superconductors of type I only. Type-I-superconductors expel a weak external magnetic field H from the bulk of their volume up to a critical field strength H_c, while immediately above this critical external field superconductivity breaks down completely in a sample whose dimensions perpendicular to the applied field are small. If the sample is not small in this sense, superconductivity will break down in parts of the sample at a value of the applied field lower than H_c, given by $H_c/(1-D)$. Here D is the so-called demagnetization coefficient. We have $0 \leq D < 1$ and D is determined by a process essentially similar to notch stress analysis and it depends on the specimen geometry. At H_c superconductivity has broken down in the whole sample and the region where magnetic flux penetrates and the electric conductivity switches to normal growths while increasing the field from $H_c/(1-D)$ to H_c. This is called the intermediate state. For type-I-superconductors the surface energy between the sections of superconductivity and normal conductivity is positive, so the extent of surfaces is minimized by minimization of the internal energy. Additionally, entropy maximization enforces disorder and as a result areas of superconduction and normal conduction form intricate patterns observable

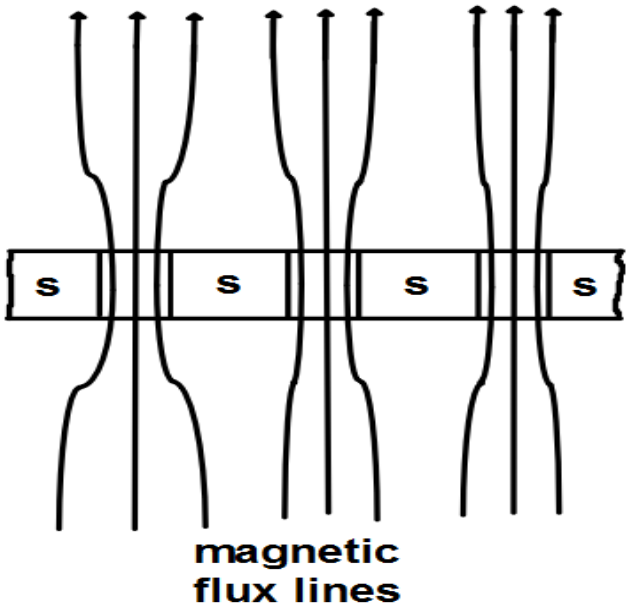

Figure 4.1: A schematic drawing of the intermediate state following Figure 2.3 in [92]. The superconducting parts are denoted by s, while the magnetic flux enters the specimen in the other parts.

in experiments, [92, chapter 2]. A schematic drawing of the intermediate state following Figure 2.3 in [92] is given in Figure 4.1.
On the contrary, type-II-superconductors, discussed first by Abrikosov in 1957 based on the GL-theory, have a negative surface energy between the sections of superconductivity and normal conductivity. They expel the magnetic field from their bulk only up to a first critical strength H_{c1}. For higher external field strengths, magnetic flux enters the superconductor by vortex lines each carrying a fixed magnetic flux quantum, but superconductivity is retained close to H_{c1}. These vortex lines form regular lattices in pure specimens, which were amply observed experimentally, [60, 92]. Only if the external magnetic field reaches the higher value H_{c2}, superconductivity breaks down completely. Depending on the circumstances, H_{c2} may be much larger than H_{c1}. In contrast to type-I-superconductors, minimization of the internal energy causes distribution of the flux lines throughout the whole sample, maximizing the "surface" between the cores of the vortex lines and the superconducting surrounding area. The distance between the flux lines is governed by the external field strength, see Figure 4.2.
GL-theory can describe both types of superconductors, as it contains the ratio κ of two length scales: The penetration depth λ introduced in 1935 by the

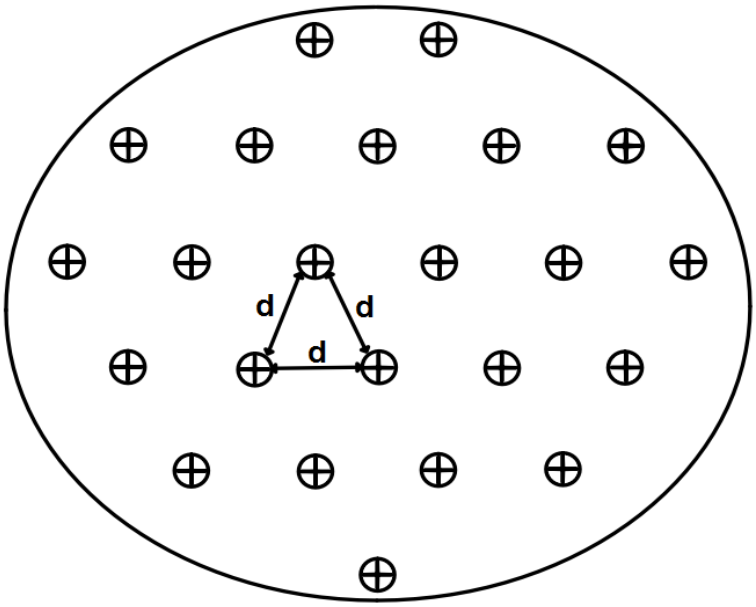

Figure 4.2: Flux line penetration perpendicular to the drawing plane in a type-II-superconductor. A regular triangular lattice is often observed. The distance d between the vortices depends on the external field strength.

brothers Fritz and Heinz London measuring the width of the surface layer, in which an exponentially decreasing magnetic field penetrates into the sample, and the coherence length ξ, new to the GL-theory, which describes the lengths scale on which the so-called order parameter changes considerably. The order parameter governs superconductivity in the GL-theory, where it corresponds to the density of superconducting electron-pairs. We shall not explain the theory in any detail, as we will not use it later on. We have $\kappa = \lambda/\xi$ and if κ is small, so the penetration depth is small compared to the coherence length, the GL-theory predicts type-I-behavior, while if κ is large, so the penetration depth is large compared to the coherence length, type-II-behavior is expected.
Now we are in a position to extend the discussion of the analogy we have in mind. On the one hand, type-I-behavior in mechanics corresponds to a material, which is initially superconducting mechanical forces, so it is a rigid body. If we put this material into an field, meaning an external load in this case, it will at first deform according to elasticity and will essentially retain its load bearing and hence force conducting capacity until a certain load is reached. At this external load, an area of allowed mass transport is created in the material at a position x obtainable from a stress distribution analysis leading

to a stress concentration factor $f(x)$, which corresponds to $1 - D$, where D is the demagnetization factor discussed above. Due to mass transport being allowed in this area, the material separates. This simply means the material fractures and the process can become unstable. The area of allowed mass transport is localized to the most highly stressed part in the specimen, but this may traverse the specimen rapidly, unless the maximum load is lowered by some intrinsic or extrinsic process. Therefore type-I-behavior for electromagnetic superconductors is identified with brittle behavior in mechanics.
On the other hand, type-II-behavior corresponds to dislocations carrying a fixed deformation quantum, corresponding to the Burgers vector, penetrating the specimen in the highly stressed region and traveling under the applied load, causing permanent deformation without fracture, until a possibly far larger external stress is reached. During this process the specimen retains a significant load bearing capacity. Hence we identify type-II-behavior with ductile failure.
In this context, the DBT is interpreted as a transition from the type-I-behavior of brittle fracture at low temperatures to the type-II-behavior of ductile fracture at high temperatures.
A major difference between the electromagnetic and mechanic superconductors is the geometric setting: While in electromagnetism the specimen of superconducting material is the setting where the process takes place, it is not in itself part of this process, though its shape and relative position with respect to the external field are relevant. In mechanics, the specimen itself is subject to the changes due to the external field/load. Therefore geometric considerations were a major issue from the very beginning of the development.
Common to both cases is the ubiquity of the phenomenon at appropriate temperatures, its occurence in numerous materials, whose microstructures do not resemble one another at all.

4.2 Consequences of the analogy

In this section we will discuss the consequences following from the notion of the rigid body as superconductor for mechanical forces. Along the way some references to relevant literature will be given, but as the author is not an expert on superconductivity, these references will not give an even nearly comprehensive picture. One general observation may still be mentioned: Researchers in superconductivity and general physics use analogies with plasticity more often than researchers in plasticity use the analogy with superconductivity.

We begin by discussing the usual stress-strain-curve recorded in a standard

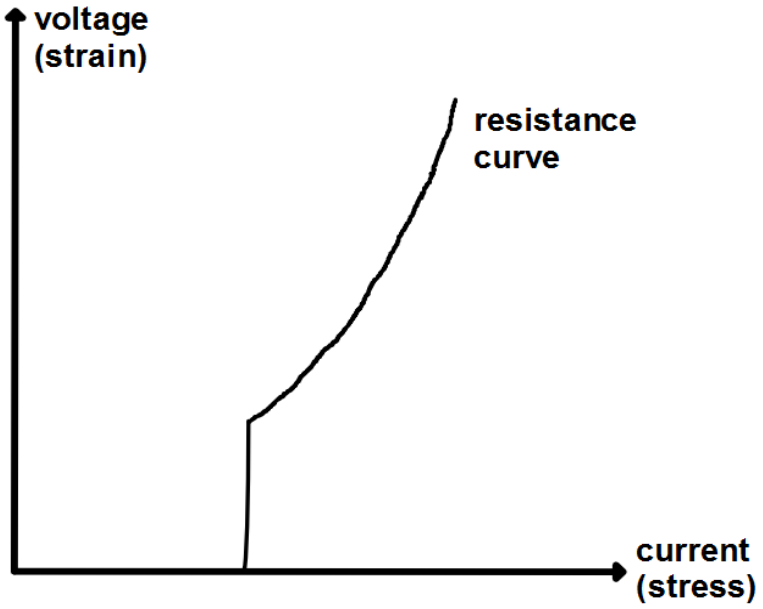

Figure 4.3: A schematic reproduction of Figure 1 in [39]. We have added the terms stress, strain and resistance line. Note the exchanged roles of stress and strain compared to the usual way to depict the stress-strain-curve, see Figure 2.2.

tensile test. The earliest article mentioning an analogy the author has studied in detail is [39], describing the following setup: A magnetic field H is applied to a superconductor of type II perpendicular to a current. H is of such a magnitude, that the specimen contains magnetic flux lines, $H_{c1} < H < H_{c2}$. Electric current and voltage are measured and Figure 1 in [39] is a plot of voltage as function of the current in the specimen at constant H, see the schematic drawing in Figure 4.3. The actual topic of [39] is not of interest, but Figure 4.3 shows our point: If the stress and hence the force conducted by the specimen is to be increased, this will result in stronger deformation, leading to a growing resistance to force conduction. In the case of a solid, the resistance will increase gradually until it breaks, resulting in a complete breakdown of force conduction, hence infinite resistance. Figure 4.3 highlights the analogy we are considering by reversing the usual role of abscissa and ordinate in the stress-strain curve. This has a bearing on the interpretation of the plastic part of the stress-strain-curve. Usually one describes the increasing part of the usual stress-strain-curve in the plastic regime by so-called hardening, a deviation from a horizontal line corresponding to perfect

plasticity. We suggest, that attempts to explain macroscopic stress-strain-curves might profitably be guided by a consideration of successive softening as deviating from elastic behavior. Explanations by hardening are common nowadays, [113], because hardening was found already in early investigations, [188], and has been thoroughly investigated empirically. The microstructure in a hardening material changes indeed, because the number of dislocations grows rapidly. Still, a true theoretical understanding is beyond the means of classical dislocation-based plasticity, while modeling has met with some empirical succes, [113].
Concerning the DBT itself, it is significant, that the GL-theory is generic and an outgrowth of Landau's theory of second order phase transitions. It applies to many different materials. From this point of view, we should not expect a criterion for the DBT based on materials properties alone, far less one of general validity. Especially from this perspective, the DBT and its microscopic origins are properties of a structure under certain conditions and not connected to a certain material, they depend on size and shape, we agree in this respect with [21].
The analogy suggestes to apply time-dependent GL-theory and a novel way to couple microscopic theory and quantum phenomena to macroscopic solid state mechanics by finding an analogy to the BCS-theory of superconductivity. A gauge theory of disorder fields has been developed by Kleinert, [108], and applied in [107] to dislocation mediated melting of crystals and the order of the superconducting phase transition. The close similarity between the GL-theory of superconductivity and his proposed theory of dislocation melting is demonstrated in the mentioned publications, but in this case of disorder field theory, Kleinert describes a finite penetration depth of stress in the material above a critical temperature. The roles of stress, mass transport and temperature are therefore reversed compared to the approach proposed here. Kleinert has written extensive monographs about the application of gauge theory to condensed matter, [109, 110].
Hove, Mo and Sudbø carried out large scale Monte-Carlo simulations to investigate the GL-equations near the critical temperature, [91, 144], and found close agreement between their simulation results and Kleinert's theory concerning the order of the superconducting phase transition. It is especially interesting, that they furthermore found a thermally induced crossover between type-I and type-II-behavior for the (electromagnetic) superconducting state. This is what we are looking for in solid state mechanics, as its analog constitutes a thermally induced DBT. There is a problem though, the works cited up to now deal only with the time-independent GL-theory. As we are interested in developing plastic zones close to cracks and notches, we need to apply the time-dependent GL-theory, whose development began around

1965. For a review of the early contributions to the time-dependent case and the problems arising therein see [48].
The mathematical theory of the GL-equations has seen major activity during the last two decades and there are by now several monographs dealing with mathematical aspects of the GL-equations, [23, 64, 89, 186]. As the time-dependent GL-theory is of special interest for the analog considerations in solid state mechanics, we specifically mention [197] and [217]. The latter actually includes an applied boundary current, which corresponds to an external force, so it deserves special attention, if the analogy is to be exploited in the future.
We close this chapter by some remarks on possible progress due especially to the superconductivity-based approach. First of all, one of the major problems in applications is the effect of the specimen size on the experimental results, as discussed at the end of chapter 3. The GL-equations shed completely new light on this question, as they contain two length scales, while the equations of equilibrium elasticity do not possess any. To assess the influence of the specimen size is one of the open problems in [186, chapter 15] and there has been recent work in [119] on the subject. Another possibly promising approach is to consider the nonlinear Schrödinger equation as applied to superfluidity and Bose-Einstein condensates, [203]. One can also consider quantized vortices in this setting. An example of its possible usefulness is the discussion of the interaction between vortices and cavitation in [67, 102]. This might shed light on plasticity-induced (cleavage) fracture, another of the problems mentioned at the end of chapter 3. In this context we give a general remark about dislocation dynamics simulations. A recent observation, [213], states that standard dislocation dynamics has not yet given explanations of effects like necking, which are observed in experiments and relate to changes of the geometry of the specimen in a test. In view of the connection between mass transport and dislocation movement, it seems mandatory to monitor mass conservation and mass transport explicitly during the simulations. The setup and boundary conditions must properly accomodate this aspect beyond the formal creation and movement of a dislocation through a necessarily finite simulation box. Otherwise, one should indeed not suppose to produce such effects intrinsically from dislocation dynamics simulations. In the opinion of the author another major challenge is the creation of a theory corresponding to the microscopic BCS-theory of superconductivity, as there is no obvious analog of the Cooper pair, a pair of two electrons, which is the charge carrier in the BCS-theory. A satisfactory BCS-theory of mechanical superconductivity should account for the fact, that there need not be any microscopic order in the arrangement of the atomic nuclei in a solid body.
We leave those developments for future work though, as their realization, if

accomplished at all, will most probably amount to material for many PhD's. Still, the author included this purely descriptive chapter, because he considers the analogy between solid state mechanics and superconductivity as fundamental and supposes that serious efforts in its investigation will finally turn out to be very profitable. A change of paradigm in the research on the microscopic origin of failure of materials from classical to modern physical theories should result in significant progress.

Chapter 5

Begriffserklärungen

- brittle fracture: Sprödbruch, tritt im Alltag z. B. bei Glas und Porzellan auf. Sprödbruch ist definiert durch die makroskopischen Eigenschaften des Bruchvorgangs. Das Material deformiert sich praktisch nicht permanent, so dass die Einzelteile nach dem Bruch in ihrer alten Form zusammengesetzt werden können. Dadurch speichert das Material wenig Energie, der Bruch erfolgt ruckartig praktisch ohne Vorwarnung und insbesondere bei Vorhandensein von gefährlichen Defekten bei verhältnismäßig geringen äußeren Kräften. Sprödbruch muss daher in der Praxis unbedingt vermieden werden.

- ductile fracture: Duktiler Bruch, wird im Alltag üblicherweise bei Stählen beobachtet und ist wie Sprödbruch durch das makroskopische Erscheinungsbild des Bruchvorgangs definiert. Das Material speichert hierbei viel Energie durch permanente Deformation, was im Extremfall zu Materialversagen durch plastische Instabilitäten wie Einschnürungen (vgl. necking) führt. Durch die entsprechende Energiespeicherung bricht das Material erst bei relativ großen äußeren Kräften und nachdem die permanente Deformation deutlich zu bemerken ist.

- cleavage fracture: Spaltbruch, wird oft synonym mit Sprödbruch verwendet, ist aber durch die Art des mikroskopischen Bruchvorgangs definiert. Bei einem Spaltbruchvorgang trennt sich das Material entlang einer wohldefinierten Ebene ohne wesentliche permanente Deformation in seiner Umgebung, was zu glatten Bruchflächen führt, die auch mit bloßem Auge als solche zu erkennen sind. Spaltbruch führt zu sprödem Materialversagen, was oft zur synonymen Verwendung beider Begriffe führt.

- creep: Kriechvorgang bei Materialversagen. Bei entsprechender Materialbelastung finden relativ langsame permanente Deformationsvorgänge innerhalb eines Materials statt, z. B. durch diffusionsartige Prozesse. Diese können bei entsprechender Dauer der Belastung zu Materialversagen durch permanente Deformation oder Bruch führen. Aufgrund der Beteiligung von Diffusion sind diese Vorgänge unter Langzeitbelastung bei hohen Temperaturen besonders relevant. Kriechtests nehmen Tage, Wochen oder noch längere Zeiträume ein und werden oft durch Belastung der Probe mit einem konstanten Gewicht durchgeführt.

- fatigue: Ermüdung, Materialversagen bei wechselnden äußeren Belastungen. Unter Wechselbelastungen versagen Proben üblicherweise bei erheblich geringeren maximalen Beanspruchungen als bei konstanter Last oder konstanter Lastrate. Die Wechselbelastung kann sowohl in einem zeitlichen Wechsel von stärkerer und geringerer Belastung z. B. durch Zug als auch in einem Wechsel von Zug- und Druckbelastung bestehen. Üblicherweise testet man durch die Wiederholung eines festgelegten Lastzyklus und zählt die Anzahl der Zyklen bis zum Materialversagen.

- transgranular fracture: intrakristalliner Bruch. Mikroskopisch bestehen Kristalle in der Regel aus einzelnen kleinen Kristallen verschiedener Orientierung, die im Deutschen Körner, im Englischen grains genannt werden. Transgranular bedeutet dann, dass der Bruchvorgang das Innere einzelner Körner durchtrennt.

- intergranular fracture: interkristalliner Bruch. Der Bruchvorgang erfolgt entlang der Grenzen verschiedener Körner.

- grain boundary sliding: Korngrenzengleiten, ein Prozess, der zum Beispiel während Kriechvorgängen auftritt. Korngrenzen gleiten gegeneinander ab, was wie Versetzungsbewegung zu permanenter Verformung führt und mit entsprechenden lokalen Spannungsüberhöhungen verbunden sein kann.

- Lüders bands: Lüdersbänder, Bänder von Versetzungen, die sich lokalisiert entlang einer Probe bewegen, so dass sich die Probe nicht als Ganzes plastisch deformiert.

- necking: Einschnürung. Bei hohen Belastungen wird die homogene plastische Verformung instabil, in der Folge konzentriert sich die plastische Deformation auf einen kleinen Bereich der Probe, in welchem diese immer dünner wird. Da dort dann ein geringerer Materialquerschnitt

eine entsprechend höhere Spannung aufnehmen muss, setzt sich dieser Prozess instabil fort und führt bei entsprechender äußerer Belastung zum Materialversagen. Dieses kann durch vollständiges Einschnüren bis auf eine schmale Spitze oder auch Sprödbruch bei genügend kleinem Materialquerschnitt eintreten.

- tensile stress, in-plane and anti-plane shear stress: Zugspannung (Mode I), Schubspannung senkrecht zur Rissfront (Mode II) und Schubspannung parallel zur Rißfront (Mode III), siehe Figure 5.1.

- uniaxial tensile stress state/test: Einachsiger Zugspannungszustand bzw. -test, biaxial zweiachsig, triaxial dreiachsig, siehe Figure 5.2. Mehrachsige Spannungszustände können auch als Druckspannungszustände oder Kombinationen aus Druck- und Zugspannung vorliegen.

- DBT: Abkürzung für ductile-brittle-transition, deutsch stets in anderer Reihenfolge: Spröd-duktil-Übergang, im Englischen ist BDT ebenfalls in Gebrauch.

- BCC: Kubisch-raumzentriertes Kristallgitter, siehe Figure 5.3.

- LEFM: Abkürzung für linear elastic fracture mechanics, linear-elastische Bruchmechanik.

- RPV: Abkürzung für reactor pressure vessel, Reaktordruckbehälter.

- VOCALIST: Abkürzung für Validation of Constraint-Based Assessment Methodology in Structural Integrity, Projekt im fünften Rahmenprogramm von EURATOM (European Atomic Energy Community).

- PERFECT: Abkürzung für Prediction of Irradiation Damage Effect in reactor Components, Projekt im sechsten Rahmenprogramm von EURATOM (European Atomic Energy Community).

- FRAME: Abkürzung für fracture mechanics based embrittlement, Projekt im fünften Rahmenprogramm von EURATOM (European Atomic Energy Community).

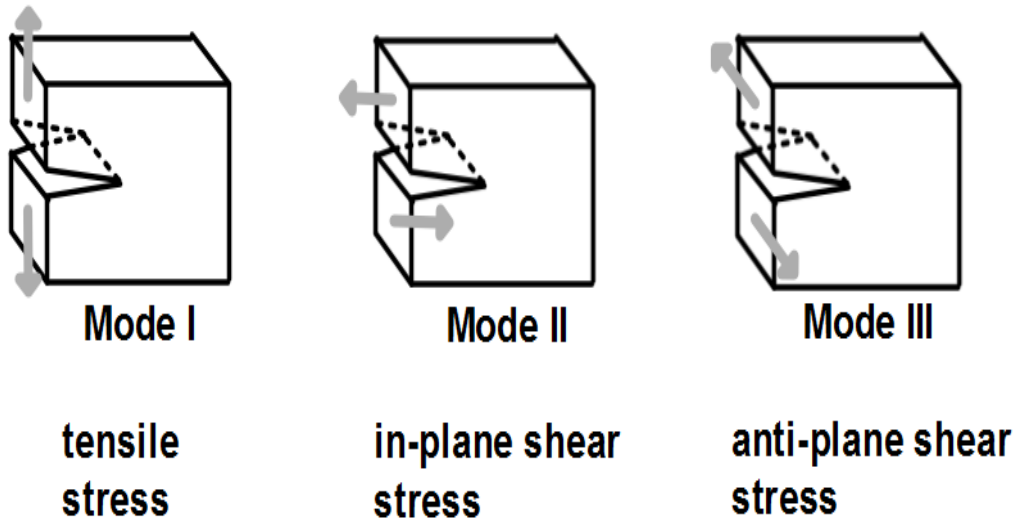

Figure 5.1: Beschreibung von Mode I, Mode II und Mode III, die grauen Pfeile verdeutlichen die angelegten Spannungen in den verschiedenen Fällen.

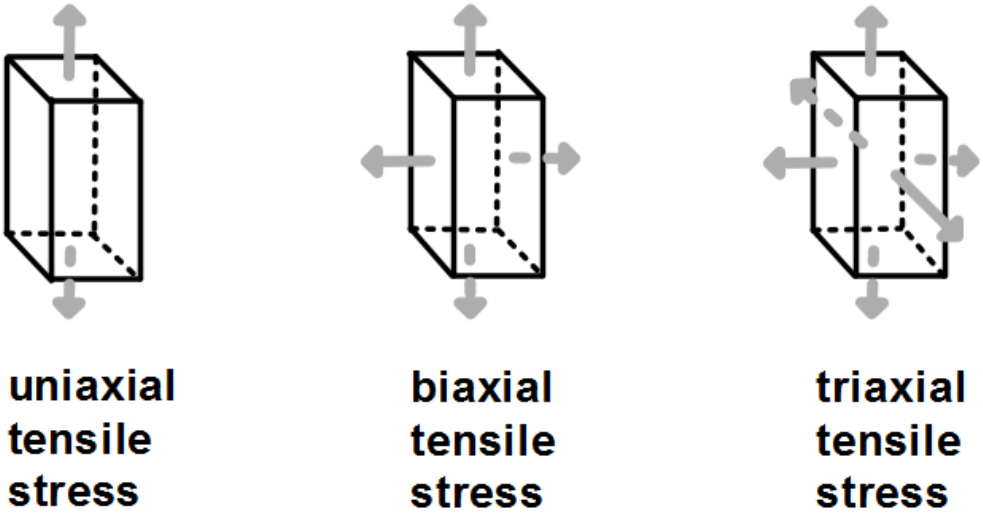

Figure 5.2: Ein-, zwei- und dreiachsige Zugspannung.

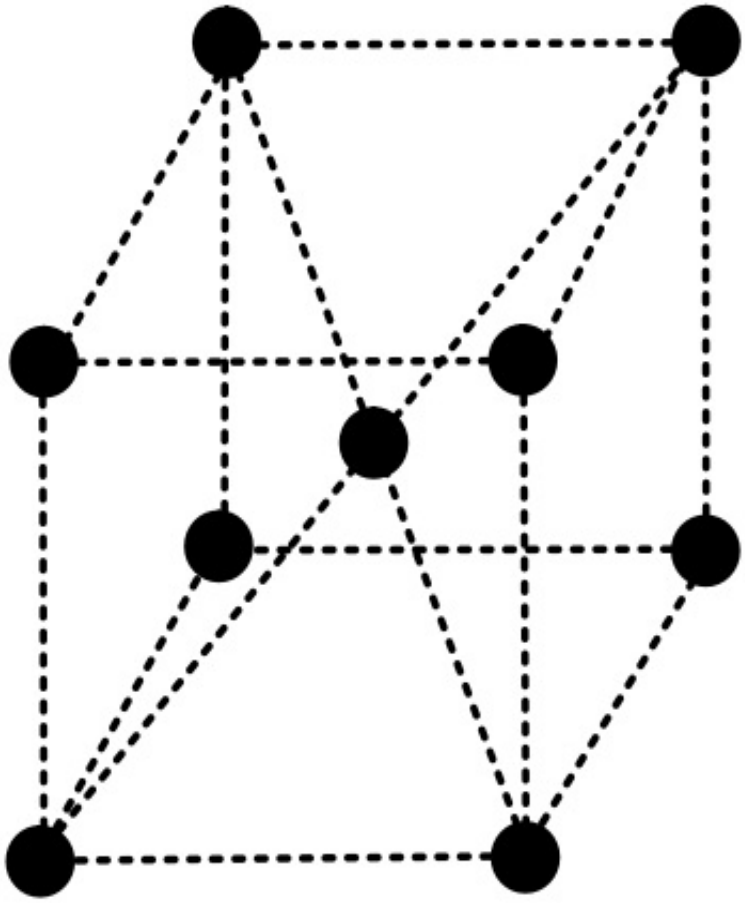

Figure 5.3: Kubisch raumzentriertes Kristallgitter, englisch body-centered cubic, BCC.

Bibliography

[1] https://fp6perfect.net/site/index.htm.

[2] E 1921 - 97: Standard Test Method for Determination of Reference Temperature, T_0, for Ferritic Steels in the Transition Range. Technical report, ASTM, 1998.

[3] G. B. Airy. On the Strains in the Interior of Beams. *Phil. Trans. R. Soc. A*, 153:49–80, 1863.

[4] S. Amelinckx. *The direct observation of dislocations*, volume Supplement 6 of *Solid State Physics*. Academic Press, 1964.

[5] T. L. Anderson. *Fracture Mechanics Fundamentals and Applications*. CRC, Taylor & Francis Group, 3 edition, 2005.

[6] A. S. Argon. Mechanics and Physics of Brittle to Ductile Transitions in Fracture. *ASME J. Eng. Mat. Tech.*, 123:1–11, 2001.

[7] A. S. Argon. *Strengthening mechanisms in plasticity*, volume 4 of *Oxford series on materials modelling*. Oxford University Press, 2008.

[8] A. S. Argon and B. J. Gally. Selection of crack-tip slip systems in the thermal arrest of cleavage cracks in dislocation-free silicon single crystals. *Scr. Mat.*, 45:1287–1294, 2001.

[9] A. S. Argon and E. Orowan. Crack nucleation in MgO Single Crystals. *Phil. Mag.*, 9:1023–1039, 1964.

[10] C. Atkinson. The interaction between a dislocation and a crack. *Int. J. Frac. Mech.*, 2:567–575, 1966.

[11] C. Atkinson and D. L. Clements. The influence of anisotropy and crystalline slip on relaxation at a crack tip. *Acta metall.*, 21:55–60, 1973.

[12] G. I. Barenblatt. The Mathematical Theory of Equilibrium Cracks in Brittle Fracture. *Adv. Appl. Mech.*, 7:55–129, 1962.

[13] E. Bayraktar, D. Kaplan, F. Schmidt, H. Paqueton, and M. Grumbach. State of art of impact tensile test (ITT): Its historical development as a simulated crash test of industrial materials and presentation of new "ductile/brittle" transition diagrams. *Journal of Materials Processing Technology*, 204(1-3):313 – 326, 2008.

[14] J.-P. Bellot. Extensional deformation assisted by mineralised fluids within the brittle-ductile transition: Insights from the southwestern Massif Central, France. *Journal of Structural Geology*, 29(2):225 – 240, 2007.

[15] G. E. Beltz, D. M. Lipkin, and L. L. Fischer. Role of Crack Blunting in Ductile Versus Brittle Response of Crystalline Materials. *Phys. Rev. Letters*, 82:4468–4471, 1999.

[16] G. E. Beltz and J. R. Rice. Dislocation nucleation at metal-ceramic interfaces. *Acta metall. mater.*, 40:S321–S331, 1992.

[17] K.-H. Bennemann and J. B. Ketterson, editors. *Superconductivity*. Springer, 2008.

[18] A. A. Benzerga. Micromechanics of coalescence in ductile fracture. *J. Mech. Phys. Solids*, 20:1331–1362, 2002.

[19] A. A. Benzerga, J. Besson, and A. Pineau. Anisotropic ductile fracture part I: experiments. *Acta Mater.*, 52:4623–4638, 2004.

[20] A. A. Benzerga, J. Besson, and A. Pineau. Anisotropic ductile fracture part II: theory. *Acta Mater.*, 52:4639–4650, 2004.

[21] A. A. Benzerga, V. Tvergaard, and A. Needleman. Size Effects in the Charpy V-Notch Test. *Int. J. Fract.*, 116:275 – 296, 2002.

[22] F. M. Beremin. A Local Criterion for Cleavage Fracture of a Nuclear Pressure Vessel Steel. *Met. Trans. A*, 14A:2277–2287, 1983.

[23] F. Bethuel, H. Brezis, and F. Hélein. *Ginzburg-Landau Vortices*, volume 13 of *Progress in Nonlinear Differential Equations and Their Applications*. Birkhäuser, 1994.

[24] W. D. Biggs. *The brittle fracture of steel*. MacDonald and Evans, 1960.

[25] B. A. Bilby, A. H. Cottrell, and K. H. Swindon. The spread of plastic yield from a notch. *Proc. R. Soc. A*, 272:304–314, 1963.

[26] J. Böhmert, H.-W. Viehrig, and A. Ulbricht. Correlation between irradiation-induced changes of microstructural parameters and mechanical properties of RPV steels. *J. Nuc. Mat.*, 334:71–78, 2004.

[27] R. Bonadé, P. Mueller, and P. Spätig. Fracture toughness behavior in the ductile-brittle transition region of the tempered martensitic Eurofer97 steel: Experiments and modeling. *Engineering Fracture Mechanics*, 75(13):3985 – 4000, 2008.

[28] C. Bouchet, B. Tanguy, J. Besson, and S. Bugat. Prediction of the effects of neutron irradiation on the Charpy ductile to brittle transition curve of an A508 pressure vessel steel. *Comp. Mat. Sci.*, 32:294–300, 2005.

[29] J. Bošanský and T. Šmida. Deformation twins - probable inherent nuclei of cleavage fracture in ferritic steels. *Mat. Sci. Eng. A*, 323:198–205, 2002.

[30] Y. Brećhet and F. Louchet. A physical approach to the toughness problem: From thermodynamics to kinetics - I. The homogeneous case. *Acta metall. mater.*, 41:783–791, 1993.

[31] M. Brede. The brittle-to-ductile transition in silicon. *Acta metall. mater.*, 41(1):211–228, 1993.

[32] M. Brede and P. Haasen. The brittle-to-ductile transition in doped silicon as a model substance. *Acta metall.*, 36(8):2003–2018, 1988.

[33] K. B. Broberg. *Cracks and Fracture*. Academic Press, San Diego, 1999.

[34] M. Brumovský, P. Novosad, M. Kytka, and J. Brynda. Surveillance Specimen Programs for WWER Type Reactors. In *Embrittlement and Mechanistic Interpretation of Reactor Pressure Vessel and Internal Materials. Selected papers from the IAEA Technical Meeting on Irradiation Effects and Mitigation in Reactor Pressure Vessel and Reactor Internals held at Gus Khrustalny, Russian Federation, May 24 - 28, 2004*, 2005.

[35] J. M. Burgers. Some considerations on the fields of stress connected with dislocations in a regular crystal lattice. I. *Proc. Kon. Nederl. Akad. Wetensch.*, 42:293–325, 1939.

[36] J. M. Burgers. Some considerations on the fields of stress connected with dislocations in a regular crystal lattice. II. *Proc. Kon. Nederl. Akad. Wetensch.*, 42:378–399, 1939.

[37] D. Caillard. Kinetics of dislocations in pure fe. part i. in situ straining experiments at room temperature. *Acta Materialia*, 58(9):3493 – 3503, 2010.

[38] D. Caillard. Kinetics of dislocations in pure fe. part ii. in situ straining experiments at low temperature. *Acta Materialia*, 58(9):3504 – 3515, 2010.

[39] C. C. Chang, J. B. McKinnon, and A. C. Rose-Innes. Peak Effect in Type II Superconductors: Yield Point of the Fluxon Lattice. *Phys. Stat. Sol.*, 36:205 –209, 1969.

[40] R. Chaouadi. On the (in)adequacy of the Charpy impact test to monitor irradiation effects of ferritic/martensitic steels. *Journal of Nuclear Materials*, 360:75–91, 2007.

[41] Z.-A. Chen, Z. Zeng, and Y. J. Chao. Effect of crack depth on the shift of the ductile-brittle-transition curve of steels. *Eng. Frac. Mech.*, 74:2437 – 2448, 2007.

[42] K. S. Cheung and S. Yip. Brittle-Ductile Transition in Intrinsic Fracture Behavior of Crystals. *Physical Review Letters*, 65:2804 – 2807, 1990.

[43] M. Coates, A. Kumar, and S. G. Roberts. Crack initiation in the brittle fracture of ferritic steels. *Fatigue Fract. Engng. Mater. Struct.*, 29:661–671, 2006.

[44] A. H. Cottrell. *Dislocations and plastic flow in crystals*. Oxford Clarendon Press, 1953.

[45] A. H. Cottrell. Theory of Brittle Fracture in Steel and Similar Metals. *Transactions of the Metallurgical Society of AIME*, 212:192–203, 1958.

[46] D. A. Curry. Cleavage micromechanisms of crack extension in steels. *Met. Sci.*, 14:319–326, 1980.

[47] D. A. Curry and J. F. Knott. The relationship between fracture toughness and microstructure in the cleavage fracture of mild steel. *Metal Sci.*, 10:1 – 6, 1976.

[48] M. Cyrot. Ginzburg-Landau theory for superconductors. *Reports on Progress in Physics*, 36:103 – 158, 1973.

[49] T. Dasgupta, U. V. Waghmare, and A. M. Umarji. Electronic signatures of ductility and brittleness. *Physical Review B*, 76:174110, 2007.

[50] D. A. DeSandre, A. A. Benzerga, V. Tvergaard, and A. Needleman. Material inertia and size effects in the charpy v-notch test. *Eur. J. Mech. A/Solids*, 23:373–386, 2004.

[51] C. Doglioni, S. Barba, E. Carminati, and F. Riguzzi. Role of the brittle-ductile transition on fault activation. *Physics of the Earth and Planetary Interiors*, 184(3-4):160 – 171, 2011.

[52] D. S. Dugdale. Yielding of steel sheets containing slits. *J. Mech. Phys. Solids*, 8:100–104, 1960.

[53] C. A. English, G. Gage, R. M. Boothby, and S. R. Ortner. Methodology for characterizing materials, Part I, Introduction. Technical report, AEA Technology plc, 1997.

[54] C. A. English, G. Gage, R. M. Boothby, and S. R. Ortner. Methodology for characterizing materials, Part II, Microstructural Techniques. Technical report, AEA Technology plc, 1997.

[55] M. EricksonKirk and M. EricksonKirk. An upper-shelf fracture toughness master curve for ferritic steels. *Int. J. Pres. Ves. Piping*, 83:571–583, 2006.

[56] J. D. Eshelby. The force on an elastic singularity. *Phil. Trans. Roy. Soc. London A*, 244:87–111, 1951.

[57] J. D. Eshelby. The Equation of Motion of a Dislocation. *Physical Review*, 90:248 – 255, 1953.

[58] J. D. Eshelby. The continuum theory of lattice defects. *Solid State Physics*, 3:79 – 144, 1956.

[59] J. D. Eshelby. *Collected Works of J. D. Eshelby The Mechanics of Defects and Inhomogeneities*, volume 133 of *Solid Mechanics and its Applications*. Springer, 2006.

[60] U. Essmann and H. Träuble. The direct observation of individual flux lines in type II superconductors. *Physics Letters*, 24A:526 – 527, 1967.

[61] European Commission. *Embrittlement and Mechanistic Interpretation of Reactor Pressure Vessel and Internal Materials. Selected papers from the IAEA Technical Meeting on Irradiation Effects and Mitigation in Reactor Pressure Vessel and Reactor Internals held at Gus Khrustalny, Russian Federation, May 24 - 28, 2004.* Office for Official Publications of the European Communities, 2005.

[62] L. L. Fischer and G. E. Beltz. The effect of crack blunting on the competition between dislocation nucleation and cleavage. *J. Mech. Phys. Solids*, 49:635–654, 2001.

[63] E. R. Fitzgerald. *Particle waves and deformation in crystalline solids.* Interscience Publishers, 1966.

[64] S. Fournais and B. Helffer. *Spectral Methods in Surface Superconductivity*, volume 77 of *Progress in Nonlinear Differential Equations and Their Applications.* Birkhäuser, 2010.

[65] J. Frenkel. Zur Theorie der Elastizitätsgrenze und der Festigkeit kristallinischer Körper. *Zeitschrift für Physik*, 37:572–609, 1926.

[66] L. B. Freund. *Dynamic fracture mechanics.* Cambridge Monographs on Mechanics and Applied Mathematics. Cambridge University Press, Cambridge, 1998. Taschenbuch.

[67] T. Frisch, Y. Pomeau, and S. Rica. Transition to Dissipation in a Model of Superflow. *Physical Review Letters*, 69:1644 – 1648, 1992.

[68] A. George and G. Michot. Dislocation loops at crack tips: nucleation and growth - an experimental study in silicon. *Mat. Sci. Eng. A*, 164:118–134, 1993.

[69] A. Giannattasio and S. G. Roberts. Strain-rate dependence of the brittle-to-ductile transition temperature in tungsten. *Philosophical Magazine*, 87:2589–2598, 2007.

[70] J. R. Greer and J. T. M. de Hosson. Plasticity in small-sized metallic systems: Intrinsic versus extrinsic size effects. *Progress in Materials Science*, 56:654 – 724, 2011.

[71] A. A. Griffith. The phenomena of rupture and flow in solids. *Phil. Trans. Roy. Soc. London*, A221:163–198, 1921.

[72] A. A. Griffith. The Theory of Rupture. In *Proceedings of the First International Congress for Applied Mechanics*, pages 55–63, 1924.

[73] A. A. Griffith and G. I. Taylor. The use of soap films in solving torsion problems. *Proceedings Inst. Mech. Eng.*, ?:755–809, 1917.

[74] D. Gross and Th. Selig. *Bruchmechanik mit einer Einführung in die Mikromechanik*. Springer, 3 edition, 2001.

[75] M. Grübler. Der Spannungszustand in Schleifsteinen und Schmirgelscheiben. *Zeitschrift VDI*, 41:860 – 864, 1897.

[76] G. T. Hahn. The influence of Microstructure on Brittle Fracture Toughness. *Metal. Trans. A*, 15:947–959, 1984.

[77] P. Hähner and H. Stamm. A dislocation dynamical Theory of the Ductile-to-Brittle Transition. *Acta metall. mater.*, 43(7):2797–2805, 1995.

[78] P. Hähner and H. Stamm. Methodology for characterizing materials, Part iv, Materials Embrittlement: Theoretical Concepts. Technical report, European Commission, Joint Research Centre, Institute for Advanced Materials, 1997.

[79] E. W. Hart. A Magnetic Analog for the Interaction of Dislocation Loops. *J. Appl. Physics*, 24:224–225, 1953.

[80] E. W. Hart. A theory for stable crack extension rates in ductile materials. *Int. J. Solids Structures*, 16:807–823, 1980.

[81] A. Hartmaier and P. Gumbsch. Thermal activation of crack-tip plasticity: The brittle or ductile response of a stationary crack loaded to failure. *Physical Review B*, 71:024108, 2005.

[82] T. Hennecke. Versetzungsdynamische Modellierung des Spröd-Duktil-Übergangs. Master's thesis, TU Braunschweig, 2005.

[83] T. Hennecke and P. Hähner. WP 3.2 JRC-IE contribution to Year 3 Progress Report; crystal plasticity based approach to the ductile-brittle transition. Technical report, JRC IE Petten, 2007.

[84] T. Hennecke and P. Hähner. Dislocation dynamics modelling of the ductile-brittle-transition. In *IOP Conf. Ser.: Mater. Sci. Eng. 3*, page 012005, 2009.

[85] P. B. Hirsch and S. G. Roberts. The brittle-ductile transition in silicon. *Phil. Mag. A*, 64:55–80, 1991.

[86] P. B. Hirsch and S. G. Roberts. Comment on the brittle-to-ductile transition: a cooperative dislocation generation instability; dislocation dynamics and the strain-rate dependence of the transition temperature. *Acta mater.*, 44:2361–2371, 1996.

[87] P. B. Hirsch and S. G. Roberts. Modelling crack tip plastic zones and brittle-ductile transitons. In K. S. Chan, editor, *George R. Irwin Symposium on Cleavage Fracture*, pages 137–145. The Minerals, Metals & Materials Society (TMS), 1997.

[88] J. P. Hirth and J. Lothe. *Theory of Dislocations*. Krieger, 1992.

[89] K.-H. Hoffmann and Q. Tang. *Ginzburg-Landau Phase Transition Theory and Superconductivity*, volume 134 of *ISNM International Series of Numerical Mathematics*. Birkhäuser, 2001.

[90] R. W. K. Honeycombe. *Steels: microstructure and properties*. Edward Arnold Publishers Ltd., 1981.

[91] J. Hove, S. Mo, and A. Sudbø. Vortex interacions and thermally induced crossover from type-I to type-II superconductivity. *Physical Review B*, 66:064524, 2002.

[92] R. P. Huebener. *Magnetic Flux Structures in Superconductors*, volume 6 of *Springer Series in Solid-State Sciences*. Springer, 1979.

[93] D. Hull and D. J. Bacon. *Introduction to Dislocations*. Butterworth and Heinemann, 2004.

[94] W. J. Ibbetson. On the Airy-Maxwell Solution of the Equations of Equilibrium of an Isotropic Elastic Solid, under Conservative Forces. *Proc. Lond. Math. Soc.*, 17:296–309, 1886.

[95] C. E. Inglis. Stresses in a plate due to the presence of cracks and sharp corners. *Transactions of the Institution of Naval Architects*, 55:219–241, 1913.

[96] G. R. Irwin. Fracture dynamics. In *Fracturing of Metals*, pages 147–166. American Society for Metals, 1948.

[97] G. R. Irwin. Analysis of Stresses and Strains Near the End of a Crack Traversing a Plate. *J. Appl. Mech.*, 24:361–364, 1957.

[98] J. Janovec, J. Pokluda, and P. Lejček. Influence of phosphorus grain boundary segregation on fracture behaviour of iron-base alloys. *Materials Science Forum*, 567 – 568:33 – 38, 2008.

[99] M. Janssen, J. Zuidema, and R. Wanhill. *Fracture Mechanics*. Spon Press, London, 2004.

[100] W. G. Johnston and J. J. Gilman. Dislocation Velocities, Dislocation Densities, and Plastic Flow in Lithium Fluoride Crystals. *J. Appl. Phys.*, 30(2):129–144, 1959.

[101] F. Jonassen, W. P. Roop, and R. T. Bayless, editors. *Fracturing of Metals. A seminar on the fracturing of metals held during the twenty-ninth national metal congress and exposition, Chicago, October 18 - 24, 1947*. American Society for Metals, 1948.

[102] C. Josserand, Y. Pomeau, and S. Rica. Cavitation versus Vortex Nucleation in a Superfluid Model. *Physical Review Letters*, 75:3150 – 3154, 1995.

[103] R. Kasada, S. G. Lee, J. Isselin, J. H. Lee, T. Omura, A. Kimura, T. Okuda, M. Inoue, S. Ukai, S. Ohnuki, T. Fujisawa, and F. Abe. Anisotropy in tensile and ductile-brittle transition behavior of ODS ferritic steels. *Journal of Nuclear Materials*, In Press, Corrected Proof:– , 2010.

[104] M. T. Kirk, M. E. Natishan, and M. Wagenhofer. Microstructural Limits of Applicability of the Master Curve. In R. Chona, editor, *Fatigue and Fracture Mechanics, 32nd volume*, ASTM STP 1406, pages 3 – 16, 2002.

[105] G. Kirsch. Die Theorie der Elastizität und die Bedürfnisse der Festigkeitslehre. *Zeitschrift VDI*, 42:797–807, 1898.

[106] F. Klein and K. Wieghardt. Über Spannungsflächen und reziproke Diagramme, mit besonderer Berücksichtigung der Maxwellschen Arbeiten,. *Arch. Math. Phys.. (Ser.3)*, 8:1–10 & 95–119, 1904.

[107] H. Kleinert. Gauge theory of dislocation melting. *Physics Letters A*, 89:294–298, 1982.

[108] H. Kleinert. Double Gauge Theory of Stresses and Defects. *Physics Letters*, 97A:51 – 54, 1983.

[109] H. Kleinert. *Gauge Fields in Condensed Matter Vol. I Superflow and Vortex Lines; Disorder Fields, Phase Transition.* World Scientific, 1990.

[110] H. Kleinert. *Gauge Fields in Condensed Matter Vol. II Stresses and Defects; Differential Geometry, Crystal Melting.* World Scientific, 1990.

[111] J. F. Knott. Some effects oof hydrostatic tension on the fracture behaviour of mild steel. *Journal of the Iron and Steel Institute*, 204:104–111, 1966.

[112] U. F. Kocks, A. S. Argon, and M. F. Ashby. *Thermodynamics and Kinetics of Slip*, volume 19 of *Progress in Materials Science*. Pergamon Press, Oxford, 1975.

[113] U. F. Kocks and H. Mecking. Physics and phenomenology of strain hardening: the FCC case. *Progress in Materials Science*, 48:171 – 273, 2003.

[114] T. Koyama, T. Araki, and H. Tanaka. Fracture Phase Separation. *Physical Review Letters*, 102:065701, 2009.

[115] E. Kröner. Dislocations and the Biot-Savart Law. *Proc. Phys. Soc. A*, 68:53–55, 1955.

[116] E. Kröner. *Kontinuumstheorie der Versetzungen und Eigenspannungen.* Ergebnisse der angewandten Mathematik 5. Springer, 1958.

[117] A. Kumar, S. G. Roberts, and A. Wilkinson. Low-temperature fracture mechanisms in a spheroidised reactor pressure vessel steel. *Int. J. Fracture*, 144:121 – 129, 2007.

[118] A. Kumar, S.G. Roberts, and A.J. Wilkinson. Relating Cleavage Nucleation to Fractured Spheroidal Carbides in A533B steel. In *Proceedings of the 16th European Conference of Fracture, held in Alexandroupolis, Greece, July 3-7, 2006*, 2006.

[119] M. Kurzke and D. Spirn. On the energy of superconductors in large and small domains. *SIAM J. Math. Anal.*, 40:2077 – 2104, 2009.

[120] L. D. Landau and E. M. Lifschitz. *Lehrbuch der theoretischen Physik Band VIII Elektrodynamik der Kontinua.* Akademie Verlag, 1990.

[121] J. S. Langer. Shear-transformation-zone theory of plastic deformation near the glassy transition. *Physical Review E*, 77:021502, 2008.

[122] B. R. Lawn. *Fracture of Brittle Solids*. Cambridge Solid State Science Series. Cambridge University Press, Cambridge, 2. edition, 1993.

[123] A. Leon. Über die Spannungsstörungen durch Kerben und Tellen und über die Spannungsverteilung in Verbundkörpern. *Österreichische Wochenzeitschrift für den öffentlichen Baudienst*, 14:770–776, 1908.

[124] A. Leon. Über die Störungen der Spannungsverteilung, die in elastischen Körpern durch Bohrungen und Bläschen entstehen. *Österreichische Wochenzeitschrift für den öffentlichen Baudienst*, 14:163–168, 1908.

[125] M. Libert, C. Rey, L. Vincent, and B. Marini. Temperature dependant polycrystal model application to bainitic steel behavior under tri-axial loading in the ductile-brittle transition. *International Journal of Solids and Structures*, 48(14-15):2196 – 2208, 2011.

[126] D. P. G. Lidbury. The ductile-to-brittle transition of ferritic steel components: some recent developments in relation to nuclear reactor pressure vessel integrity. *Int. J. Pres. Ves. & Piping*, 64:191–197, 1995.

[127] D. P. G. Lidbury, A. H. Sharry, B. R. Bass, P. Gilles, D. Connors, U. Eisele, E. Keim, H. Keinanen, K. Wallin, D. Lauerova, S. Marie, G. Nagel, K. Nilsson, D. Siegele, and Y. Wadier. Validation of constraint-based methodology in structural integrity of ferritic steels for nuclear reactor pressure vessels. *Fatigue Fract. Engng. Mater. Struct.*, 29:829–849, 2006.

[128] I.-H. Lin and R. Thomson. Cleavage, dislocation emission, and shielding for cracks under general loading. *Acta metall.*, 34(2):187–206, 1986.

[129] T. C. Lindley, G. Oates, and C. E. Richards. A critical appraisal of carbide cracking mechanisms in ferride/carbide aggregates. *Acta metall.*, 18:1127–1136, 1970.

[130] R. Löfstedt. Brittleness, ductility, and the Griffith crack. *Physical Review E*, 55:6726–6730, 1997.

[131] R. Löfstedt. Thermodynamic approach to creep and plasticity. *Physical Review E*, 55:6719–6725, 1997.

[132] F. Louchet and Y. Bréchet. Physics of Toughness A Kinetic Approach of the Brittle-Ductile Transition and of the Role of Plastic Instabilities. *Phys. Stat. Sol. (a)*, 131:529–537, 1992.

[133] F. Louchet and Y. Bréchet. A physical approach to the toughness problem: From thermodynamics to kinetics - II. The heterogeneous case. *Acta metall. mater.*, 41:793–800, 1993.

[134] A. E. H. Love. *A treatise on the mathematical theory of elasticity.* Dover, 1944.

[135] J. R. Low. *The Fracture of Metals*, volume 12 of *Progress in Materials Science*. Pergamon Press, 1963.

[136] M. A. Loyola de Oliveira and G. Michot. Three dimensional analysis of the interaction between a crack and a dislocation loop. *Acta mater.*, 46:1371–1383, 1998.

[137] B. Z. Margolin, V. A. Shvetsova, A. G. Gulenko, and V. I. Kostylev. Application of a new cleavage fracture criterion for fracture toughness prediction for RPV steels. *Fatigue Fract. Engng. Mater. Struct.*, 29:697–713, 2006.

[138] J. C. Maxwell. *The Scientific Papers of James Clerk Maxwell Volume I.* Dover Phoenix Editions. Dover, 2003.

[139] J. C. Maxwell. *The Scientific Papers of James Clerk Maxwell Volume II.* Dover Phoenix Editions. Dover, 2003.

[140] C. J. McMahon Jr. and M. Cohen. Initiation of cleavage in polycristalline iron. *Acta Met.*, 13:591–604, 1965.

[141] V. V. Meleshko. Selected topics in the history of the two-dimensional biharmonic problem. *Applied Mechanics Review*, 56:33–85, 2003.

[142] G. Michot and A. George. Fracture and crack tip plasticity in silicon and gallium arsenide. In S. G. Roberts, D. B. Holt, and P. R. Wilshaw, editors, *Proceedings of the 6th International Conference on Dislocations in Semiconductors*, volume 104 of *IOP Conference Series*, pages 385–396, 1989.

[143] G. Michot and M. A. Loyola de Oliveira. Plastic relaxation at crack tip: from brittle to ductile behaviour. *Mater. Transactions JIM*, 42:14–19, 2001.

[144] S. Mo, J. Hove, and A. Sudbø. Order of the metal-to-superconductor transition. *Physical Review B*, 65:104501, 2002.

[145] J. W. Morris Jr. Metallurgical Control of the Ductile-Brittle Transition in High-Strength Structural Steels. In G. E. Beltz, R. L. Blumberg Selinger, K.-S. Kim, and M. P. Marder, editors, *Fracture and Ductile vs. Brittle Behaviour - Theory, Modelling and Experiment; Symposium held November 30 - December 3, 1998, Boston, Massachusetts*, volume 539 of *MRS Symposium Procedings*, 1999.

[146] R. Moskovic. Application of the competing risks analysis to fracture toughness of silicon-killed C-Mn plate steels. *Fatigue Fract. Engng. Mater. Struct.*, 29:738–751, 2006.

[147] F. R. N. Nabarro. *Theory of Crystal Dislocations*. Dover Publications, New York, 1987.

[148] E. Nadgornyi. *Dislocation dynamics and mechanical properties of crystals*, volume 31 of *Progress in Materials Science*. Pergamon Press, 1988.

[149] A. Nazari, A. A. Milani, and M. Zakeri. Modeling ductile to brittle transition temperature of functionally graded steels by artificial neural networks. *Computational Materials Science*, 50(7):2028 – 2037, 2011.

[150] H. Neuber. Ein neuer Ansatz zur Lösung räumlicher Probleme der Elastizitätstheorie. Der Hohlkegel unter Einzellast als Beispiel. *ZAMM*, 14:203–212, 1934.

[151] H. Neuber. *Kerbspannungslehre*. Springer, 4 edition, 2001.

[152] R. W. D. Nickalls. A new approach to solving the cubic: Cardan's solution revealed. *The Mathematical Gazette*, 77:354–359, 1993.

[153] Y. A. Nikolaev, A. V. Nikolaeva, and Y. I. Shtrombakh. Radiation embrittlement of low-alloy steels. *Int. J. Pres. Vess. Piping*, 79:619–636, 2002.

[154] G. R. Odette and M. Y. He. A cleavage toughness master curve model. *J. Nuc. Mat.*, 283-287:120–127, 2000.

[155] G. R. Odette, T. Yamamoto, H. J. Rathbun, M. Y. He, M. L. Hribernik, and J. W. Rensman. Cleavage fracture and irradiation embrittlement of fusion reactor alloys: mechanisms, multiscale models,toughness measurements and implications to structural integrity assessment. *J. Nuc. Mat.*, 323:313–340, 2003.

[156] S. M. Ohr. An Electron Microscope Study of Crack Tip Deformation and its Impact on the Dislocation Theory of Fracture. *Mat. Sci. Eng.*, 72:1–35, 1985.

[157] S. M. Ohr et al. Viewpoint set on dislocation emission from crack tips. *Scripta Met.*, 20:1465–1505, 1986.

[158] E. Orowan. Zur Kristallplastizität. III. Über den Mechanismus des Gleitvorganges. *Z. Physik*, 89:634–659, 1934.

[159] E. Orowan. Problems of plastic gliding. *Proc. Phys. Soc.*, 52:8 – 22, 1940.

[160] E. Orowan. Energy criteria of fracture. *The Welding Journal Research Supplement*, 34:157s – 160s, 1955.

[161] S. R. Ortner. Factors affecting the shape of the ductile-to-brittle transition. *Int. J. Pres. Ves. Piping*, 79:693–700, 2002.

[162] S. R. Ortner and C. A. Hippsley. Two component description of ductile to brittle transition in ferritic steel. *Mat. Sci. Tech.*, 12:1035–1042, 1996.

[163] J. Paglione and R. L. Greene. High-temperature superconductivity in iron-based materials. *Nature Physics*, 6:645 – 658, 2010.

[164] R. D. Parks, editor. *Superconductivity (in two Volumes) Volume 1.* Marcel Dekker, 1969.

[165] R. D. Parks, editor. *Superconductivity (in two Volumes) Volume 2.* Marcel Dekker, 1969.

[166] M. Peach and J. S. Koehler. The forces exerted on dislocations and the stress fields produced by them. *Physical Review*, 80:436–439, 1950.

[167] A. Pineau. Global and Local Aproaches of Fracture - Transferability of Laboratory Test Results to Components. In A. S. Argon, editor, *Topics in Fracture and Fatigue*, pages 197 – 234. Springer, 1992.

[168] A. Pineau. Development of the local approach to fracture over the past 25 years: theory and applications. *Int. J. Frac.*, 138:139 – 166, 2006.

[169] A. Pineau. Modeling ductile to brittle fracture transition in steels - micromechanical and physical challenges. *Int. J. Fract.*, 150:129 – 156, 2008.

[170] M. Polanyi. Über eine Art Gitterstörung, die einen Kristall plastisch machen könnte. *Z. Physik*, 89:660–664, 1934.

[171] G. D. Quinn and et al. Standard Reference Material 2100: Fracture Toughness of Ceramics. In R. Chona, editor, *Fatigue and Fracture Mechanics, 32nd volume, ASTM STP 1406*, 2002.

[172] W. T. Read Jr. *Dislocations in Crystals*. McGraw-Hill, 1953.

[173] J. R. Rice. Dislocation nucleation from a crack tip: an analysis based on the Peierls concept. *J. Mech. Phys. Solids*, 40(2):239–271, 1992.

[174] J. R. Rice and G. E. Beltz. The activation energy for dislocation nucleation at a crack. *J. Mech. Phys. Solids*, 42(2):333–360, 1994.

[175] J. R. Rice and R. Thomson. Ductile versus brittle behaviour of crystals. *Phil. Mag.*, 29:73–97, 1974.

[176] R. O. Ritchie, J. F. Knott, and J. R. Rice. On the relationship between critical tensile stress and fracture toughness in mild steel. *J. Mech. Phys. Sol.*, 21:395–410, 1973.

[177] S. G. Roberts. Modelling the brittle to ductile transition in single crystals. In H. O. Kirchner, L. P. Kubin, and V. Pontikis, editors, *Computer Simulation in Materials Science - nano/meso/macroscopic space and time scales*, volume 308 of *NATO ASI Series E*, pages 409–434. Kluwer Acad. Publishers, 1996.

[178] S. G. Roberts. Modelling crack tip plastic zones and brittle-ductile transitions. *Mat. Sci. Eng. A*, 234-236:52–58, 1997.

[179] S. G. Roberts. Depths of cracks produced by abrasion of brittle materials. *Scripta Materialia*, 40:101–108, 1999.

[180] S. G. Roberts. Modelling brittle-ductile transitions. In *Multiscale Phenomena in plasticity*, volume 367 of *NATO Science Series E*, pages 349–364. Kluwer Acad. Publishers, 2000.

[181] S. G. Roberts, P. B. Hirsch, A. S. Booth, M. Ellis, and F. C. Serbena. Dislocations, cracks and brittleness in single crystals. *Physica Scripta*, T49:420–426, 1993.

[182] A. R. Rosenfield. Micromechanics of cleavage fracture. In K. S. Chan, editor, *George R. Irwin Symposium on Cleavage Fracture*, pages 229–236. The Minerals, Metals & Materials Society (TMS), 1997.

[183] H. P. Rossmanith. An introduction to K. Wieghardt's historical paper "On splitting and cracking of elastic bodies". *Fatigue Fract. Engng. Mater. Struct.*, 18:1367–1369, 1995.

[184] H. P. Rossmanith. Fracture mechanics and materials testing: forgotten pioneers of the early 20th century. *Fatigue Fract. Engng. Mater. Struct.*, 22:781–797, 1999.

[185] T. Saario, K. Wallin, and K. Törronen. On the microstructural basis of cleavage fracture initiation in ferritic and bainitic steels. *J. Eng. Mat. Tech.*, 106:173–177, 1984.

[186] E. Sandier and S. Serfaty. *Vortices in the Magnetic Ginzburg-Landau Model*. Birkhäuser, 2007.

[187] L. Schäfer. Tensile and impact behavior of the reduced-activation steels OPTIFER and F82H mod. *J. Nuc. Mat.*, 283-287:707–710, 2000.

[188] E. Schmid and W. Boas. *Kristallplastizität mit besonderer Berücksichtigung der Metalle*, volume XVII of *Struktur und Eigenschaften der Materie*. Springer, 1935.

[189] G. Schöck. Dislocation emission from crack tips. *Phil. Mag. A*, 63(1):111–120, 1991.

[190] G. Schöck. Dislocation emission from crack tips as a variational problem of the crack energy. *J. Mech. Phys. Solids*, 44(3):413–437, 1996.

[191] G. Schöck. The formation of dislocation rings on a crack front. *Phil. Mag. A*, 74(2):419–430, 1996.

[192] G. Schöck. The emission of dislocations from crack tips. A critical assessment. *Mat. Sci. Eng. A*, 356:93–101, 2003.

[193] G. Schöck and W. Püschl. The formation of dislocation loops at crack tips in three dimensions. *Phil. Mag. A*, 64(4):931–949, 1991.

[194] A. Seeger. The Temperature and Strain-Rate Dependence of the Flow Stress of Body-Centred Cubic Metals: A Theory Based on Kink-Kink Interactions. *Zeitschrift für Metallkunde*, 72:369 – 380, 1981.

[195] P. G. Shewmon and V. F. Zackay, editors. *Response of metals to high velocity deformation. Proceedings of a technical conference held at Estes Park, Colorado, July 11 - 12, 1960*. Interscience Publishers, 1961.

[196] G. E. Smith, A. G. Crocker, R. Moskovic, and P. E. J. Flewitt. Competing fracture mechanisms in the brittle-to-ductile transition region of ferritic steels. *Materials Science and Engineering A*, 387-389:367 – 371, 2004. 13th International Conference on the Strength of Materials.

[197] D. Spirn. Vortex Dynamics of the Full Time-Dependent Ginzburg-Landau Equations. *Communications on Pure and Applied Mathematics*, 55:537 – 581, 2002.

[198] C. St. John. The brittle-to-ductile transition in pre-cleaved silicon single crystals. *Phil. Mag.*, 32:1193–1212, 1975.

[199] M. Steigemann. *Verallgemeinerte Eigenfunktionen und lokale Integralcharakteristiken bei quasi-statischer Rissausbreitung in anisotropen Materialien*. PhD thesis, Universität Kassel, 2008.

[200] A. N. Stroh. The formation of cracks as a result of plastic flow. *Proc. Roy. Soc. London*, A223:404–414, 1954.

[201] A. N. Stroh. The formation of cracks in plastic flow. II. *Proc. Roy. Soc. London*, A232:548 – 560, 1955.

[202] A. N. Stroh. A Theory of the Fracture of Metals. *Advances in Physics*, 6:418–465, 1957.

[203] C. Sulem and P.-L. Sulem. *The Nonlinear Schrödinger Equation Self-Focusing and Wave Collapse*, volume 139 of *Applied Mathematical Sciences*. Springer, 1999.

[204] Y. Sun and G. E. Beltz. Dislocation nucleation from a crack tip: a formulation based on anisotropic elasticity. *J. Mech. Phys. Solids*, 42(12):1905–1932, 1994.

[205] Y. Sun, G. E. Beltz, and J. R. Rice. Estimates from atomic models of tension-shear coupling in dislocation nucleation from a crack tip. *Mat. Sci. Eng. A*, 170:67–85, 1993.

[206] T. Tagawa, Y. Kayamori, and H. Hira. Statistical scatter of fracture toughness in the ductile-brittle transition of a structural steel. *Engineering Fracture Mechanics*, 77(16):3077 – 3086, 2010.

[207] M. Tanaka, E. Tarleton, and S. G. Roberts. The brittle-ductile transition in single-crystal iron. *Acta Materialia*, 56(18):5123–5129, 2008.

[208] D. Tanguy. Constained molecular dynamics for quantifying intrinsic ductility versus brittleness. *Physical Review B*, 76:144115, 2007.

[209] E. Tarleton and S. G. Roberts. Dislocation dynamic model of the brittle-ductile transition in tungsten. *Philosophical Magazine*, 89:2759 – 2769, 2009.

[210] G. I. Taylor. The Mechanism of Plastic Deformation of Crystals. Part I. - Theoretical. *Proc. Roy. Soc.*, A145:366–387, 1934.

[211] G. I. Taylor. The Mechanism of Plastic Deformation of Crystals. Part II. - Comparison with Oservations. *Proc. Roy. Soc.*, A145:388–404, 1934.

[212] G. I. Taylor. Plastic strain in metals. *J. Inst. Metals*, 62:307–324, 1938.

[213] D. Terentyev. Personal communication, 2008.

[214] D. Terentyev and X. He. Properties of grain boundaries in BCC iron and iron-based alloys. An atomistic study. Technical Report BLG-1072, SCK-CEN, 2010.

[215] A. S. Tetelman and A. J. McEvily Jr. *Fracture of Structural Materials.* John Wiley & Sons, Inc., 1967.

[216] R. Thomson. Fundamentals of fracture: a 1993 prologue, and other comments. *Mat. Sci. Eng.*, A176:1 – 7, 1994.

[217] I. Tice. Ginzburg-Landau Vortex Dynamics Driven by an Applied Boundary Current. *Communications on Pure and Applied Mathematics*, 63:1622 – 1676, 2010.

[218] S. P. Timoshenko. *History of Strength of Materials.* Dover, 1982.

[219] A. A. Timpe. Probleme der Spannungsverteilung in ebenen Systemen, einfach gelöst mit Hilfe der Airyschen Funktion. *Zeitschrift Math. Phys.*, 52:348–383, 1905.

[220] A. A. Timpe. Die Torsion von Umdrehungskörpern. *Math. Annalen*, 71:480 – 509, 1911.

[221] A. A. Timpe. Die Airysche Funktion für den Ellipsenring. *Math. Zeitschrift*, 17:189 – 205, 1923.

[222] A. A. Timpe. Achsensymmetrische Torsionszustände und ihre Inversion. *ZAMM*, 11:8 – 15, 1931.

[223] M. Tinkham. *Introduction to Superconductivity*. Dover, 2004.

[224] C. Truesdell. Invariant and Complete Stress Functions for General Continua. *Arch. Rat. Mech. Analysis*, 4:1–29, 1959.

[225] T. Šmida and J. Bošanský. Deformation twinning and its possible influence on the ductile brittle transition temperature of ferritic steels. *Mat. Sci. Eng. A*, 287:107–115, 2000.

[226] T. Šmida and J. Bošanský. Fracture mode transition phenomena in steels as a consequence of the change of operating deformation mode. *Mat. Sci. Eng. A*, 323:21–26, 2002.

[227] M. Valo, K. Wallin, E. Lucon, M. Kytka, M. Brumovsky, B. Acosta, L. Debarberis, J. Kohopää, F. Gillemot, and M. Horvath. The Euratom 5th Framework Programme Project FRAME (fracture mechanics based embrittlement); description of the project and first results. *Nuc. Eng. Des.*, 235:445–455, 2005.

[228] I. R. Vatne, E. Østby, C. Thaulow, and D. Farkas. Quasicontinuum simulation of crack propagation in BCC-Fe. *Mat. Sci. Eng. A*, 528:5122 – 5134, 2011.

[229] M. von Laue. *Theorie der Supraleitung*. Springer, 1947.

[230] K. Wallin. The scatter in K_{IC}-results. *Eng. Frac. Mech.*, 19:1085–1093, 1984.

[231] K. Wallin. The size effect in K_{IC}-results. *Eng. Frac. Mech.*, 22:149–163, 1985.

[232] K. Wallin. Irradiation damage effects on the fracture toughness transition curve shape for reactor pressure vessel steels. *Int. J. Pres. Ves. & Piping*, 55:61–79, 1993.

[233] K. Wallin. Effect of strain rate on the fracture toughness reference temperature T_0 for ferritic steels. In R. K. Mahidhara, A. B. Geltmacher, P. Matic, and K. Sadananda, editors, *Recent advances in fracture - Proceedings of a symposium held at the Annual Meeting of The Minerals, Metals & Materials Society in Orlando, Florida, February 10-13, 1997*. TMMMS, 1997.

[234] K. Wallin. Master curve analysis of the "Euro" fracture toughness dataset. *Eng. Frac. Mech.*, 69:451–481, 2002.

[235] K. Wallin, T. Saario, and K. Törrönen. Statistical model for carbide induced brittle fracture in steel. *Met. Sci.*, 18:13–16, 1984.

[236] G. Z. Wang, H. Wang, F. Z. Xuan, S. T. Tu, and Z. D. Wang. Effects of void damage induced by warm prestressing (WPS) on cleavage fracture of notched steel specimens. *Engineering Fracture Mechanics*, 76(8):1010 – 1023, 2009.

[237] J. Weertman. *Dislocation Based Fracture Mechanics*. World Scientific, Singapore, 1996.

[238] J. Weertman and J. R. Weertman. *Elementary Dislocation Theory*. Oxford University Press, New York, 1992.

[239] K. Wieghardt. Über ein Verfahren, verwickelte theoretische Spannungsverteilungen auf experimentellem Wege zu finden. *Zeitschrift VDI*, 49:1568–1569, 1905.

[240] K. Wieghardt. Über das Spalten und Zerreißen elastischer Körper. *Zeitschrift für Mathematik und Physik*, 55:60–103, 1907.

[241] K. Wieghardt. Über Spannungsverteilungen in Balken aus Eisenbeton. *Zeitschrift für Mathematik und Physik*, 56:119–137, 1908.

[242] K. Wieghardt. Über einige wirklich durchführbare Ansätze zur Berechnung von Spannungszuständen des elastischen Kreisringes. *Sitzungsberichte Akad. Wiss. Wien, Math.-Nat. Kl.*, 124:1119–1142, 1915.

[243] K. Wieghardt. On splitting and cracking of elastic bodies. *Fatigue Fract. Engng. Mater. Struct.*, 18:1371–1405, 1995. Translated from german to english by H. P. Rossmanith.

[244] K. Wolf. Zur Bruchtheorie von A. Griffith. *ZAMM*, 3:107–112, 1923.

[245] K.-C. Wu and E. W. Hart. Steady state crack growth in elastic-viscoplastic materials. *Int. J. Frac.*, 33:175–194, 1987.

[246] L. Xia and C. Fong Shih. Ductile crack growth - I. A numerical study using computational cells with microstructurally-based length scales. *J. Mech. Phys. Solids*, 43:233–259, 1995.

[247] L. Xia and C. Fong Shih. Ductile crack growth - II. Void nucleation and geometry effects on macroscopic fracture behavior. *J. Mech. Phys. Solids*, 43:1953–1981, 1995.

[248] L. Xia and C. Fong Shih. Ductile crack growth - III. Transition to cleavage fracture incorporating statistics. *J. Mech. Phys. Solids*, 44:603–639, 1996.

[249] G. Xu, A. S. Argon, and M. Ortiz. Nucleation of dislocations from crack tips under mixed modes of loading: implications for brittle against ductile behaviour of crystals. *Phil. Mag. A*, 72(2):415–451, 1995.

[250] G. Xu, A. S. Argon, and M. Ortiz. Critical configurations for dislocation nucleation from crack tips. *Phil. Mag. A*, 75(2):341–367, 1997.

[251] G. Xu and M. Ortiz. A variational boundary integral method for the analysis of 3-d cracks of arbitrary geometry modelled as continuous distributions of dislocation loops. *Int. J. Num. Meth. Eng.*, 36:3675–3701, 1993.

[252] T. Yuritzinn, L. Ferry, S. Chapuliot, D. Moinereau, A. Dahl, and P. Gilles. Warm pre-stressing tests on specimens with semi-elliptical cracks and analysis of the results. *Engineering Fracture Mechanics*, 77(1):71 – 83, 2010.

[253] C. Zener. The micro-mechanics of fracture. In *Fracturing of Metals*, pages 3–31. American Society for Metals, 1948.

[254] F. J. Zerilli and R. W. Armstrong. Dislocation-mechanics-based constitutive relations for material dynamics calculations. *J. Appl. Phys.*, 61:1816–1825, 1987.

[255] M.-C. Zhao, T.-Y. Zeng, J.-L. Li, H. Xiaofang, Y.-C. Zhao, and A. Atrens. Identification of the effective grain size responsible for the ductile to brittle transition temperature for steel with an ultrafine grain size ferrite/cementite microstructure with a bimodal ferrite grain size distribution. *Materials Science and Engineering: A*, 528(12):4217 – 4221, 2011.

[256] S. J. Zhou and R. Thomson. Dislocation emission at ledges on cracks. *J. Mater. Res.*, 6:639–653, 1991.

[257] L. M. Zubov. *Nonlinear Theory of Dislocations and Disclinations in Elastic Bodies*. Springer, 1997.